# GRANIS: A Model for the Assessment of External Photon Irradiation from Contaminated Media of Infinite Lateral Extent

**R Kowe, A D Carey*, J A Jones and S F Mobbs**

***Now at UKAEA, Harwell**

## ABSTRACT

GRANIS (**G**amma **R**adiation **A**bove **N**uclides **I**n **S**oil) is a model developed at HPA-RPD to calculate the external photon dose from layers of contaminated material which have finite thickness yet are effectively infinite in horizontal extent. The model allows different vertical activity profiles to be considered, so has particular application for the prediction of external gamma irradiation following the deposition of radionuclides to ground following short or continuous releases of radionuclides to the environment. GRANIS calculates effective dose and equivalent dose for four tissues. This report describes the theory behind the GRANIS version 3 (v3) model and includes results calculated by GRANIS v3 for a set of typical cases. The report describes intercomparisons made of the results of GRANIS v3 with standard theoretical methods, published papers and other radiation transport codes. GRANIS v3 was found to agree well with other results, particularly for photon energies in the range 0.1 to 4 MeV, which is of interest for exposure assessments.

This work was undertaken under the Environmental Assessments and Emergency Response Group's Quality Management System, which has been approved by Lloyd's Register Quality Assurance to the Quality Management Standards ISO 9001:2000 and TickIT Guide Issue 5, certificate number 956546.


Centre for Radiation, Chemical and Environmental Hazards
Radiation Protection Division
Chilton, Didcot, Oxfordshire OX11 0RQ

Approval: September 2007
Publication: October 2007
£20.00
ISBN 978-0-85951-606-8

# EXECUTIVE SUMMARY

GRANIS (**G**amma **R**adiation **A**bove **N**uclides **I**n **S**oil) version 3 (v3) is a model developed at HPA-RPD to calculate the external photon dose from layers of contaminated material which have finite thickness yet are effectively infinite in horizontal extent. The model allows different vertical activity concentration profiles to be considered, and is therefore particularly appropriate for the prediction of external gamma irradiation following the deposition of radionuclides to ground. A soil migration model, not described by this report, can generate such activity concentration profiles. GRANIS allows calculation of photon irradiation from contaminated material of any composition, such as soils, sands, sediments and water as well as man-made materials such as concrete and steel sheet. The advantage of this model compared to other codes currently available is that it also allows the assessment of the effects of shielding layers, for example where contaminated soil is shielded by uncontaminated layers of soil, concrete or tarmac following redevelopment. GRANIS is also capable of estimating the variation of dose rate with height above the ground.

The parameters calculated by GRANIS include air kerma, effective dose and equivalent dose for four tissues (gonads, breast, thyroid and skin).

This report describes the theory behind GRANIS and includes results calculated by GRANIS v3 for three cases, namely variation of photon dose and dose rate with time following an instantaneous deposit of radionuclides to ground; variation of photon dose and dose rate with time following the continuous deposit of radionuclides to ground for a single year followed by no deposition; and the instantaneous dose rate above unit radionuclide concentrations (and unit concentrations of mono-energetic photons) in varying thicknesses of soil and sewage sludge. The variation of the radionuclide concentration profiles with time and any progeny ingrowth were generated by another code.

The report describes intercomparisons of the results of GRANIS v3 with standard theoretical methods, published papers and other radiation transport codes. GRANIS v3 was found to agree with well with other results for photon energies in the range 0.1 to 4 MeV - photon energies of importance for radionuclides found in the environment. However the underlying equation on which GRANIS v3 is based, which describes the relationship between absorbed dose rate in air and the particle flux density, is accurate up to a gamma radiation energy of about 3 MeV but at higher energies is less reliable. However, HPA-RPD recommends that GRANIS v3 should replace the earlier NRPB code, BOXDOSE (Charles et al, 1982).

# CONTENTS

# 1 INTRODUCTION

The computer model GRANIS (**G**amma **R**adiation **A**bove **N**uclides **I**n **S**oil) has been developed to calculate the gamma dose and dose rate above layers of contaminated material of finite thickness and infinite lateral extent. By considering external irradiation from layers of contaminated material, the model allows variations in radionuclide activity concentrations with depth to be considered. In this way the model can calculate the dose above areas of material contaminated with gamma emitting radionuclides with any activity profile. The model is also capable of calculating photon exposure above contaminated bodies of water and man-made materials such as concrete and steel sheeting so long as the lateral extent of the contaminated material is such that it can be considered to be infinite. GRANIS was developed as an update of the BOXDOSE code (Charles et al, 1982).

GRANIS was originally developed for a VAX mainframe computer and has now been converted to PC format. This report gives the theory of version 3 (v3) of the GRANIS model. The report shows a set of typical results for environmental scenarios in which GRANIS v3 is used in conjunction with a compartmental soil model. Details of the GRANIS v3 model verification are given in Appendix A and the GRANIS v3 library files are given in Appendix B.

GRANIS v3 results are used in several departmental applications including the contaminated land methodology (Oatway and Mobbs, 2003), the UK recovery handbook for radiation incidents (Mobbs et al, 2005), and a version of the GRANIS code is used in PC-CREAM (Mayall et al, 1997).

## 1.1 Capability of the GRANIS model

As mentioned above, calculation of gamma dose and gamma dose rate using GRANIS v3 is not restricted to environmental media (soils, sediments and sands). The dose rate in the vicinity of an effectively infinite area of contaminated material of any composition, such as the dose rate above contaminated water, contaminated concrete and above large contaminated steel sheets, can be calculated. The model can also calculate the dose rate above contaminated material shielded by a layer of uncontaminated material, for example an area of land previously contaminated then developed as a car park or factory, i.e., the contaminated soil is shielded by a layer of tarmac or concrete.

It is normal in the types of analysis above to calculate the dose and/or dose rate at a height of 1 metre above the material surface, a height generally used in assessing whole body exposure. However GRANIS v3 can calculate dose and dose rate at any height.

GRANIS v3 cannot be used to calculate the dose rate in the vicinity of objects of finite size. However, in some cases an object, although finite, can be adequately represented as infinite. The accuracy of this approximation is dependent on radionuclide photon energies, the size and density of the contaminated material and the height requested for calculation of dose rate (see Jaeger et al, 1968). Other codes such as MICROSHIELD (Negin, 1986) have the capability of calculating doses from finite and infinite objects. However unlike MICROSHIELD, GRANIS v3 has the capability of modelling multiple media above contaminated layers in soil. In addition, given activity concentration values supplied from other codes (see next paragraph), GRANIS v3 can calculate the aggregated exposure from several contaminated soil layers.

GRANIS v3 can also be used to assess the dose and dose rate on land contaminated with radionuclides as a result of releases from, for example, nuclear facilities during normal or accidental conditions. For this type of assessment use is normally made of the HPA-RPD compartmental soil model (Brown and Simmonds, 1995), which uses a compartmental solution code, to provide radionuclide activity concentrations in soil or sediment layers. The soil model calculates the transfer of deposited radionuclides through soil layers over time and simultaneously models the process of radionuclide decay and progeny ingrowth. Thus it can provide time integrated radionuclide activity concentrations that GRANIS v3 can use to calculate integrated dose results.

It is also possible to input a set of radionuclide activity concentrations directly into GRANIS v3 from, for example, environmental radionuclide activity concentration measurements, to enable the calculation of an instantaneous dose rate. However, GRANIS v3 is not capable of calculating integrated dose from measured input.

### 1.2 PC GRANIS

A version of GRANIS with limited functionality has been developed as part of the PC-CREAM (Mayall et al, 1997) suite of models. This version is called PC GRANIS and should not be confused with the stand alone version of GRANIS on the PC (GRANIS v3). CREAM (**C**onsequences of **R**eleases to the **E**nvironment: **A**ssessment **M**ethodology) has been developed for evaluating the radiological consequences primarily from routine discharges of radioactive effluents to the environment. Thus the functions of PC GRANIS have been limited to the calculation of integrated effective and organ doses resulting from continuous deposition. The shortest period of time that can be considered is one year. Deposition rates, and up to 20 integration times can be specified by the user for a range of radionuclides. PC GRANIS uses a two-stage process to calculate doses. Firstly, the HPA-RPD compartment soil model is used to calculate the activity concentrations and integrated activity concentrations of radionuclides in soil at various depths at the specified integration times resulting from a calculated deposition from atmosphere. Secondly, doses resulting from the distribution of radionuclides in the soil are calculated using PC GRANIS. The user can choose one of two soil models to describe migration, one for undisturbed soil (i.e., pasture) or one for well mixed soil (i.e., ploughed fields).

## 2 THEORETICAL BASIS FOR THE CODE

### 2.1 Theory

Figure 1 shows a layer of contaminated material of finite thickness (L2-L1) and infinite lateral extent, buried beneath a thickness of material, which may or may not be of the same material type. To calculate the photon dose rate the GRANIS v3 model calculates total photon flux density from such a layer by first considering the flux density from an annulus of a simple disc at the top of the contaminated layer and then integrating over all disks within the layer.

The relationship between absorbed dose rate in air, and the particle flux density for mono energetic radiation under conditions of electron equilibrium (Goussev, 1968) is determined by:

$$D = P.E.\left(\frac{\mu_a}{\rho}\right)_{air}.\psi \qquad (2.1)$$

where

D = absorbed dose rate in air ( $Gy\ h^{-1}$ )

P = constant ($9.6\ 10^{-12}$ J $MeV^{-1}$ $s\ h^{-1}$).

ψ = particle flux density ( photons $s^{-1}$ $m^{-2}$ )

$(\mu_a/\rho)_{air}$= mass attenuation coefficient of air ($m^2$ $kg^{-1}$) for photons of energy E

ρ = density of air (kg $m^{-3}$)

Equation (2.1) is accurate up to a gamma radiation energy of about 3 MeV; at higher energies electron equilibrium is difficult to attain. There are a few important nuclides which have photons with gamma energies above 3 MeV (e.g $^{238}$Pu, $^{240}$Pu) but the mean energy of the rest of their gamma energy spectrum is normally below 3 MeV. However comparison of GRANIS v3 with other codes justifies its use for energies up to 4 MeV (see Appendix A2.4).

From Goussev et al (1968) for a disk source with a slab shield, ie, the disk of activity at the top of the contaminated layer as shown in Figure 1, shielded by the slab of contaminated material above it, the radiation flux at a point on the centre line of the disk source may be obtained by the integration of the attenuation function for point sources which make up an annulus of the disk. The flux from the differential ring source (annulus) contained between the circles of radii r and r + dr is:

$$d\psi = BC_A\left(\frac{2\pi r\,dr}{4\pi y^2}\right)e^{-\mu_s x}e^{-\mu_a(y-x)} \qquad (2.2)$$

where

B is the build-up factor for scattered radiation (see below).

$C_A$ is the number of photons of initial energy E (MeV), emitted per second per $m^2$ of surface and per cm depth of soil in the layer considered.

x, y and r are lengths (metres) indicated in Figure 1.

$\mu_a$ and $\mu_s$ are the linear attenuation coefficients for the photons of energy E in air and material respectively ($m^{-1}$).

The build-up factor is used to account for the effects of photon scattering which occur in the material of the contaminated layer, shielding layer and the air layer. This scatters photons from their initial trajectory, which was away from the reference point, back to the reference point. The amount of scattering and thus the size of the build-up factor for each annulus is dependent on the shield material, and naturally varies with photon energy and attenuation depth of the annulus. Generally, build-up is higher for low atomic number materials.

Combining equations (2.1) and (2.2), the following is obtained:

$$dD(r, l, E) = \frac{PE}{2}\left(\frac{\mu_a}{\rho}\right)_{air} C_A B\left(\frac{r\,dr}{y^2}\right) e^{-\mu_s x} e^{-\mu_a (y-x)} \qquad (2.3)$$

where

dD(r,l,E) is the component of dose in Gy per year due to photons of energy E MeV from an annular source between r and r+dr, at a depth of l in the material (see Figure 1).

l is the depth of a disk annulus.

To calculate the exposure from a whole layer of contaminated material, equation (2.3) (the dose from a potentially buried annulus) requires integration over the radius of the annulus (r = 0 to infinity) and over the vertical thickness of the layer (L1 to L2 in Figure 1).

If equation (2.3) is written in terms of a variable φ, the number of mean free paths (though air and material) through which a gamma ray must pass in travelling from dr at a depth l to the reference point at height h above the material air interface, and variable dependencies are included, the following is obtained:

$$D = \frac{PE}{2}\left(\frac{\mu_a}{\rho}\right)_{air} C_A \int_{l_1}^{l_2} \int_{c(h+)}^{\infty} B(\phi, l, E)\, \frac{e^{-\phi(l,E)}}{\phi(l, E)}\, d\phi dl \qquad (2.4)$$

where

$$\phi = cy \quad \text{where } c = \left(\frac{h\mu_a + l\mu_s}{h + l}\right)$$

Equation (2.4) is solved in the GRANIS v3 code for each defined material layer using numerical quadrature methods.

GRANIS v3 is an updating of an earlier code, BOXDOSE (Charles et al, 1982), which was based on a model for dose rate above contaminated soil taken from earlier work by CEA (NRPB and CEA, 1979). The model used there is somewhat simpler than that included in GRANIS v3. This results in several differences in the codes, which are discussed in Appendix A3.1.

### 2.2 Radionuclide decay chains

GRANIS v3 can model a single radionuclide, a set of radionuclides in secular equilibrium (e.g., $^{137}$Cs+$^{137m}$Ba) and radionuclide chains as a sequence of single radionuclides and radionuclide sets (e.g., $^{238}$U etc). For radionuclides in secular equilibrium GRANIS v3 uses the activity concentration of the parent radionuclide to calculate the contribution to the overall dose from the daughter.

Radionuclides in a chain are in secular equilibrium when the activities of both radionuclides are nearly equal. For secular equilibrium to be established, the parent radionuclide must have a half-life much longer than that of the daughter. For secular equilibrium to be established in a chain, the parent radionuclide must have a half-life much longer than of any other radionuclide in the series. Secondly, for chains with more than one daughter, a sufficiently long period of time must have elapsed, for example ten half-lives of the decay product having the longest half-life, to allow for ingrowth of the decay products. Under secular equilibrium, the activity of the parent radionuclide undergoes no appreciable changes during many half-lives of its decay products.

The radionuclide chains are defined in a compartmental solution code and are written to a data file that also contains the time series of activity and integrated activity concentrations in the soil layers that are to be read into GRANIS v3. Table 1 gives details of the radionuclide chains used by the compartmental solution code for the instantaneous and continuous deposit to ground and for sewage sludge. A parent and daughter nuclide are assumed to be in secular equilibrium if the half life of the daughter is less than a hundredth of its parent, and the half-life is less than 1/7 of the minimum non-zero output time. The minimum non-zero output time is 6 hours for the instantaneous deposit to ground and one year for the continuous deposit to ground. Table 1 uses the following notation to show how the decay chains are handled. "$^{90}$Sr + $^{90}$Y" indicates that the parent nuclide $^{90}$Sr is assumed to be in secular equilibrium with its daughter $^{90}$Y. "$^{90}$Sr $^{90}$Y" indicates that the ingrowth of the daughter $^{90}$Y is modelled explicitly. For the GRANIS v3 calculations involving deposition to ground it is assumed that when two radionuclides are in secular equilibrium both the parent and the daughter are deposited in equal activity concentrations.

### 2.3 GRANIS calculational limits

Table 2 summarises the limits of the calculational capabilities of GRANIS v3.

## 3 GRANIS LIBRARY DATA

GRANIS v3 uses a number of data libraries, as described below.

## 3.1 Attenuation coefficient data

Photon attenuation coefficient data used by GRANIS v3 have been obtained from the work of Hubbell (1982) and are in the form of mass attenuation coefficients ($\mu/\rho$ in $cm^2\ g^{-1}$) at twelve different energy levels for twenty elements. The elements have been selected to cover the elemental compositions of the materials likely to be encountered in external dose analyses at HPA-RPD. The elements available in the library are shown in Table 3. Table 4 gives the generic elemental composition used to generate material specific attenuation coefficients. The mass attenuation coefficients given in the file x_sectors.lib (version 1) are shown in Table B1 of Appendix B.

## 3.2 Build up data

The build-up data available in GRANIS v3 are for concrete, water, iron, lead and air. The build-up values for concrete, water, iron and lead have been generated from Jaeger et al (1968). The air build-up library is based on Table 4.3-11 of Jaeger et al (1968). The build-up data given in the file buildup.lib (version 1) for the various materials are shown Tables B2 to B6 of Appendix B.

## 3.3 Fluence and dose conversion coefficients

The two sets of dose conversion libraries which were used in BOXDOSE (Charles et al, 1982) are also utilized with GRANIS v3: these are based on ICRP Publication 51 (1987) or ICRP Publication 74 (1996) respectively. Both libraries consider rotational irradiation geometry. Rotational irradiation geometry has been shown to be the most appropriate for exposure in a standing position from contamination deposited to ground (Jacob et al, 1986). Both libraries provide air absorbed dose conversion (Gy $cm^2$), whole body dose conversion (effective dose or effective dose equivalent) (Sv $cm^2$) and tissue or organ dose conversions (equivalent dose or dose equivalent) for four tissues (organs), gonads, breast, thyroid and skin (Sv $cm^2$). However, the ICRP Publication 74 values have modified tissue-weighting factors based on more recent data. The two sets of dose conversion factors are contained in the single file dose_factors.lib (version 1). The ICRP Publication 51 dose conversion factors are shown in Table B7 of Appendix B, and the ICRP Publication 74 modified dose conversion factors are shown in Table B8.

## 3.4 Radionuclide gamma ray production data

GRANIS v3 requires information on gamma production from radionuclide decay processes. Oak Ridge National Laboratory produced data files (Eckerman et al, 1993) containing all the decay data in ICRP Publication 38 (ICRP, 1983), and it is these data files that are used in GRANIS v3.

The photon emissions for each radionuclide are provided by this data library using a twelve-point energy scheme. The gamma ray production data are given in the file orlnspec.dat (version 1). The data for a few selected radionuclides are shown in Table B9 of Appendix B.

# 4 GRANIS VERIFICATION

The results of the GRANIS v3 model have been compared with analytical solutions, published calculations (Chen, 1991; Eckerman and Ryman, 1993), other radiation transport codes, BOXDOSE (Charles et al, 1982) the predecessor of GRANIS, and MICROSHIELD (Negin, 1986). The results of the comparisons are given below. Details of the verification work are described in Appendix A.

GRANIS v3 has been compared with analytical methods, a number of computer codes and published results for the calculation of dose from contaminated slabs of material of infinite lateral extent of a variety of thicknesses. The differences between GRANIS v3 and the other codes are generally less than a factor of two across the energy spectrum 0.1 to 4 MeV. The best agreement with other calculational methods has been observed at energies between 0.1 to 4 MeV, where many of the comparisons show agreement within about 10%. Below 0.1 MeV many of the comparisons show agreement within 40%. Therefore it has been concluded that GRANIS v3 is an appropriate model for calculating dose rates above contaminated material with an infinite lateral spread, with particular reliability within the energy range 0.1 to 4 MeV.

Within its stated limitations (Table 2) GRANIS v3 has been also shown to accurately predict the effects of shielding materials above contaminated materials, and is thus appropriate for use in the calculation of dose for scenarios where contaminated land has been re-developed as a car-park or factory, where tarmac or concrete provide radiation shielding.

GRANIS v3 has also been shown to be acceptable for the assessment of the variation of dose above the ground, up to a height of 10 metres, particularly at photon energies in excess of 0.1 MeV. However, for heights above 10 m, care needs to be taken in the choice of build-up factors. In this case the user is referred to Chilton et al (1984) who list build-up factors in air at different values of mean free path for different photon energies.

# 5 GRANIS – EXAMPLE RESULTS

GRANIS v3 has been used to generate a set of typical results for selected radionuclides and mono-energetic photons. These analyses and results are described below.

## 5.1 Instantaneous deposits of selected radionuclides to ground

GRANIS v3 and a compartmental solution code have been used in combination to calculate the dose and dose rate at various times following the instantaneous deposit to ground of 1 Bq $m^{-2}$ for selected radionuclides. Following the deposit to ground, in-growth of daughters and migration of the radionuclides through undisturbed soil have been considered. The migration of radionuclides through soil has been considered using the models of Brown and Simmonds (1995). Tables 5 and 6 show the dose rate and integrated dose respectively at 1 metre above the ground following an instantaneous release of 1 Bq m$^{-2}$ on undisturbed soil at various times.

### 5.2 Continuous deposits of selected radionuclides to ground for 1 year

GRANIS v3 and a compartmental solution code have been used to calculate the dose and dose rate at various times following a continuous and constant deposit of 1 Bq m$^{-2}$ s$^{-1}$ for a single year, for selected radionuclides. Following the deposit, the ingrowth of daughters and migration of the radionuclides through undisturbed soil have been considered. The migration of radionuclides through soil has been considered using the models of Brown and Simmonds (1995). Tables 7 and 8 show dose rate and integrated dose values respectively at 1 metre above the ground following a continuous release of 1 Bq m$^{-2}$ on undisturbed soil at various times.

### 5.3 Soil uniformly contaminated with selected radionuclides

GRANIS v3 has been used to calculate instantaneous dose rates at 1 metre above soil and sewage sludge, uniformly contaminated at an activity concentration of 1 Bq cm$^{-3}$, from the material surface to a series of depths. Table 9 shows the results of these analyses for a selection of radionuclides. Similar results for mono-energetic photons from 0.01 to 4 MeV are given in Table 10 and Figure 2. Section 4 gives caveats on the use of GRANIS v3 for photon energies below 0.1 MeV.

## 6 REFERENCES

Brown J and Simmonds JR (1995). FARMLAND. A dynamic model for the transfer of radionuclides through terrestrial food chains. Chilton, NRPB-R273.

BSI. BS 4094 (1966). Recommendation for data on shielding from ionising radiation. Part I Shielding from gamma radiation. Appendix A.

Charles D, Crick MJ, Fell TP and Greenhalgh JR (1982). DOSE-MARC: The dosimetric module in the methodology for assessing the radiological consequences of accidental releases. Chilton, NRPB-M74.

Chen SY (1991). Calculation of effective dose-equivalent responses for external exposures from residual photon emitters in soil. *Health Phys*, **60**(3), 411-426.

Chilton AB, Shultis KJ and Faw RE (1984). ‘Principles of Radiation Shielding’, Appendix 4. Prentice-Hall, Englewood Cliffs, NJ.

Eckerman KF and Ryman JC (1993). External exposure to radionuclides in air, water and soil. US EPA, Federal Guidance Report No 12.

Eckerman K F, Westfall R J, Ryman J C and Cristy M (1993). Nuclear decay data files of the dosimetry research group. Health Sciences Division, Oak Ridge National Laboratory, ORNL/TM-12350.

Goussev NG (1968). Relationship between absorbed dose rate (in air) and particle flux density or energy flux density (X- and gamma rays). IN : Engineering Compendium on Radiation Shielding **1**, Shielding Fundamentals and Methods, Section 1.3.1 (Jaeger RG et al, eds). New York, Springer and Verlag.

Goussev NG, Kovalev E and Foderaro A (1968). Derivation of formulae. IN : Engineering Compendium on Radiation Shielding **1**, Shielding Fundamentals and Methods, Section 6.6.2.2 (Jaeger RG et al, eds). New York, Springer and Verlag.

Negin CA (1986). MICROSHIELD - A Microcomputer Program for Analysing Dose Rate and Gamma Shielding. CONF-861102, ISSN 0003-018X CODEN TANSA. *Trans Am Nucl Soc*, **53**, 421-422.

Hubbell JH (1982). Photon mass attenuation and energy-absorption coefficients from 1 keV to 20 MeV. *Int J Appl Radiat Isot*, **33**, 1269-1290.

ICRP (1983). Radionuclide transformations: energy and intensity of emissions. ICRP Publication 38. *Ann ICRP*, **11–13**.

ICRP (1987). Data for use in protection against external radiation. ICRP Publication 51. *Ann ICRP*, **17**(2/3).

ICRP (1996). Conversion coefficients for use in radiological protection against external radiation. ICRP Publication 74. A*nn ICRP*, **26**(3/4).

Jacob P et al (1986). Effective dose equivalents for photon exposures. *Rad Prot Dosim*, **14**(4), 299-310.

Jaeger R G et al (Eds) (1968). Engineering Compendium on Radiation Shielding **1**, Shielding Fundamentals and Methods. New York, Springer and Verlag

Jones JA (1980). ESCLOUD: a computer program to calculate the air concentration, deposition rate and external dose rate from a continuous discharge of radioactive material to atmosphere. Chilton, NRPB-R101.

Mayall A, Cabianca T, Attwood CA, Fayers CA, Smith JG, Penfold J, Steadman D, Martin G, Morris TP and Simmonds JR (1997). *PC CREAM 97*. Chilton, NRPB-SR296. EUR 17791 (Code updated in 1998-PC CREAM 98).

Mobbs SF, Nisbet AF, Mercer J, Mortimer KT, Roberts G and Hesketh N (2005). UK recovery handbook for radiation incidents. HPA-RPD-002.

NRPB and CEA (1979). Methodology for evaluating the radiological consequences of radioactive effluents released via normal operations. Luxembourg, CEC, Doc No V/3865/79.

Oatway WB and Mobbs SF (2003). Methodology for estimating the doses to members of the public from the future use of land previously contaminated with radioactivity. Chilton, NRPB-W36.

# 7 TABLES AND FIGURES

**Table 1 Radionuclide decay chain for instantaneous and continuous deposit to the ground and for sewage sludge**

| Instantaneous deposit | Continuous deposit | Sewage sludge |
|---|---|---|
| $^{90}$Sr $^{90}$Y | $^{90}$Sr + $^{90}$Y | $^{90}$Sr + $^{90}$Y |
| $^{95}$Zr $^{95}$Nb | $^{95}$Zr $^{95}$Nb | $^{99}$Mo + $^{99m}$Tc + $^{99}$Tc |
| $^{99}$Mo $^{99m}$Tc $^{99}$Tc | $^{99}$Mo $^{99m}$Tc $^{99}$Tc | $^{106}$Ru + $^{106}$Rh |
| $^{106}$Ru + $^{106}$Rh | $^{106}$Ru + $^{106}$Rh | $^{137}$Cs + $^{137m}$Ba |
| $^{127m}$Te $^{127}$Te | $^{127m}$Te + $^{127}$Te | $^{144}$Ce + $^{144}$Pr |
| $^{129m}$Te $^{129}$Te $^{129}$I | $^{129m}$Te + $^{129}$Te $^{129}$I | $^{210}$Pb + $^{210}$Bi |
| $^{132}$Te $^{132}$I | $^{132}$Te $^{132}$I | $^{226}$Ra + $^{222}$Rn + $^{218}$Po $^{214}$Pb $^{214}$Bi + $^{214}$Po |
| $^{133}$I $^{133}$Xe | $^{133}$I $^{133}$Xe | $^{228}$Ra + $^{228}$Ac |
| $^{135}$I $^{135}$Xe $^{135}$Cs | $^{135}$I $^{135}$Xe $^{135}$Cs | $^{227}$Ac + $^{227}$Th + $^{223}$Ra+ $^{219}$Rn + $^{215}$Po $^{211}$Pb $^{211}$Bi + $^{207}$Tl |
| $^{137}$Cs + $^{137m}$Ba | $^{137}$Cs + $^{137m}$Ba | $^{228}$Th + $^{224}$Ra+ $^{220}$Rn + $^{216}$Po $^{212}$Pb $^{212}$Bi + $^{208}$Tl + $^{212}$Po |
| $^{140}$Ba $^{140}$La | $^{140}$Ba $^{140}$La | $^{235}$U + $^{231}$Th |
| $^{144}$Ce + $^{144}$Pr | $^{144}$Ce + $^{144}$Pr | $^{238}$U + $^{234}$Th + $^{234}$Pa |
| $^{226}$Ra $^{222}$Rn + $^{218}$Po $^{214}$Pb $^{214}$Bi + $^{214}$Po $^{210}$Pb $^{210}$Bi | $^{226}$Ra + $^{222}$Rn + $^{218}$Po $^{214}$Pb $^{214}$Bi + $^{214}$Po $^{210}$Pb + $^{210}$Bi | $^{237}$Np + $^{233}$Pa |
| $^{235}$U $^{231}$Th $^{231}$Pa $^{227}$Ac $^{227}$Th $^{223}$Ra + $^{219}$Rn + $^{215}$Po | $^{235}$U + $^{231}$Th $^{231}$Pa $^{227}$Ac + $^{227}$Th $^{223}$Ra + $^{219}$Rn + $^{215}$Po | |
| $^{238}$U $^{234}$Th + $^{234m}$Pa $^{234}$U $^{230}$Th $^{226}$Ra $^{222}$Rn + $^{218}$Po | $^{238}$U + $^{234}$Th + $^{234m}$Pa $^{234}$U $^{230}$Th $^{226}$Ra + $^{222}$Rn + $^{218}$Po | |
| $^{238}$Pu $^{234}$U $^{230}$Th $^{226}$Ra $^{222}$Rn + $^{218}$Po $^{214}$Pb $^{214}$Bi | $^{238}$Pu $^{234}$U $^{230}$Th $^{226}$Ra + $^{222}$Rn + $^{218}$Po $^{214}$Pb $^{214}$Bi | |
| $^{239}$Pu $^{235}$U $^{231}$Th $^{231}$Pa $^{227}$Ac $^{227}$Th $^{223}$Rn + $^{219}$Rn | $^{239}$Pu $^{235}$U + $^{231}$Th $^{231}$Pa $^{227}$Ac + $^{227}$Th $^{223}$Rn + $^{219}$Rn | |
| $^{241}$Pu $^{241}$Am $^{237}$Np $^{233}$Pa $^{233}$U $^{229}$Th $^{225}$Ra $^{225}$Ac | $^{241}$Pu $^{241}$Am $^{237}$Np + $^{233}$Pa $^{233}$U $^{229}$Th + $^{225}$Ra $^{225}$Ac | |
| $^{241}$Am $^{237}$Np $^{233}$Pa $^{233}$U $^{229}$Th $^{225}$Ra $^{225}$Ac + $^{221}$Fr | $^{241}$Am $^{237}$Np + $^{233}$Pa $^{233}$U $^{229}$Th + $^{225}$Ra $^{225}$Ac + $^{221}$Fr | |

Note: A single radionuclide is described by the element symbol preceded by the mass number in superscript, e.g. $^{238}$U or $^{230}$Th. Radionuclides in a secular equilibrium set are separated by a "+", e.g. $^{137}$Cs+$^{137m}$Ba. A decay chain of radionuclides is given as a sequence of radionuclide sets separated by a space, e.g. $^{228}$Th + $^{224}$Ra+ $^{220}$Rn + $^{216}$Po $^{212}$Pb $^{212}$Bi + $^{208}$Tl + $^{212}$Po, which illustrates the $^{228}$Th chain modelled using three separate radionuclide sets. See Section 2.2.

**Table 2 Calculational limits of GRANIS v3**

| Parameter description | Parameter limit |
|---|---|
| Maximum thickness of material considered | 100 cm |
| No. of user defined material layers | 20 |
| No. of material layers | 20 |
| No. of input times | 70 |
| No. of radionuclides in input file | 50 |
| No. of ‘organs’ | 6 |
| No. of radionuclides in a secular equilibrium set | 10 |
| No. of radionuclide sets in a chain | 10 |
| Energy range | 0.01 - 4 MeV |
| Restricted to contaminated objects of infinite lateral extent | |

**TABLE 3 Elements for which attenuation coefficients are provided**

| Element | Name | Atomic number |
|---|---|---|
| H | Hydrogen | 1 |
| C | Carbon | 6 |
| N | Nitrogen | 7 |
| O | Oxygen | 8 |
| F | Fluorine | 9 |
| Na | Sodium | 11 |
| Mg | Magnesium | 12 |
| Al | Aluminium | 13 |
| Si | Silicon | 14 |
| P | Phosphorus | 15 |
| S | Sulphur | 16 |
| Ar | Argon | 18 |
| K | Potassium | 19 |
| Ca | Calcium | 20 |
| Ti | Titanium | 22 |
| Mn | Manganese | 25 |
| Fe | Iron | 26 |
| Ba | Barium | 56 |
| Ce | Cerium | 58 |
| Pb | Lead | 82 |

**TABLE 4 Generic material compositions**

| Material | | Density ($g\ cm^{-3}$) | Elemental composition (fraction by weight) | | | | | | | | |
|---|---|---|---|---|---|---|---|---|---|---|---|
| | | | H 1 | C 6 | N 7 | O 8 | Al 13 | Si 14 | Ca 20 | Fe 26 | Pb 82 |
| Air[1] | | $1.293\ 10^{-3}$ | - | - | 0.78 | 0.21 | - | - | - | - | - |
| Soil | - dry | 1.25 | - | 0.10 | - | 0.46 | 0.04 | 0.38 | - | 0.02 | - |
| | - wet | 1.5 | 0.04 | 0.07 | - | 0.6 | 0.03 | 0.25 | - | 0.01 | - |
| Sediment | - dry | 1.5 | - | 0.05 | - | 0.49 | 0.05 | 0.38 | - | 0.03 | - |
| | - wet | 1.7 | 0.03 | 0.04 | - | 0.58 | 0.04 | 0.28 | - | 0.03 | - |
| Sewage sludge (wet) | | 1.0 | 0.11 | 0.05 | - | 0.84 | - | - | - | - | - |
| Sand | - dry | 1.8 | - | - | - | 0.53 | - | 0.47 | - | - | - |
| | - wet | 1.95 | 0.01 | - | - | 0.56 | - | 0.43 | - | - | - |
| Earth crust (dry)[2] | | 1.0 | - | - | - | 0.45 | 0.09 | 0.28 | 0.04 | 0.06 | - |
| Concrete [3] | | 2.35 | 0.01 | - | - | 0.52 | 0.02 | 0.37 | 0.06 | 0.02 | - |
| Water | | 1.0 | 0.11 | - | - | 0.89 | - | - | - | - | - |
| Lead | | 11.35 | - | - | - | - | - | - | - | - | 1.0 |

1 Trace element - Ar 0.01.
2 Trace elements - Na 0.03, Mg 0.02 and K 0.03 from Chen (1991).
3 Portland concrete composition from Goussev (1968).

## TABLE 5 Effective dose rate at 1 m above the ground after an instantaneous deposit of 1 Bq $m^{-2}$ on undisturbed soil[1]

| | Dose rate (Sv $h^{-1}$) | | | | | | | | | | | |
|---|---|---|---|---|---|---|---|---|---|---|---|---|
| Radionuclide[2] | 0 | 6 hours | 12 hours | 1 day | 2 days | 7 days | 30 days | 1 year | 2 years | 5 years | 10 years | 50 years | Infinity |
| $^{51}$Cr | 7.38 $10^{-14}$ | 7.33 $10^{-14}$ | 7.29 $10^{-14}$ | 7.19 $10^{-14}$ | 7.01 $10^{-14}$ | 6.18 $10^{-14}$ | 3.45 $10^{-14}$ | 7.07 $10^{-18}$ | 1.03 $10^{-21}$ | 1.55 $10^{-24}$ | 1.40 $10^{-28}$ | 0[3] | 0 |
| $^{54}$Mn | 1.94 $10^{-12}$ | 1.93 $10^{-12}$ | 1.93 $10^{-12}$ | 1.93 $10^{-12}$ | 1.93 $10^{-12}$ | 1.90 $10^{-12}$ | 1.79 $10^{-12}$ | 7.66 $10^{-13}$ | 3.07 $10^{-13}$ | 2.06 $10^{-14}$ | 2.61 $10^{-16}$ | 8.52 $10^{-24}$ | 0 |
| $^{59}$Fe | 2.69 $10^{-12}$ | 2.68 $10^{-12}$ | 2.67 $10^{-12}$ | 2.65 $10^{-12}$ | 2.60 $10^{-12}$ | 2.40 $10^{-12}$ | 1.67 $10^{-12}$ | 8.17 $10^{-15}$ | 2.53 $10^{-17}$ | 2.96 $10^{-21}$ | 8.27 $10^{-25}$ | 0 | 0 |
| $^{60}$Co | 5.64 $10^{-12}$ | 5.64 $10^{-12}$ | 5.64 $10^{-12}$ | 5.63 $10^{-12}$ | 5.63 $10^{-12}$ | 5.61 $10^{-12}$ | 5.52 $10^{-12}$ | 4.41 $10^{-12}$ | 3.49 $10^{-12}$ | 1.81 $10^{-12}$ | 6.89 $10^{-13}$ | 9.87 $10^{-16}$ | 0 |
| $^{65}$Zn | 1.32 $10^{-12}$ | 1.32 $10^{-12}$ | 1.32 $10^{-12}$ | 1.32 $10^{-12}$ | 1.32 $10^{-12}$ | 1.29 $10^{-12}$ | 1.20 $10^{-12}$ | 4.18 $10^{-13}$ | 1.33 $10^{-13}$ | 4.56 $10^{-15}$ | 1.86 $10^{-17}$ | 8.22 $10^{-24}$ | 0 |
| $^{75}$Se | 8.87 $10^{-13}$ | 8.86 $10^{-13}$ | 8.85 $10^{-13}$ | 8.82 $10^{-13}$ | 8.77 $10^{-13}$ | 8.50 $10^{-13}$ | 7.38 $10^{-13}$ | 9.47 $10^{-14}$ | 1.02 $10^{-14}$ | 1.34 $10^{-17}$ | 7.39 $10^{-22}$ | 2.26 $10^{-26}$ | 0 |
| $^{86}$Rb | 2.16 $10^{-13}$ | 2.14 $10^{-13}$ | 2.12 $10^{-13}$ | 2.08 $10^{-13}$ | 2.00 $10^{-13}$ | 1.66 $10^{-13}$ | 7.01 $10^{-14}$ | 2.61 $10^{-19}$ | 1.34 $10^{-22}$ | 0 | 0 | 0 | 0 |
| $^{89}$Sr | 1.95 $10^{-16}$ | 1.94 $10^{-16}$ | 1.94 $10^{-16}$ | 1.92 $10^{-16}$ | 1.90 $10^{-16}$ | 1.77 $10^{-16}$ | 1.28 $10^{-16}$ | 1.16 $10^{-18}$ | 6.96 $10^{-21}$ | 1.55 $10^{-25}$ | 0 | 0 | 0 |
| $^{90}$Sr | 0 | 8.70 $10^{-21}$ | 1.69 $10^{-20}$ | 3.16 $10^{-20}$ | 5.60 $10^{-20}$ | 1.15 $10^{-19}$ | 1.35 $10^{-19}$ | 1.06 $10^{-19}$ | 8.13 $10^{-20}$ | 3.66 $10^{-20}$ | 9.76 $10^{-21}$ | 5.00 $10^{-24}$ | 0 |
| $^{95}$Zr | 1.72 $10^{-12}$ | 1.72 $10^{-12}$ | 1.72 $10^{-12}$ | 1.73 $10^{-12}$ | 1.75 $10^{-12}$ | 1.81 $10^{-12}$ | 1.89 $10^{-12}$ | 9.39 $10^{-14}$ | 1.62 $10^{-15}$ | 4.55 $10^{-20}$ | 1.60 $10^{-23}$ | 0 | 0 |
| $^{95}$Nb | 1.78 $10^{-12}$ | 1.77 $10^{-12}$ | 1.76 $10^{-12}$ | 1.74 $10^{-12}$ | 1.71 $10^{-12}$ | 1.55 $10^{-12}$ | 9.74 $10^{-13}$ | 1.18 $10^{-15}$ | 8.66 $10^{-19}$ | 7.46 $10^{-23}$ | 1.31 $10^{-26}$ | 0 | 0 |
| $^{99}$Mo | 3.46 $10^{-13}$ | 4.53 $10^{-13}$ | 4.87 $10^{-13}$ | 4.69 $10^{-13}$ | 3.65 $10^{-13}$ | 8.67 $10^{-14}$ | 1.16 $10^{-16}$ | 0 | 0 | 0 | 0 | 0 | 0 |
| $^{103}$Ru | 1.11 $10^{-12}$ | 1.11 $10^{-12}$ | 1.10 $10^{-12}$ | 1.09 $10^{-12}$ | 1.07 $10^{-12}$ | 9.81 $10^{-13}$ | 6.49 $10^{-13}$ | 1.58 $10^{-15}$ | 2.28 $10^{-18}$ | 2.92 $10^{-22}$ | 6.57 $10^{-26}$ | 0 | 0 |
| $^{106}$Ru | 4.81 $10^{-13}$ | 4.80 $10^{-13}$ | 4.80 $10^{-13}$ | 4.80 $10^{-13}$ | 4.78 $10^{-13}$ | 4.73 $10^{-13}$ | 4.50 $10^{-13}$ | 2.15 $10^{-13}$ | 9.69 $10^{-14}$ | 9.37 $10^{-15}$ | 2.17 $10^{-16}$ | 2.79 $10^{-24}$ | 0 |
| $^{110m}$Ag | 6.32 $10^{-12}$ | 6.31 $10^{-12}$ | 6.31 $10^{-12}$ | 6.30 $10^{-12}$ | 6.28 $10^{-12}$ | 6.18 $10^{-12}$ | 5.76 $10^{-12}$ | 2.05 $10^{-12}$ | 6.68 $10^{-12}$ | 2.45 $10^{-14}$ | 1.13 $10^{-16}$ | 5.93 $10^{-23}$ | 0 |
| $^{125}$Sb | 9.86 $10^{-13}$ | 9.86 $10^{-13}$ | 9.86 $10^{-13}$ | 9.85 $10^{-13}$ | 9.84 $10^{-13}$ | 9.79 $10^{-13}$ | 9.57 $10^{-13}$ | 6.81 $10^{-13}$ | 4.75 $10^{-13}$ | 1.70 $10^{-13}$ | 3.46 $10^{-14}$ | 3.62 $10^{-19}$ | 0 |
| $^{127m}$Te | 6.61 $10^{-15}$ | 1.07 $10^{-14}$ | 1.33 $10^{-14}$ | 1.60 $10^{-14}$ | 1.75 $10^{-14}$ | 1.73 $10^{-14}$ | 1.48 $10^{-14}$ | 1.53 $10^{-15}$ | 1.30 $10^{-16}$ | 8.64 $10^{-20}$ | 2.91 $10^{-23}$ | 0 | 0 |
| $^{129m}$Te | 7.32 $10^{-14}$ | 1.53 $10^{-13}$ | 1.54 $10^{-13}$ | 1.51 $10^{-13}$ | 1.46 $10^{-13}$ | 1.24 $10^{-13}$ | 5.98 $10^{-14}$ | 3.81 $10^{-18}$ | 2.01 $10^{-22}$ | 7.87 $10^{-23}$ | 5.10 $10^{-23}$ | 1.05 $10^{-23}$ | 1.61 $10^{-25}$ |
| $^{132}$Te | 4.96 $10^{-13}$ | 4.73 $10^{-12}$ | 5.18 $10^{-12}$ | 4.78 $10^{-12}$ | 3.87 $10^{-12}$ | 1.33 $10^{-12}$ | 9.97 $10^{-15}$ | 0 | 0 | 0 | 0 | 0 | 0 |
| $^{129}$I | 1.69 $10^{-14}$ | 1.69 $10^{-14}$ | 1.69 $10^{-14}$ | 1.69 $10^{-14}$ | 1.69 $10^{-14}$ | 1.68 $10^{-14}$ | 1.66 $10^{-14}$ | 1.36 $10^{-14}$ | 1.09 $10^{-14}$ | 5.89 $10^{-15}$ | 2.39 $10^{-15}$ | 1.01 $10^{-16}$ | 5.33 $10^{-23}$ |
| $^{131}$I | 8.94 $10^{-13}$ | 8.75 $10^{-13}$ | 8.56 $10^{-13}$ | 8.20 $10^{-13}$ | 7.52 $10^{-13}$ | 4.88 $10^{-13}$ | 6.66 $10^{-14}$ | 1.49 $10^{-22}$ | 1.03 $10^{-25}$ | 0 | 0 | 0 | 0 |

**TABLE 5 Cont'd Effective dose rate at 1 m above the ground after an instantaneous deposit of 1 Bq $m^{-2}$ on undisturbed soil**

| | Dose rate (Sv $h^{-1}$) | | | | | | | | | | | |
|---|---|---|---|---|---|---|---|---|---|---|---|---|
| Radionuclide | 0 | 6 hours | 12 hours | 1 day | 2 days | 7 days | 30 days | 1 year | 2 years | 5 years | 10 years | 50 years | Infinity |
| $^{132}$I | 5.27 $10^{-12}$ | 8.63 $10^{-13}$ | 1.42 $10^{-13}$ | 3.84 $10^{-15}$ | 1.13 $10^{-17}$ | 1.36 $10^{-23}$ | 0 | 0 | 0 | 0 | 0 | 0 | 0 |
| $^{133}$I | 1.43 $10^{-12}$ | 1.13 $10^{-12}$ | 8.92 $10^{-13}$ | 5.59 $10^{-13}$ | 2.22 $10^{-13}$ | 6.36 $10^{-15}$ | 2.14 $10^{-16}$ | 4.91 $10^{-26}$ | 0 | 0 | 0 | 0 | 0 |
| $^{134}$I | 6.03 $10^{-12}$ | 5.27 $10^{-14}$ | 7.45 $10^{-16}$ | 2.95 $10^{-19}$ | 2.23 $10^{-22}$ | 0 | 0 | 0 | 0 | 0 | 0 | 0 | 0 |
| $^{135}$I | 3.52 $10^{-12}$ | 2.03 $10^{-12}$ | 1.18 $10^{-12}$ | 4.06 $10^{-13}$ | 5.23 $10^{-14}$ | 6.96 $10^{-18}$ | 4.07 $10^{-22}$ | 0 | 0 | 0 | 0 | 0 | 0 |
| $^{134}$Cs | 3.62 $10^{-12}$ | 3.62 $10^{-12}$ | 3.62 $10^{-12}$ | 3.61 $10^{-12}$ | 3.61 $10^{-12}$ | 3.59 $10^{-12}$ | 3.48 $10^{-12}$ | 2.30 $10^{-12}$ | 1.48 $10^{-12}$ | 4.11 $10^{-13}$ | 5.51 $10^{-14}$ | 2.31 $10^{-20}$ | 0 |
| $^{136}$Cs | 4.97 $10^{-12}$ | 4.90 $10^{-12}$ | 4.84 $10^{-12}$ | 4.71 $10^{-12}$ | 4.47 $10^{-12}$ | 3.42 $10^{-12}$ | 1.01 $10^{-12}$ | 1.09 $10^{-19}$ | 8.03 $10^{-23}$ | 0 | 0 | 0 | 0 |
| $^{137}$Cs | 1.39 $10^{-12}$ | 1.39 $10^{-12}$ | 1.39 $10^{-12}$ | 1.39 $10^{-12}$ | 1.39 $10^{-12}$ | 1.39 $10^{-12}$ | 1.38 $10^{-12}$ | 1.21 $10^{-12}$ | 1.06 $10^{-12}$ | 7.48 $10^{-13}$ | 4.76 $10^{-13}$ | 4.37 $10^{-14}$ | 0 |
| $^{140}$Ba | 4.22 $10^{-13}$ | 9.18 $10^{-13}$ | 1.36 $10^{-12}$ | 2.09 $10^{-12}$ | 3.10 $10^{-12}$ | 4.01 $10^{-12}$ | 1.23 $10^{-12}$ | 7.08 $10^{-20}$ | 5.33 $10^{-23}$ | 0 | 0 | 0 | 0 |
| $^{140}$La | 5.16 $10^{-12}$ | 4.65 $10^{-12}$ | 4.20 $10^{-12}$ | 3.41 $10^{-12}$ | 2.26 $10^{-12}$ | 2.86 $10^{-13}$ | 2.46 $10^{-17}$ | 0 | 0 | 0 | 0 | 0 | 0 |
| $^{144}$Ce | 1.09 $10^{-13}$ | 1.09 $10^{-13}$ | 1.09 $10^{-13}$ | 1.09 $10^{-13}$ | 1.08 $10^{-13}$ | 1.07 $10^{-13}$ | 1.00 $10^{-13}$ | 3.89 $10^{-14}$ | 1.40 $10^{-14}$ | 6.94 $10^{-16}$ | 5.29 $10^{-18}$ | 1.90 $10^{-25}$ | 0 |
| $^{169}$Yb | 6.03 $10^{-13}$ | 6.00 $10^{-13}$ | 5.97 $10^{-13}$ | 5.90 $10^{-13}$ | 5.77 $10^{-13}$ | 5.17 $10^{-13}$ | 3.11 $10^{-13}$ | 1.92 $10^{-16}$ | 7.79 $10^{-20}$ | 1.08 $10^{-22}$ | 1.47 $10^{-26}$ | 0 | 0 |
| $^{192}$Ir | 1.92 $10^{-12}$ | 1.92 $10^{-12}$ | 1.92 $10^{-12}$ | 1.91 $10^{-12}$ | 1.89 $10^{-12}$ | 1.80 $10^{-12}$ | 1.44 $10^{-12}$ | 5.60 $10^{-14}$ | 1.65 $10^{-15}$ | 6.32 $10^{-20}$ | 2.15 $10^{-23}$ | 0 | 0 |
| $^{226}$Ra | 1.50 $10^{-14}$ | 1.67 $10^{-13}$ | 3.30 $10^{-13}$ | 6.35 $10^{-13}$ | 1.17 $10^{-12}$ | 2.79 $10^{-12}$ | 3.88 $10^{-12}$ | 3.51 $10^{-12}$ | 3.16 $10^{-12}$ | 2.42 $10^{-12}$ | 1.76 $10^{-12}$ | 4.60 $10^{-13}$ | 0 |
| $^{235}$U | 3.41 $10^{-13}$ | 3.45 $10^{-13}$ | 3.48 $10^{-13}$ | 3.52 $10^{-13}$ | 3.58 $10^{-13}$ | 3.63 $10^{-13}$ | 3.60 $10^{-13}$ | 3.20 $10^{-13}$ | 2.83 $10^{-13}$ | 2.07 $10^{-13}$ | 1.40 $10^{-13}$ | 2.44 $10^{-14}$ | 5.85 $10^{-16}$ |
| $^{238}$U | 1.22 $10^{-14}$ | 1.25 $10^{-14}$ | 1.28 $10^{-14}$ | 1.34 $10^{-14}$ | 1.45 $10^{-14}$ | 1.98 $10^{-14}$ | 3.61 $10^{-14}$ | 4.79 $10^{-14}$ | 4.25 $10^{-14}$ | 3.13 $10^{-14}$ | 2.17 $10^{-14}$ | 4.91 $10^{-15}$ | 1.47 $10^{-16}$ |
| $^{238}$Pu | 2.13 $10^{-16}$ | 2.13 $10^{-16}$ | 2.13 $10^{-16}$ | 2.13 $10^{-16}$ | 2.13 $10^{-16}$ | 2.12 $10^{-16}$ | 2.09 $10^{-16}$ | 1.68 $10^{-16}$ | 1.33 $10^{-16}$ | 6.70 $10^{-17}$ | 2.37 $10^{-17}$ | 7.21 $10^{-19}$ | 4.28 $10^{-21}$ |
| $^{239}$Pu | 1.75 $10^{-16}$ | 1.75 $10^{-16}$ | 1.75 $10^{-16}$ | 1.75 $10^{-16}$ | 1.75 $10^{-16}$ | 1.75 $10^{-16}$ | 1.73 $10^{-16}$ | 1.47 $10^{-16}$ | 1.24 $10^{-16}$ | 7.95 $10^{-17}$ | 4.55 $10^{-17}$ | 7.15 $10^{-18}$ | 3.75 $10^{-20}$ |
| $^{241}$Pu | 3.31 $10^{-18}$ | 3.35 $10^{-18}$ | 3.39 $10^{-18}$ | 3.47 $10^{-18}$ | 3.63 $10^{-18}$ | 4.42 $10^{-18}$ | 8.03 $10^{-18}$ | 5.51 $10^{-17}$ | 9.67 $10^{-17}$ | 1.81 $10^{-16}$ | 2.49 $10^{-16}$ | 3.06 $10^{-16}$ | 7.29 $10^{-19}$ |
| $^{241}$Am | 3.65 $10^{-14}$ | 3.65 $10^{-14}$ | 3.65 $10^{-14}$ | 3.65 $10^{-14}$ | 3.65 $10^{-14}$ | 3.64 $10^{-14}$ | 3.60 $10^{-14}$ | 3.06 $10^{-14}$ | 2.59 $10^{-14}$ | 1.65 $10^{-14}$ | 9.25 $10^{-15}$ | 8.86 $10^{-16}$ | 1.65 $10^{-18}$ |

1 Generic wet soil of 1.5 g $cm^{-3}$ assumed in calculation
2 See Table 1 for radionuclide chains
3 Cut-off value for zero is 1 $10^{-30}$

## TABLE 6 Integrated effective dose rate at 1 m above the ground after an instantaneous deposit of 1 Bq $m^{-2}$ on undisturbed soil[1]

| | Dose (Sv) | | | | | | | | | | |
|---|---|---|---|---|---|---|---|---|---|---|---|
| Radionuclide[2] | 6 hours | 12 hours | 1 day | 2 days | 7 days | 30 days | 1 year | 2 years | 5 years | 10 years | 50 years | Infinity |
| $^{51}$Cr | 4.41 $10^{-13}$ | 8.80 $10^{-13}$ | 1.75 $10^{-12}$ | 3.45 $10^{-12}$ | 1.14 $10^{-11}$ | 3.72 $10^{-11}$ | 6.98 $10^{-11}$ | 6.98 $10^{-11}$ | 6.98 $10^{-11}$ | 6.98 $10^{-11}$ | 6.98 $10^{-11}$ | 6.98 $10^{-11}$ |
| $^{54}$Mn | 1.16 $10^{-11}$ | 2.32 $10^{-11}$ | 4.64 $10^{-11}$ | 9.26 $10^{-11}$ | 3.22 $10^{-10}$ | 1.34 $10^{-9}$ | 1.10 $10^{-8}$ | 1.54 $10^{-8}$ | 1.82 $10^{-8}$ | 1.84 $10^{-8}$ | 1.84 $10^{-8}$ | 1.84 $10^{-8}$ |
| $^{59}$Fe | 1.61 $10^{-11}$ | 3.21 $10^{-11}$ | 6.40 $10^{-11}$ | 1.27 $10^{-10}$ | 4.27 $10^{-10}$ | 1.54 $10^{-9}$ | 4.05 $10^{-9}$ | 4.06 $10^{-9}$ | 4.06 $10^{-9}$ | 4.06 $10^{-9}$ | 4.06 $10^{-9}$ | 4.06 $10^{-9}$ |
| $^{60}$Co | 3.38 $10^{-11}$ | 6.76 $10^{-11}$ | 1.35 $10^{-10}$ | 2.70 $10^{-10}$ | 9.45 $10^{-10}$ | 4.02 $10^{-9}$ | 4.38 $10^{-8}$ | 7.82 $10^{-8}$ | 1.45 $10^{-7}$ | 1.95 $10^{-7}$ | 2.30 $10^{-7}$ | 2.30 $10^{-7}$ |
| $^{65}$Zn | 7.94 $10^{-12}$ | 1.59 $10^{-11}$ | 3.17 $10^{-11}$ | 6.33 $10^{-11}$ | 2.20 $10^{-10}$ | 9.09 $10^{-10}$ | 6.88 $10^{-9}$ | 9.06 $10^{-9}$ | 1.01 $10^{-8}$ | 1.01 $10^{-8}$ | 1.01 $10^{-8}$ | 1.01 $10^{-8}$ |
| $^{75}$Se | 5.32 $10^{-12}$ | 1.06 $10^{-11}$ | 2.12 $10^{-11}$ | 4.23 $10^{-11}$ | 1.46 $10^{-10}$ | 5.84 $10^{-10}$ | 3.10 $10^{-9}$ | 3.43 $10^{-9}$ | 3.47 $10^{-9}$ | 3.47 $10^{-9}$ | 3.47 $10^{-9}$ | 3.47 $10^{-9}$ |
| $^{86}$Rb | 1.29 $10^{-12}$ | 2.56 $10^{-12}$ | 5.08 $10^{-12}$ | 9.97 $10^{-12}$ | 3.19 $10^{-11}$ | 9.33 $10^{-11}$ | 1.38 $10^{-10}$ | 1.38 $10^{-10}$ | 1.38 $10^{-10}$ | 1.38 $10^{-10}$ | 1.38 $10^{-10}$ | 1.38 $10^{-10}$ |
| $^{89}$Sr | 1.17 $10^{-15}$ | 2.33 $10^{-15}$ | 4.65 $10^{-16}$ | 9.22 $10^{-15}$ | 3.12 $10^{-14}$ | 1.15 $10^{-13}$ | 3.31 $10^{-13}$ | 3.33 $10^{-13}$ | 3.33 $10^{-13}$ | 3.33 $10^{-13}$ | 3.33 $10^{-13}$ | 3.33 $10^{-13}$ |
| $^{90}$Sr | 2.64 $10^{-20}$ | 1.03 $10^{-19}$ | 3.96 $10^{-19}$ | 1.46 $10^{-18}$ | 1.25 $10^{-17}$ | 8.58 $10^{-17}$ | 1.05 $10^{-15}$ | 1.87 $10^{-15}$ | 3.34 $10^{-15}$ | 4.23 $10^{-15}$ | 4.56 $10^{-15}$ | 4.56 $10^{-15}$ |
| $^{95}$Zr | 1.03 $10^{-11}$ | 2.07 $10^{-11}$ | 4.14 $10^{-11}$ | 8.31 $10^{-11}$ | 2.97 $10^{-10}$ | 1.33 $10^{-9}$ | 7.26 $10^{-9}$ | 7.46 $10^{-9}$ | 7.46 $10^{-9}$ | 7.46 $10^{-9}$ | 7.46 $10^{-9}$ | 7.46 $10^{-9}$ |
| $^{95}$Nb | 1.06 $10^{-11}$ | 2.12 $10^{-11}$ | 4.23 $10^{-11}$ | 8.37 $10^{-11}$ | 2.79 $10^{-10}$ | 9.62 $10^{-10}$ | 2.13 $10^{-9}$ | 2.13 $10^{-9}$ | 2.13 $10^{-9}$ | 2.13 $10^{-9}$ | 2.13 $10^{-9}$ | 2.13 $10^{-9}$ |
| $^{99}$Mo | 2.45 $10^{-12}$ | 5.29 $10^{-12}$ | 1.11 $10^{-11}$ | 2.11 $10^{-11}$ | 4.44 $10^{-11}$ | 5.16 $10^{-11}$ | 5.16 $10^{-11}$ | 5.16 $10^{-11}$ | 5.16 $10^{-11}$ | 5.16 $10^{-11}$ | 5.16 $10^{-11}$ | 5.16 $10^{-11}$ |
| $^{103}$Ru | 6.66 $10^{-12}$ | 1.33 $10^{-11}$ | 2.65 $10^{-11}$ | 5.25 $10^{-11}$ | 1.76 $10^{-10}$ | 6.19 $10^{-10}$ | 1.48 $10^{-9}$ | 1.49 $10^{-9}$ | 1.49 $10^{-9}$ | 1.49 $10^{-9}$ | 1.49 $10^{-9}$ | 1.49 $10^{-9}$ |
| $^{106}$Ru | 2.88 $10^{-12}$ | 5.76 $10^{-12}$ | 1.15 $10^{-11}$ | 2.30 $10^{-11}$ | 8.01 $10^{-11}$ | 3.35 $10^{-10}$ | 2.89 $10^{-9}$ | 4.19 $10^{-9}$ | 5.17 $10^{-9}$ | 5.27 $10^{-9}$ | 5.27 $10^{-9}$ | 5.27 $10^{-9}$ |
| $^{110m}$Ag | 3.79 $10^{-11}$ | 7.58 $10^{-11}$ | 1.51 $10^{-10}$ | 3.02 $10^{-10}$ | 1.05 $10^{-9}$ | 4.34 $10^{-9}$ | 3.32 $10^{-8}$ | 4.39 $10^{-8}$ | 4.90 $10^{-8}$ | 4.92 $10^{-8}$ | 4.92 $10^{-8}$ | 4.92 $10^{-8}$ |
| $^{125}$Sb | 5.92 $10^{-12}$ | 1.18 $10^{-11}$ | 2.37 $10^{-11}$ | 4.73 $10^{-11}$ | 1.65 $10^{-10}$ | 6.99 $10^{-10}$ | 7.22 $10^{-9}$ | 1.22 $10^{-8}$ | 2.00 $10^{-8}$ | 2.37 $10^{-8}$ | 2.47 $10^{-8}$ | 2.47 $10^{-8}$ |
| $^{127m}$Te | 5.29 $10^{-14}$ | 1.26 $10^{-13}$ | 3.04 $10^{-13}$ | 7.13 $10^{-13}$ | 2.82 $10^{-12}$ | 1.16 $10^{-11}$ | 5.86 $10^{-11}$ | 6.35 $10^{-11}$ | 6.40 $10^{-11}$ | 6.40 $10^{-11}$ | 6.40 $10^{-11}$ | 6.40 $10^{-11}$ |
| $^{129m}$Te | 9.27 $10^{-13}$ | 1.98 $10^{-12}$ | 4.05 $10^{-12}$ | 8.10 $10^{-12}$ | 2.63 $10^{-11}$ | 7.92 $10^{-11}$ | 1.29 $10^{-10}$ | 1.29 $10^{-10}$ | 1.29 $10^{-10}$ | 1.29 $10^{-10}$ | 1.29 $10^{-10}$ | 1.29 $10^{-10}$ |
| $^{132}$Te | 1.96 $10^{-11}$ | 4.99 $10^{-11}$ | 1.10 $10^{-10}$ | 2.14 $10^{-10}$ | 4.99 $10^{-10}$ | 6.48 $10^{-10}$ | 6.50 $10^{-10}$ | 6.50 $10^{-10}$ | 6.50 $10^{-10}$ | 6.50 $10^{-10}$ | 6.50 $10^{-10}$ | 6.50 $10^{-10}$ |
| $^{129}$I | 1.01 $10^{-13}$ | 2.02 $10^{-13}$ | 4.05 $10^{-13}$ | 8.09 $10^{-13}$ | 2.83 $10^{-12}$ | 1.20 $10^{-11}$ | 1.33 $10^{-10}$ | 2.39 $10^{-10}$ | 4.53 $10^{-10}$ | 6.20 $10^{-10}$ | 8.11 $10^{-10}$ | 8.29 $10^{-10}$ |
| $^{131}$I | 5.31 $10^{-12}$ | 1.05 $10^{-11}$ | 2.06 $10^{-11}$ | 3.94 $10^{-11}$ | 1.13 $10^{-10}$ | 2.29 $10^{-10}$ | 2.48 $10^{-10}$ | 2.48 $10^{-10}$ | 2.48 $10^{-10}$ | 2.48 $10^{-10}$ | 2.48 $10^{-10}$ | 2.48 $10^{-10}$ |
| $^{132}$I | 1.46 $10^{-11}$ | 1.70 $10^{-11}$ | 1.75 $10^{-11}$ | 1.75 $10^{-11}$ | 1.75 $10^{-11}$ | 1.75 $10^{-11}$ | 1.75 $10^{-11}$ | 1.75 $10^{-11}$ | 1.75 $10^{-11}$ | 1.75 $10^{-11}$ | 1.75 $10^{-11}$ | 1.75 $10^{-11}$ |
| $^{133}$I | 7.62 $10^{-12}$ | 1.37 $10^{-11}$ | 2.22 $10^{-11}$ | 3.10 $10^{-11}$ | 3.71 $10^{-11}$ | 3.79 $10^{-11}$ | 3.79 $10^{-11}$ | 3.79 $10^{-11}$ | 3.79 $10^{-11}$ | 3.79 $10^{-11}$ | 3.79 $10^{-11}$ | 3.79 $10^{-11}$ |
| $^{134}$I | 7.56 $10^{-12}$ | 7.62 $10^{-12}$ | 7.63 $10^{-12}$ | 7.63 $10^{-12}$ | 7.63 $10^{-12}$ | 7.63 $10^{-12}$ | 7.63 $10^{-12}$ | 7.63 $10^{-12}$ | 7.63 $10^{-12}$ | 7.63 $10^{-12}$ | 7.63 $10^{-12}$ | 7.63 $10^{-12}$ |
| $^{135}$I | 1.62 $10^{-11}$ | 2.56 $10^{-11}$ | 3.43 $10^{-11}$ | 3.84 $10^{-11}$ | 3.90 $10^{-11}$ | 3.90 $10^{-11}$ | 3.90 $10^{-11}$ | 3.90 $10^{-11}$ | 3.90 $10^{-11}$ | 3.90 $10^{-11}$ | 3.90 $10^{-11}$ | 3.90 $10^{-11}$ |
| $^{134}$Cs | 2.17 $10^{-11}$ | 4.34 $10^{-11}$ | 8.68 $10^{-11}$ | 1.73 $10^{-10}$ | 6.05 $10^{-10}$ | 2.56 $10^{-9}$ | 2.55 $10^{-8}$ | 4.17 $10^{-8}$ | 6.35 $10^{-8}$ | 7.12 $10^{-8}$ | 7.24 $10^{-8}$ | 7.24 $10^{-8}$ |

**TABLE 6 Cont'd Integrated effective dose rate at 1 m above the ground after an instantaneous deposit of 1 Bq m$^{-2}$ on undisturbed soil**

| | Dose (Sv) | | | | | | | | | | | |
|---|---|---|---|---|---|---|---|---|---|---|---|---|
| Radionuclide | 6 hours | 12 hours | 1 day | 2 days | 7 days | 30 days | 1 year | 2 years | 5 years | 10 years | 50 years | Infinity |
| $^{136}$Cs | $2.96\ 10^{-11}$ | $5.88\ 10^{-11}$ | $1.16\ 10^{-10}$ | $2.26\ 10^{-10}$ | $6.97\ 10^{-10}$ | $1.79\ 10^{-9}$ | $2.24\ 10^{-9}$ | $2.24\ 10^{-9}$ | $2.24\ 10^{-9}$ | $2.24\ 10^{-9}$ | $2.24\ 10^{-9}$ | $2.24\ 10^{-9}$ |
| $^{137}$Cs | $8.35\ 10^{-12}$ | $1.67\ 10^{-11}$ | $3.34\ 10^{-11}$ | $6.68\ 10^{-11}$ | $2.34\ 10^{-10}$ | $9.96\ 10^{-10}$ | $1.14\ 10^{-8}$ | $2.13\ 10^{-8}$ | $4.46\ 10^{-8}$ | $7.07\ 10^{-8}$ | $1.30\ 10^{-7}$ | $1.38\ 10^{-7}$ |
| $^{140}$Ba | $4.05\ 10^{-12}$ | $1.09\ 10^{-11}$ | $3.18\ 10^{-11}$ | $9.53\ 10^{-11}$ | $5.62\ 10^{-10}$ | $1.91\ 10^{-9}$ | $2.45\ 10^{-9}$ | $2.45\ 10^{-9}$ | $2.45\ 10^{-9}$ | $2.45\ 10^{-9}$ | $2.45\ 10^{-9}$ | $2.45\ 10^{-9}$ |
| $^{140}$La | $2.94\ 10^{-11}$ | $5.59\ 10^{-11}$ | $1.01\ 10^{-10}$ | $1.68\ 10^{-10}$ | $2.83\ 10^{-10}$ | $2.99\ 10^{-10}$ | $2.99\ 10^{-10}$ | $2.99\ 10^{-10}$ | $2.99\ 10^{-10}$ | $2.99\ 10^{-10}$ | $2.99\ 10^{-10}$ | $2.99\ 10^{-10}$ |
| $^{144}$Ce | $6.53\ 10^{-13}$ | $1.31\ 10^{-12}$ | $2.61\ 10^{-12}$ | $5.21\ 10^{-12}$ | $1.81\ 10^{-11}$ | $7.51\ 10^{-11}$ | $5.95\ 10^{-10}$ | $8.08\ 10^{-10}$ | $9.24\ 10^{-10}$ | $9.30\ 10^{-10}$ | $9.30\ 10^{-10}$ | $9.30\ 10^{-10}$ |
| $^{169}$Yb | $3.61\ 10^{-12}$ | $7.20\ 10^{-12}$ | $1.43\ 10^{-11}$ | $2.83\ 10^{-11}$ | $9.39\ 10^{-11}$ | $3.18\ 10^{-10}$ | $6.56\ 10^{-10}$ | $6.56\ 10^{-10}$ | $6.56\ 10^{-10}$ | $6.56\ 10^{-10}$ | $6.56\ 10^{-10}$ | $6.56\ 10^{-10}$ |
| $^{192}$Ir | $1.15\ 10^{-11}$ | $2.30\ 10^{-11}$ | $4.60\ 10^{-11}$ | $9.15\ 10^{-11}$ | $3.13\ 10^{-10}$ | $1.20\ 10^{-9}$ | $4.63\ 10^{-9}$ | $4.76\ 10^{-9}$ | $4.76\ 10^{-9}$ | $4.76\ 10^{-9}$ | $4.76\ 10^{-9}$ | $4.76\ 10^{-9}$ |
| $^{226}$Ra | $5.07\ 10^{-13}$ | $2.00\ 10^{-12}$ | $7.82\ 10^{-12}$ | $2.97\ 10^{-11}$ | $2.81\ 10^{-10}$ | $2.29\ 10^{-9}$ | $3.20\ 10^{-8}$ | $6.12\ 10^{-8}$ | $1.34\ 10^{-7}$ | $2.24\ 10^{-7}$ | $5.40\ 10^{-7}$ | $1.12\ 10^{-6}$ |
| $^{235}$U | $2.06\ 10^{-12}$ | $4.13\ 10^{-12}$ | $8.33\ 10^{-12}$ | $1.69\ 10^{-11}$ | $6.03\ 10^{-11}$ | $2.60\ 10^{-10}$ | $2.99\ 10^{-9}$ | $5.63\ 10^{-9}$ | $1.20\ 10^{-8}$ | $1.94\ 10^{-8}$ | $4.09\ 10^{-8}$ | $1.40\ 10^{-5}$ |
| $^{238}$U | $7.41\ 10^{-14}$ | $1.50\ 10^{-13}$ | $3.07\ 10^{-13}$ | $6.42\ 10^{-13}$ | $2.71\ 10^{-12}$ | $1.86\ 10^{-11}$ | $4.12\ 10^{-10}$ | $8.07\ 10^{-10}$ | $1.76\ 10^{-9}$ | $2.90\ 10^{-9}$ | $6.54\ 10^{-9}$ | $3.52\ 10^{-6}$ |
| $^{238}$Pu | $1.28\ 10^{-15}$ | $2.56\ 10^{-15}$ | $5.11\ 10^{-15}$ | $1.02\ 10^{-14}$ | $3.57\ 10^{-14}$ | $1.52\ 10^{-13}$ | $1.66\ 10^{-12}$ | $2.97\ 10^{-12}$ | $5.49\ 10^{-12}$ | $7.29\ 10^{-12}$ | $8.84\ 10^{-12}$ | $2.09\ 10^{-8}$ |
| $^{239}$Pu | $1.05\ 10^{-15}$ | $2.10\ 10^{-15}$ | $4.21\ 10^{-15}$ | $8.41\ 10^{-15}$ | $2.94\ 10^{-14}$ | $1.25\ 10^{-13}$ | $1.41\ 10^{-12}$ | $2.59\ 10^{-12}$ | $5.20\ 10^{-12}$ | $7.83\ 10^{-12}$ | $1.41\ 10^{-11}$ | $9.18\ 10^{-10}$ |
| $^{241}$Pu | $2.00\ 10^{-17}$ | $4.02\ 10^{-17}$ | $8.14\ 10^{-17}$ | $1.67\ 10^{-16}$ | $6.50\ 10^{-16}$ | $4.09\ 10^{-15}$ | $2.65\ 10^{-13}$ | $9.36\ 10^{-13}$ | $4.69\ 10^{-12}$ | $1.43\ 10^{-11}$ | $1.19\ 10^{-10}$ | $2.88\ 10^{-8}$ |
| $^{241}$Am | $2.19\ 10^{-13}$ | $4.38\ 10^{-13}$ | $8.76\ 10^{-13}$ | $1.75\ 10^{-12}$ | $6.12\ 10^{-12}$ | $2.61\ 10^{-11}$ | $2.93\ 10^{-10}$ | $5.40\ 10^{-10}$ | $1.09\ 10^{-9}$ | $1.63\ 10^{-9}$ | $2.73\ 10^{-9}$ | $6.38\ 10^{-8}$ |

1 Generic wet soil of 1.5 g cm$^{-3}$ assumed in calculation
2 See Table 1 for radionuclide chains

## TABLE 7 Effective dose rate at 1 m above the ground following a continuous deposit of 1 Bq $m^{-2}$ $s^{-1}$ to undisturbed soil for 1 year[1]

| | Dose-rate (Sv $h^{-1}$) | | | | | | | | | | |
|---|---|---|---|---|---|---|---|---|---|---|---|
| Radionuclide[2] | 1 year | 5 years | 10 years | 20 years | 30 years | 40 years | 50 years | 100 years | 200 years | 500 years | $10^5$ years |
| $^{51}$Cr | $2.51\ 10^{-7}$ | $4.04\ 10^{-22}$ | 0[3] | 0 | 0 | 0 | 0 | 0 | 0 | 0 | 0 |
| $^{54}$Mn | $3.98\ 10^{-5}$ | $1.05\ 10^{-6}$ | $1.31\ 10^{-8}$ | $2.56\ 10^{-12}$ | $5.50\ 10^{-16}$ | $1.25\ 10^{-19}$ | $2.09\ 10^{-22}$ | 0 | 0 | 0 | 0 |
| $^{59}$Fe | $1.46\ 10^{-5}$ | $1.33\ 10^{-15}$ | $3.60\ 10^{-22}$ | $1.03\ 10^{-25}$ | 0 | 0 | 0 | 0 | 0 | 0 | 0 |
| $^{60}$Co | $1.58\ 10^{-4}$ | $6.36\ 10^{-5}$ | $2.39\ 10^{-5}$ | $4.21\ 10^{-6}$ | $8.14\ 10^{-7}$ | $1.63\ 10^{-7}$ | $3.37\ 10^{-8}$ | $1.75\ 10^{-11}$ | $1.08\ 10^{-17}$ | $2.28\ 10^{-25}$ | 0 |
| $^{65}$Zn | $2.48\ 10^{-5}$ | $2.65\ 10^{-7}$ | $1.06\ 10^{-9}$ | $2.16\ 10^{-14}$ | $4.89\ 10^{-19}$ | $5.47\ 10^{-22}$ | $6.12\ 10^{-25}$ | 0 | 0 | 0 | 0 |
| $^{75}$Se | $1.12\ 10^{-5}$ | $1.55\ 10^{-9}$ | $2.73\ 10^{-14}$ | $7.79\ 10^{-22}$ | $6.13\ 10^{-25}$ | 0 | 0 | 0 | 0 | 0 | 0 |
| $^{86}$Rb | $4.98\ 10^{-7}$ | $2.33\ 10^{-23}$ | 0 | 0 | 0 | 0 | 0 | 0 | 0 | 0 | 0 |
| $^{89}$Sr | $1.19\ 10^{-9}$ | $1.58\ 10^{-18}$ | $3.19\ 10^{-26}$ | 0 | 0 | 0 | 0 | 0 | 0 | 0 | 0 |
| $^{90}$Sr | $3.83\ 10^{-12}$ | $1.32\ 10^{-12}$ | $3.52\ 10^{-13}$ | $2.63\ 10^{-14}$ | $2.57\ 10^{-15}$ | $4.91\ 10^{-16}$ | $1.66\ 10^{-16}$ | $2.08\ 10^{-18}$ | $3.61\ 10^{-22}$ | 0 | 0 |
| $^{95}$Nb | $7.66\ 10^{-6}$ | $1.69\ 10^{-18}$ | $2.87\ 10^{-22}$ | $3.83\ 10^{-26}$ | 0 | 0 | 0 | 0 | 0 | 0 | 0 |
| $^{95}$Zr | $2.61\ 10^{-5}$ | $3.54\ 10^{-12}$ | $2.86\ 10^{-20}$ | $1.78\ 10^{-23}$ | $1.10\ 10^{-26}$ | 0 | 0 | 0 | 0 | 0 | 0 |
| $^{99}$Mo | $1.86\ 10^{-7}$ | $9.89\ 10^{-28}$ | 0 | 0 | 0 | 0 | 0 | 0 | 0 | 0 | 0 |
| $^{103}$Ru | $5.34\ 10^{-6}$ | $2.28\ 10^{-17}$ | $1.33\ 10^{-22}$ | $2.59\ 10^{-26}$ | 0 | 0 | 0 | 0 | 0 | 0 | 0 |
| $^{106}$Ru | $1.04\ 10^{-5}$ | $4.45\ 10^{-7}$ | $1.01\ 10^{-8}$ | $6.64\ 10^{-12}$ | $4.79\ 10^{-15}$ | $3.59\ 10^{-18}$ | $2.93\ 10^{-21}$ | $1.07\ 10^{-24}$ | $2.55\ 10^{-28}$ | 0 | 0 |
| $^{110m}$Ag | $1.19\ 10^{-4}$ | $1.40\ 10^{-6}$ | $6.35\ 10^{-9}$ | $1.64\ 10^{-13}$ | $4.68\ 10^{-18}$ | $2.26\ 10^{-21}$ | $2.62\ 10^{-24}$ | $3.20\ 10^{-28}$ | 0 | 0 | 0 |
| $^{125}$Sb | $2.60\ 10^{-5}$ | $6.35\ 10^{-6}$ | $1.28\ 10^{-6}$ | $6.55\ 10^{-8}$ | $3.71\ 10^{-9}$ | $2.18\ 10^{-10}$ | $1.31\ 10^{-11}$ | $1.51\ 10^{-17}$ | $1.16\ 10^{-25}$ | 0 | 0 |
| $^{127m}$Te | $2.11\ 10^{-7}$ | $1.15\ 10^{-11}$ | $6.62\ 10^{-17}$ | $7.15\ 10^{-24}$ | $5.89\ 10^{-27}$ | 0 | 0 | 0 | 0 | 0 | 0 |
| $^{129m}$Te | $7.34\ 10^{-7}$ | $1.12\ 10^{-15}$ | $1.12\ 10^{-15}$ | $1.12\ 10^{-15}$ | $1.12\ 10^{-15}$ | $1.12\ 10^{-15}$ | $1.12\ 10^{-15}$ | $1.12\ 10^{-15}$ | $1.12\ 10^{-15}$ | $1.12\ 10^{-15}$ | $1.11\ 10^{-15}$ |
| $^{132}$Te | $2.34\ 10^{-6}$ | $9.31\ 10^{-25}$ | 0 | 0 | 0 | 0 | 0 | 0 | 0 | 0 | 0 |
| $^{129}$I | $4.78\ 10^{-7}$ | $2.05\ 10^{-7}$ | $8.20\ 10^{-8}$ | $2.33\ 10^{-8}$ | $1.09\ 10^{-8}$ | $5.88\ 10^{-9}$ | $3.28\ 10^{-9}$ | $2.34\ 10^{-10}$ | $1.37\ 10^{-11}$ | $2.41\ 10^{-13}$ | $1.89\ 10^{-15}$ |
| $^{131}$I | $8.92\ 10^{-7}$ | $1.49\ 10^{-22}$ | 0 | 0 | 0 | 0 | 0 | 0 | 0 | 0 | 0 |
| $^{132}$I | $6.29\ 10^{-8}$ | $1.38\ 10^{-23}$ | 0 | 0 | 0 | 0 | 0 | 0 | 0 | 0 | 0 |
| $^{133}$I | $1.37\ 10^{-7}$ | $1.58\ 10^{-24}$ | 0 | 0 | 0 | 0 | 0 | 0 | 0 | 0 | 0 |
| $^{134}$I | $2.75\ 10^{-8}$ | $6.22\ 10^{-24}$ | 0 | 0 | 0 | 0 | 0 | 0 | 0 | 0 | 0 |
| $^{135}$I | $1.40\ 10^{-7}$ | $1.45\ 10^{-29}$ | 0 | 0 | 0 | 0 | 0 | 0 | 0 | 0 | 0 |

**TABLE 7 Cont'd Effective dose rate at 1 m above the ground following a continuous deposit of 1 Bq $m^{-2}$ $s^{-1}$ to undisturbed soil for 1 year**

| Radionuclide | Dose-rate (Sv $h^{-1}$) # | | | | | | | | | | |
|---|---|---|---|---|---|---|---|---|---|---|---|
| | 1 year | 5 years | 10 years | 20 years | 30 years | 40 years | 50 years | 100 years | 200 years | 500 years | $10^5$ years |
| $^{134}$Cs | 9.17 $10^{-5}$ | 1.61 $10^{-5}$ | 2.13 $10^{-6}$ | 4.71 $10^{-8}$ | 1.15 $10^{-9}$ | 2.91 $10^{-11}$ | 7.55 $10^{-13}$ | 1.34 $10^{-20}$ | 5.69 $10^{-25}$ | 0 | 0 |
| $^{136}$Cs | 8.06 $10^{-6}$ | 2.37 $10^{-21}$ | 6.64 $10^{-26}$ | 0 | 0 | 0 | 0 | 0 | 0 | 0 | 0 |
| $^{137}$Cs | 4.09 $10^{-5}$ | 2.49 $10^{-5}$ | 1.56 $10^{-5}$ | 7.78 $10^{-6}$ | 4.26 $10^{-6}$ | 2.42 $10^{-6}$ | 1.42 $10^{-6}$ | 1.37 $10^{-7}$ | 3.26 $10^{-9}$ | 5.72 $10^{-13}$ | 7.02 $10^{-29}$ |
| $^{140}$Ba | 8.81 $10^{-6}$ | 6.06 $10^{-22}$ | 1.49 $10^{-26}$ | 0 | 0 | 0 | 0 | 0 | 0 | 0 | 0 |
| $^{140}$La | 1.08 $10^{-6}$ | 2.00 $10^{-21}$ | 7.65 $10^{-29}$ | 0 | 0 | 0 | 0 | 0 | 0 | 0 | 0 |
| $^{144}$Ce | 2.14 $10^{-6}$ | 3.75 $10^{-8}$ | 2.81 $10^{-10}$ | 2.04 $10^{-14}$ | 1.66 $10^{-18}$ | 3.56 $10^{-22}$ | 4.93 $10^{-25}$ | 8.60 $10^{-29}$ | 0 | 0 | 0 |
| $^{169}$Yb | 2.36 $10^{-6}$ | 3.07 $10^{-20}$ | 4.21 $10^{-24}$ | 3.91 $10^{-28}$ | 0 | 0 | 0 | 0 | 0 | 0 | 0 |
| $^{192}$Ir | 1.67 $10^{-5}$ | 1.28 $10^{-11}$ | 3.81 $10^{-19}$ | 2.84 $10^{-22}$ | 2.13 $10^{-25}$ | 1.60 $10^{-28}$ | 0 | 0 | 0 | 0 | 0 |
| $^{226}$Ra | 1.16 $10^{-4}$ | 7.96 $10^{-5}$ | 5.71 $10^{-5}$ | 3.69 $10^{-5}$ | 2.62 $10^{-5}$ | 1.94 $10^{-5}$ | 1.47 $10^{-5}$ | 5.23 $10^{-6}$ | 1.57 $10^{-6}$ | 5.06 $10^{-7}$ | 3.27 $10^{-25}$ |
| $^{235}$U | 1.32 $10^{-5}$ | 8.46 $10^{-6}$ | 5.67 $10^{-6}$ | 3.31 $10^{-6}$ | 2.15 $10^{-6}$ | 1.45 $10^{-6}$ | 1.01 $10^{-6}$ | 2.45 $10^{-7}$ | 5.47 $10^{-8}$ | 1.27 $10^{-8}$ | 1.76 $10^{-8}$ |
| $^{238}$U | 1.62 $10^{-6}$ | 1.04 $10^{-6}$ | 7.10 $10^{-7}$ | 4.34 $10^{-7}$ | 2.98 $10^{-7}$ | 2.13 $10^{-7}$ | 1.58 $10^{-7}$ | 5.15 $10^{-8}$ | 1.48 $10^{-8}$ | 4.70 $10^{-9}$ | 4.53 $10^{-9}$ |
| $^{238}$Pu | 5.98 $10^{-9}$ | 2.37 $10^{-9}$ | 8.23 $10^{-10}$ | 1.78 $10^{-10}$ | 7.58 $10^{-11}$ | 4.08 $10^{-11}$ | 2.34 $10^{-11}$ | 2.35 $10^{-12}$ | 1.73 $10^{-13}$ | 6.37 $10^{-14}$ | 1.05 $10^{-10}$ |
| $^{239}$Pu | 5.06 $10^{-9}$ | 2.69 $10^{-9}$ | 1.51 $10^{-9}$ | 7.61 $10^{-10}$ | 4.84 $10^{-10}$ | 3.28 $10^{-10}$ | 2.29 $10^{-10}$ | 5.88 $10^{-11}$ | 1.32 $10^{-11}$ | 2.41 $10^{-12}$ | 1.11 $10^{-12}$ |
| $^{241}$Pu | 9.52 $10^{-10}$ | 5.35 $10^{-9}$ | 7.70 $10^{-9}$ | 9.30 $10^{-9}$ | 9.70 $10^{-9}$ | 9.75 $10^{-9}$ | 9.67 $10^{-9}$ | 8.97 $10^{-9}$ | 7.65 $10^{-9}$ | 4.74 $10^{-9}$ | 4.30 $10^{-11}$ |
| $^{241}$Am | 1.06 $10^{-6}$ | 5.60 $10^{-7}$ | 3.07 $10^{-7}$ | 1.40 $10^{-7}$ | 7.90 $10^{-8}$ | 4.69 $10^{-8}$ | 2.86 $10^{-8}$ | 3.80 $10^{-9}$ | 4.91 $10^{-10}$ | 9.06 $10^{-11}$ | 9.35 $10^{-11}$ |

1Generic wet soil of 1.5 g $cm^{-3}$ assumed in calculation
2 See Table 1 for radionuclide chains
3 Cut-off value for zero is 1 $10^{-30}$

**TABLE 8 Integrated effective dose rate at 1 m above the ground following a continuous deposit of 1 Bq $m^{-2}$ $s^{-1}$ to undisturbed soil for 1 year[1]**

| | Dose (Sv) | | | | | | | | | | |
|---|---|---|---|---|---|---|---|---|---|---|---|
| Radionuclide[2] | 1 year | 5 years | 10 years | 20 years | 30 years | 40 years | 50 years | 100 years | 200 years | 500 years | $10^5$ years |
| $^{51}$Cr | 1.96 $10^{-3}$ | 2.20 $10^{-3}$ | 2.20 $10^{-3}$ | 2.20 $10^{-3}$ | 2.20 $10^{-3}$ | 2.20 $10^{-3}$ | 2.20 $10^{-3}$ | 2.20 $10^{-3}$ | 2.20 $10^{-3}$ | 2.20 $10^{-3}$ | 2.20 $10^{-3}$ |
| $^{54}$Mn | 2.01 $10^{-1}$ | 5.70 $10^{-1}$ | 5.81 $10^{-1}$ | 5.81 $10^{-1}$ | 5.81 $10^{-1}$ | 5.81 $10^{-1}$ | 5.81 $10^{-1}$ | 5.81 $10^{-1}$ | 5.81 $10^{-1}$ | 5.81 $10^{-1}$ | 5.81 $10^{-1}$ |
| $^{59}$Fe | 1.06 $10^{-1}$ | 1.28 $10^{-1}$ | 1.28 $10^{-1}$ | 1.28 $10^{-1}$ | 1.28 $10^{-1}$ | 1.28 $10^{-1}$ | 1.28 $10^{-1}$ | 1.28 $10^{-1}$ | 1.28 $10^{-1}$ | 1.28 $10^{-1}$ | 1.28 $10^{-1}$ |
| $^{60}$Co | 7.18 $10^{-1}$ | 4.31 $10^{0}$ | 6.06 $10^{0}$ | 7.04 $10^{0}$ | 7.22 $10^{0}$ | 7.26 $10^{0}$ | 7.26 $10^{0}$ | 7.27 $10^{0}$ | 7.27 $10^{0}$ | 7.27 $10^{0}$ | 7.27 $10^{0}$ |
| $^{65}$Zn | 1.29 $10^{-1}$ | 3.16 $10^{-1}$ | 3.18 $10^{-1}$ | 3.18 $10^{-1}$ | 3.18 $10^{-1}$ | 3.18 $10^{-1}$ | 3.18 $10^{-1}$ | 3.18 $10^{-1}$ | 3.18 $10^{-1}$ | 3.18 $10^{-1}$ | 3.18 $10^{-1}$ |
| $^{75}$Se | 6.58 $10^{-2}$ | 1.10 $10^{-1}$ | 1.10 $10^{-1}$ | 1.10 $10^{-1}$ | 1.10 $10^{-1}$ | 1.10 $10^{-1}$ | 1.10 $10^{-1}$ | 1.10 $10^{-1}$ | 1.10 $10^{-1}$ | 1.10 $10^{-1}$ | 1.10 $10^{-1}$ |
| $^{86}$Rb | 4.04 $10^{-3}$ | 4.36 $10^{-3}$ | 4.36 $10^{-3}$ | 4.36 $10^{-3}$ | 4.36 $10^{-3}$ | 4.36 $10^{-3}$ | 4.36 $10^{-3}$ | 4.36 $10^{-3}$ | 4.36 $10^{-3}$ | 4.36 $10^{-3}$ | 4.36 $10^{-3}$ |
| $^{89}$Sr | 8.46 $10^{-6}$ | 1.05 $10^{-5}$ | 1.05 $10^{-5}$ | 1.05 $10^{-5}$ | 1.05 $10^{-5}$ | 1.05 $10^{-5}$ | 1.05 $10^{-5}$ | 1.05 $10^{-5}$ | 1.05 $10^{-5}$ | 1.05 $10^{-5}$ | 1.05 $10^{-5}$ |
| $^{90}$Sr | 1.75 $10^{-8}$ | 1.00 $10^{-7}$ | 1.32 $10^{-7}$ | 1.43 $10^{-7}$ | 1.44 $10^{-7}$ | 1.44 $10^{-7}$ | 1.44 $10^{-7}$ | 1.44 $10^{-7}$ | 1.44 $10^{-7}$ | 1.44 $10^{-7}$ | 1.44 $10^{-7}$ |
| $^{95}$Nb | 5.80 $10^{-2}$ | 6.71 $10^{-2}$ | 6.71 $10^{-2}$ | 6.71 $10^{-2}$ | 6.71 $10^{-2}$ | 6.71 $10^{-2}$ | 6.71 $10^{-2}$ | 6.71 $10^{-2}$ | 6.71 $10^{-2}$ | 6.71 $10^{-2}$ | 6.71 $10^{-2}$ |
| $^{95}$Zr | 1.63 $10^{-1}$ | 2.35 $10^{-1}$ | 2.35 $10^{-1}$ | 2.35 $10^{-1}$ | 2.35 $10^{-1}$ | 2.35 $10^{-1}$ | 2.35 $10^{-1}$ | 2.35 $10^{-1}$ | 2.35 $10^{-1}$ | 2.35 $10^{-1}$ | 2.35 $10^{-1}$ |
| $^{99}$Mo | 1.61 $10^{-3}$ | 1.63 $10^{-3}$ | 1.63 $10^{-3}$ | 1.63 $10^{-3}$ | 1.63 $10^{-3}$ | 1.63 $10^{-3}$ | 1.63 $10^{-3}$ | 1.63 $10^{-3}$ | 1.63 $10^{-3}$ | 1.63 $10^{-3}$ | 1.63 $10^{-3}$ |
| $^{103}$Ru | 3.97 $10^{-2}$ | 4.68 $10^{-2}$ | 4.68 $10^{-2}$ | 4.68 $10^{-2}$ | 4.68 $10^{-2}$ | 4.68 $10^{-2}$ | 4.68 $10^{-2}$ | 4.68 $10^{-2}$ | 4.68 $10^{-2}$ | 4.68 $10^{-2}$ | 4.68 $10^{-2}$ |
| $^{106}$Ru | 5.16 $10^{-2}$ | 1.61 $10^{-1}$ | 1.66 $10^{-1}$ | 1.66 $10^{-1}$ | 1.66 $10^{-1}$ | 1.66 $10^{-1}$ | 1.66 $10^{-1}$ | 1.66 $10^{-1}$ | 1.66 $10^{-1}$ | 1.66 $10^{-1}$ | 1.66 $10^{-1}$ |
| $^{110m}$Ag | 6.19 $10^{-1}$ | 1.54 $10^{0}$ | 1.55 $10^{0}$ | 1.55 $10^{0}$ | 1.55 $10^{0}$ | 1.55 $10^{0}$ | 1.55 $10^{0}$ | 1.55 $10^{0}$ | 1.55 $10^{0}$ | 1.55 $10^{0}$ | 1.55 $10^{0}$ |
| $^{125}$Sb | 1.21 $10^{-1}$ | 6.04 $10^{-1}$ | 7.41 $10^{-1}$ | 7.76 $10^{-1}$ | 7.78 $10^{-1}$ | 7.78 $10^{-1}$ | 7.78 $10^{-1}$ | 7.78 $10^{-1}$ | 7.78 $10^{-1}$ | 7.78 $10^{-1}$ | 7.78 $10^{-1}$ |
| $^{127m}$Te | 1.27 $10^{-3}$ | 2.02 $10^{-3}$ | 2.02 $10^{-3}$ | 2.02 $10^{-3}$ | 2.02 $10^{-3}$ | 2.02 $10^{-3}$ | 2.02 $10^{-3}$ | 2.02 $10^{-3}$ | 2.02 $10^{-3}$ | 2.02 $10^{-3}$ | 2.02 $10^{-3}$ |
| $^{129m}$Te | 3.54 $10^{-3}$ | 3.70 $10^{-3}$ | 3.70 $10^{-3}$ | 3.70 $10^{-3}$ | 3.70 $10^{-3}$ | 3.70 $10^{-3}$ | 3.70 $10^{-3}$ | 3.70 $10^{-3}$ | 3.70 $10^{-3}$ | 3.70 $10^{-3}$ | 3.70 $10^{-3}$ |
| $^{132}$Te | 2.02 $10^{-2}$ | 2.05 $10^{-2}$ | 2.05 $10^{-2}$ | 2.05 $10^{-2}$ | 2.05 $10^{-2}$ | 2.05 $10^{-2}$ | 2.05 $10^{-2}$ | 2.05 $10^{-2}$ | 2.05 $10^{-2}$ | 2.05 $10^{-2}$ | 2.05 $10^{-2}$ |
| $^{129}$I | 2.17 $10^{-3}$ | 1.34 $10^{-2}$ | 1.92 $10^{-2}$ | 2.31 $10^{-2}$ | 2.45 $10^{-2}$ | 2.52 $10^{-2}$ | 2.56 $10^{-2}$ | 2.60 $10^{-2}$ | 2.61 $10^{-2}$ | 2.61 $10^{-2}$ | 2.61 $10^{-2}$ |
| $^{131}$I | 7.57 $10^{-3}$ | 7.82 $10^{-3}$ | 7.82 $10^{-3}$ | 7.82 $10^{-3}$ | 7.82 $10^{-3}$ | 7.82 $10^{-3}$ | 7.82 $10^{-3}$ | 7.82 $10^{-3}$ | 7.82 $10^{-3}$ | 7.82 $10^{-3}$ | 7.82 $10^{-3}$ |
| $^{132}$I | 5.51 $10^{-4}$ | 5.51 $10^{-4}$ | 5.51 $10^{-4}$ | 5.51 $10^{-4}$ | 5.51 $10^{-4}$ | 5.51 $10^{-4}$ | 5.51 $10^{-4}$ | 5.51 $10^{-4}$ | 5.51 $10^{-4}$ | 5.51 $10^{-4}$ | 5.51 $10^{-4}$ |
| $^{133}$I | 1.19 $10^{-3}$ | 1.20 $10^{-3}$ | 1.20 $10^{-3}$ | 1.20 $10^{-3}$ | 1.20 $10^{-3}$ | 1.20 $10^{-3}$ | 1.20 $10^{-3}$ | 1.20 $10^{-3}$ | 1.20 $10^{-3}$ | 1.20 $10^{-3}$ | 1.20 $10^{-3}$ |
| $^{134}$I | 2.40 $10^{-4}$ | 2.41 $10^{-4}$ | 2.41 $10^{-4}$ | 2.41 $10^{-4}$ | 2.41 $10^{-4}$ | 2.41 $10^{-4}$ | 2.41 $10^{-4}$ | 2.41 $10^{-4}$ | 2.41 $10^{-4}$ | 2.41 $10^{-4}$ | 2.41 $10^{-4}$ |
| $^{135}$I | 1.23 $10^{-3}$ | 1.23 $10^{-3}$ | 1.23 $10^{-3}$ | 1.23 $10^{-3}$ | 1.23 $10^{-3}$ | 1.23 $10^{-3}$ | 1.23 $10^{-3}$ | 1.23 $10^{-3}$ | 1.23 $10^{-3}$ | 1.23 $10^{-3}$ | 1.23 $10^{-3}$ |

**TABLE 8 Cont'd Integrated effective dose rate at 1 m above the ground following a continuous deposit of 1 Bq m$^{-2}$ s$^{-1}$ to undisturbed soil for 1 year**

| | Dose (Sv) | | | | | | | | | | |
|---|---|---|---|---|---|---|---|---|---|---|---|
| Radionuclide | 1 year | 5 years | 10 years | 20 years | 30 years | 40 years | 50 years | 100 years | 200 years | 500 years | $10^5$ years |
| $^{134}$Cs | $4.32\ 10^{-1}$ | $1.94\ 10^{0}$ | $2.24\ 10^{0}$ | $2.28\ 10^{0}$ | $2.28\ 10^{0}$ | $2.28\ 10^{0}$ | $2.28\ 10^{0}$ | $2.28\ 10^{0}$ | $2.28\ 10^{0}$ | $2.28\ 10^{0}$ | $2.28\ 10^{0}$ |
| $^{136}$Cs | $6.70\ 10^{-2}$ | $7.06\ 10^{-2}$ | $7.06\ 10^{-2}$ | $7.06\ 10^{-2}$ | $7.06\ 10^{-2}$ | $7.06\ 10^{-2}$ | $7.06\ 10^{-2}$ | $7.06\ 10^{-2}$ | $7.06\ 10^{-2}$ | $7.06\ 10^{-2}$ | $7.06\ 10^{-2}$ |
| $^{137}$Cs | $1.83\ 10^{-1}$ | $1.30\ 10^{0}$ | $2.16\ 10^{0}$ | $3.13\ 10^{0}$ | $3.65\ 10^{0}$ | $3.93\ 10^{0}$ | $4.09\ 10^{0}$ | $4.32\ 10^{0}$ | $4.35\ 10^{0}$ | $4.35\ 10^{0}$ | $4.35\ 10^{0}$ |
| $^{140}$Ba | $7.28\ 10^{-2}$ | $7.72\ 10^{-2}$ | $7.72\ 10^{-2}$ | $7.72\ 10^{-2}$ | $7.72\ 10^{-2}$ | $7.72\ 10^{-2}$ | $7.72\ 10^{-2}$ | $7.72\ 10^{-2}$ | $7.72\ 10^{-2}$ | $7.72\ 10^{-2}$ | $7.72\ 10^{-2}$ |
| $^{140}$La | $9.38\ 10^{-3}$ | $9.44\ 10^{-3}$ | $9.44\ 10^{-3}$ | $9.44\ 10^{-3}$ | $9.44\ 10^{-3}$ | $9.44\ 10^{-3}$ | $9.44\ 10^{-3}$ | $9.44\ 10^{-3}$ | $9.44\ 10^{-3}$ | $9.44\ 10^{-3}$ | $9.44\ 10^{-3}$ |
| $^{144}$Ce | $1.10\ 10^{-2}$ | $2.90\ 10^{-2}$ | $2.93\ 10^{-2}$ | $2.93\ 10^{-2}$ | $2.93\ 10^{-2}$ | $2.93\ 10^{-2}$ | $2.93\ 10^{-2}$ | $2.93\ 10^{-2}$ | $2.93\ 10^{-2}$ | $2.93\ 10^{-2}$ | $2.93\ 10^{-2}$ |
| $^{169}$Yb | $1.81\ 10^{-2}$ | $2.07\ 10^{-2}$ | $2.07\ 10^{-2}$ | $2.07\ 10^{-2}$ | $2.07\ 10^{-2}$ | $2.07\ 10^{-2}$ | $2.07\ 10^{-2}$ | $2.07\ 10^{-2}$ | $2.07\ 10^{-2}$ | $2.07\ 10^{-2}$ | $2.07\ 10^{-2}$ |
| $^{192}$Ir | $1.09\ 10^{-1}$ | $1.50\ 10^{-1}$ | $1.50\ 10^{-1}$ | $1.50\ 10^{-1}$ | $1.50\ 10^{-1}$ | $1.50\ 10^{-1}$ | $1.50\ 10^{-1}$ | $1.50\ 10^{-1}$ | $1.50\ 10^{-1}$ | $1.50\ 10^{-1}$ | $1.50\ 10^{-1}$ |
| $^{226}$Ra | $5.08\ 10^{-1}$ | $3.88\ 10^{0}$ | $6.81\ 10^{0}$ | $1.08\ 10^{1}$ | $1.35\ 10^{1}$ | $1.55\ 10^{1}$ | $1.70\ 10^{1}$ | $2.08\ 10^{1}$ | $2.34\ 10^{1}$ | $2.54\ 10^{1}$ | $3.53\ 10^{1}$ |
| $^{235}$U | $5.92\ 10^{-2}$ | $4.29\ 10^{-1}$ | $7.31\ 10^{-1}$ | $1.11\ 10^{0}$ | $1.34\ 10^{0}$ | $1.50\ 10^{0}$ | $1.60\ 10^{0}$ | $1.83\ 10^{0}$ | $1.93\ 10^{0}$ | $1.99\ 10^{0}$ | $1.53\ 10^{1}$ |
| $^{238}$U | $7.21\ 10^{-3}$ | $5.25\ 10^{-2}$ | $8.99\ 10^{-2}$ | $1.38\ 10^{-1}$ | $1.70\ 10^{-1}$ | $1.92\ 10^{-1}$ | $2.08\ 10^{-1}$ | $2.48\ 10^{-1}$ | $2.72\ 10^{-1}$ | $2.90\ 10^{-1}$ | $4.13\ 10^{0}$ |
| $^{238}$Pu | $2.72\ 10^{-5}$ | $1.63\ 10^{-4}$ | $2.27\ 10^{-4}$ | $2.61\ 10^{-4}$ | $2.71\ 10^{-4}$ | $2.76\ 10^{-4}$ | $2.79\ 10^{-4}$ | $2.83\ 10^{-4}$ | $2.83\ 10^{-4}$ | $2.83\ 10^{-4}$ | $5.32\ 10^{-2}$ |
| $^{239}$Pu | $2.28\ 10^{-5}$ | $1.53\ 10^{-4}$ | $2.40\ 10^{-4}$ | $3.33\ 10^{-4}$ | $3.86\ 10^{-4}$ | $4.21\ 10^{-4}$ | $4.45\ 10^{-4}$ | $4.97\ 10^{-4}$ | $5.22\ 10^{-4}$ | $5.35\ 10^{-4}$ | $1.67\ 10^{-3}$ |
| $^{241}$Pu | $2.98\ 10^{-6}$ | $1.24\ 10^{-4}$ | $4.17\ 10^{-4}$ | $1.18\ 10^{-3}$ | $2.01\ 10^{-3}$ | $2.87\ 10^{-3}$ | $3.72\ 10^{-3}$ | $7.80\ 10^{-3}$ | $1.51\ 10^{-2}$ | $3.11\ 10^{-2}$ | $9.17\ 10^{-2}$ |
| $^{241}$Am | $4.76\ 10^{-3}$ | $3.18\ 10^{-2}$ | $4.99\ 10^{-2}$ | $6.80\ 10^{-2}$ | $7.73\ 10^{-2}$ | $8.27\ 10^{-2}$ | $8.59\ 10^{-2}$ | $9.10\ 10^{-2}$ | $9.22\ 10^{-2}$ | $9.26\ 10^{-2}$ | $1.68\ 10^{-1}$ |

1 Generic wet soil of 1.5 g cm$^{-3}$ assumed in calculation
2 See Table 1 for radionuclide chains

**TABLE 9 Instantaneous effective gamma dose rate at 1 m above of soil and sewage sludge uniformly contaminated at 1 Bq cm$^{-3}$ from the material surface to a series of depths[1]**

| | Dose-rate (Sv h$^{-1}$) | | | | | |
|---|---|---|---|---|---|---|
| | Soil[2] | | | | | Sewage sludge[2] |
| Radionuclide[3] | 1cm | 5cm | 15cm | 30cm | 1 metre | 1 metre |
| $^{55}$Fe | 9.04 10$^{-14}$ | 9.04 10$^{-14}$ | 9.04 10$^{-14}$ | 9.04 10$^{-14}$ | 9.04 10$^{-14}$ | 3.88 10$^{-13}$ |
| $^{60}$Co | 5.64 10$^{-8}$ | 1.72 10$^{-7}$ | 2.90 10$^{-7}$ | 3.45 10$^{-7}$ | 3.65 10$^{-7}$ | 5.49 10$^{-7}$ |
| $^{59}$Ni | 1.28 10$^{-13}$ | 1.28 10$^{-13}$ | 1.28 10$^{-13}$ | 1.28 10$^{-13}$ | 1.28 10$^{-13}$ | 5.52 10$^{-13}$ |
| $^{65}$Zn | 1.32 10$^{-8}$ | 4.01 10$^{-8}$ | 6.70 10$^{-8}$ | 7.87 10$^{-8}$ | 8.26 10$^{-8}$ | 1.25 10$^{-7}$ |
| $^{90}$Sr | 1.38 10$^{-15}$ | 1.39 10$^{-15}$ | 1.39 10$^{-15}$ | 1.39 10$^{-15}$ | 1.39 10$^{-15}$ | 6.70 10$^{-15}$ |
| $^{99}$Mo | 6.20 10$^{-9}$ | 1.77 10$^{-8}$ | 2.68 10$^{-8}$ | 2.95 10$^{-8}$ | 3.01 10$^{-8}$ | 6.17 10$^{-8}$ |
| $^{106}$Ru | 4.81 10$^{-9}$ | 1.43 10$^{-8}$ | 2.29 10$^{-8}$ | 2.60 10$^{-8}$ | 2.67 10$^{-8}$ | 4.31 10$^{-8}$ |
| $^{110m}$Ag | 6.32 10$^{-8}$ | 1.90 10$^{-7}$ | 3.14 10$^{-7}$ | 3.64 10$^{-7}$ | 3.80 10$^{-7}$ | 5.87 10$^{-7}$ |
| $^{137}$Cs | 1.39 10$^{-8}$ | 4.15 10$^{-8}$ | 6.70 10$^{-8}$ | 7.64 10$^{-8}$ | 7.88 10$^{-8}$ | 1.25 10$^{-7}$ |
| $^{144}$Ce | 1.09 10$^{-9}$ | 3.14 10$^{-9}$ | 4.98 10$^{-9}$ | 5.74 10$^{-9}$ | 6.07 10$^{-9}$ | 1.14 10$^{-8}$ |
| $^{210}$Pb | 2.64 10$^{-11}$ | 4.61 10$^{-11}$ | 4.85 10$^{-11}$ | 4.85 10$^{-11}$ | 4.85 10$^{-11}$ | 3.10 10$^{-10}$ |
| $^{210}$Po | 1.97 10$^{-13}$ | 5.91 10$^{-13}$ | 9.67 10$^{-13}$ | 1.12 10$^{-12}$ | 1.16 10$^{-12}$ | 1.80 10$^{-12}$ |
| $^{226}$Ra | 3.94 10$^{-8}$ | 1.19 10$^{-7}$ | 1.98 10$^{-7}$ | 2.33 10$^{-7}$ | 2.47 10$^{-7}$ | 3.84 10$^{-7}$ |
| $^{228}$Ra | 2.20 10$^{-8}$ | 6.62 10$^{-8}$ | 1.09 10$^{-7}$ | 1.26 10$^{-7}$ | 1.32 10$^{-7}$ | 2.07 10$^{-7}$ |
| $^{227}$Ac | 8.86 10$^{-9}$ | 2.52 10$^{-8}$ | 3.78 10$^{-8}$ | 4.11 10$^{-8}$ | 4.17 10$^{-8}$ | 8.62 10$^{-8}$ |
| $^{228}$Th | 7.78 10$^{-8}$ | 2.40 10$^{-7}$ | 4.12 10$^{-7}$ | 5.01 10$^{-7}$ | 5.49 10$^{-7}$ | 8.30 10$^{-7}$ |
| $^{230}$Th | 7.83 10$^{-12}$ | 1.82 10$^{-11}$ | 2.34 10$^{-11}$ | 2.41 10$^{-11}$ | 2.41 10$^{-11}$ | 8.61 10$^{-11}$ |
| $^{232}$Th | 3.89 10$^{-12}$ | 8.19 10$^{-12}$ | 1.00 10$^{-11}$ | 1.03 10$^{-11}$ | 1.03 10$^{-11}$ | 4.14 10$^{-11}$ |
| $^{231}$Pa | 8.35 10$^{-10}$ | 2.38 10$^{-9}$ | 3.59 10$^{-9}$ | 3.92 10$^{-9}$ | 3.96 10$^{-9}$ | 7.79 10$^{-9}$ |
| $^{234}$U | 3.40 10$^{-12}$ | 6.24 10$^{-12}$ | 7.46 10$^{-12}$ | 7.60 10$^{-12}$ | 7.61 10$^{-12}$ | 3.14 10$^{-11}$ |
| $^{235}$U | 3.64 10$^{-9}$ | 1.01 10$^{-8}$ | 1.42 10$^{-8}$ | 1.49 10$^{-8}$ | 1.50 10$^{-8}$ | 3.79 10$^{-8}$ |
| $^{236}$U | 2.23 10$^{-12}$ | 3.48 10$^{-12}$ | 3.94 10$^{-12}$ | 3.99 10$^{-12}$ | 3.99 10$^{-12}$ | 1.82 10$^{-11}$ |
| $^{238}$U | 5.36 10$^{-10}$ | 1.50 10$^{-9}$ | 2.32 10$^{-9}$ | 2.63 10$^{-9}$ | 2.73 10$^{-9}$ | 5.49 10$^{-9}$ |
| $^{237}$Np | 4.98 10$^{-9}$ | 1.40 10$^{-8}$ | 2.07 10$^{-8}$ | 2.23 10$^{-8}$ | 2.26 10$^{-8}$ | 4.92 10$^{-8}$ |
| $^{238}$Pu | 2.14 10$^{-12}$ | 2.57 10$^{-12}$ | 2.71 10$^{-12}$ | 2.72 10$^{-12}$ | 2.72 10$^{-12}$ | 1.32 10$^{-11}$ |
| $^{239}$Pu | 1.75 10$^{-12}$ | 3.54 10$^{-12}$ | 4.73 10$^{-12}$ | 5.02 10$^{-12}$ | 5.06 10$^{-12}$ | 1.46 10$^{-11}$ |
| $^{240}$Pu | 2.22 10$^{-12}$ | 2.91 10$^{-12}$ | 3.25 10$^{-12}$ | 3.35 10$^{-12}$ | 3.38 10$^{-12}$ | 1.45 10$^{-11}$ |
| $^{241}$Pu | 3.31 10$^{-14}$ | 8.47 10$^{-14}$ | 1.10 10$^{-13}$ | 1.13 10$^{-13}$ | 1.13 10$^{-13}$ | 3.84 10$^{-13}$ |
| $^{241}$Am | 3.65 10$^{-10}$ | 7.55 10$^{-10}$ | 8.74 10$^{-10}$ | 8.83 10$^{-10}$ | 8.83 10$^{-10}$ | 4.38 10$^{-9}$ |

1 Generic wet soil density of 1.5 g cm$^{-3}$ and sewage sludge density 1.0 g cm$^{-3}$ assumed
2 Compositions of materials as given in Table 4
3 See Table 1 for radionuclide chains

**TABLE 10 Instantaneous effective dose rate at 1 m above depths of soil and sewage sludge contaminated with mono-energetic photons at 1 photon $cm^{-3}$**

| Photon energy(MeV) | Dose-rate ($Sv\ h^{-1}$)[1] | | | | | |
|---|---|---|---|---|---|---|
| | Soil[2] | | | | | Sewage sludge[2] |
| | 1 cm | 5 cm | 15 cm | 30 cm | 1 metre | 1 metre |
| 0.01 | $5.35\ 10^{-13}$ | $5.35\ 10^{-13}$ | $5.35\ 10^{-13}$ | $5.35\ 10^{-13}$ | $5.35\ 10^{-13}$ | $2.30\ 10^{-12}$ |
| 0.015 | $7.46\ 10^{-12}$ | $7.47\ 10^{-12}$ | $7.47\ 10^{-12}$ | $7.47\ 10^{-12}$ | $7.47\ 10^{-12}$ | $3.50\ 10^{-11}$ |
| 0.02 | $3.45\ 10^{-11}$ | $3.50\ 10^{-11}$ | $3.50\ 10^{-11}$ | $3.50\ 10^{-11}$ | $3.50\ 10^{-11}$ | $1.72\ 10^{-10}$ |
| 0.03 | $1.78\ 10^{-10}$ | $2.13\ 10^{-10}$ | $2.13\ 10^{-10}$ | $2.13\ 10^{-10}$ | $2.13\ 10^{-10}$ | $1.22\ 10^{-9}$ |
| 0.05 | $7.23\ 10^{-10}$ | $1.31\ 10^{-9}$ | $1.38\ 10^{-9}$ | $1.38\ 10^{-9}$ | $1.38\ 10^{-9}$ | $8.90\ 10^{-9}$ |
| 0.1 | $2.06\ 10^{-9}$ | $5.27\ 10^{-9}$ | $6.70\ 10^{-9}$ | $6.82\ 10^{-9}$ | $6.83\ 10^{-9}$ | $2.51\ 10^{-8}$ |
| 0.2 | $4.58\ 10^{-9}$ | $1.30\ 10^{-8}$ | $1.89\ 10^{-8}$ | $1.99\ 10^{-8}$ | $2.00\ 10^{-8}$ | $4.57\ 10^{-8}$ |
| 0.5 | $1.19\ 10^{-8}$ | $3.51\ 10^{-8}$ | $5.54\ 10^{-8}$ | $6.18\ 10^{-8}$ | $6.29\ 10^{-8}$ | $1.05\ 10^{-7}$ |
| 1 | $2.30\ 10^{-8}$ | $6.92\ 10^{-8}$ | $1.15\ 10^{-7}$ | $1.34\ 10^{-7}$ | $1.39\ 10^{-7}$ | $2.12\ 10^{-7}$ |
| 1.5 | $3.33\ 10^{-8}$ | $1.02\ 10^{-7}$ | $1.75\ 10^{-7}$ | $2.11\ 10^{-7}$ | $2.25\ 10^{-7}$ | $3.36\ 10^{-7}$ |
| 2 | $4.23\ 10^{-8}$ | $1.31\ 10^{-7}$ | $2.28\ 10^{-7}$ | $2.79\ 10^{-7}$ | $3.04\ 10^{-7}$ | $4.42\ 10^{-7}$ |
| 4 | $7.46\ 10^{-8}$ | $2.39\ 10^{-7}$ | $4.35\ 10^{-7}$ | $5.58\ 10^{-7}$ | $6.46\ 10^{-7}$ | $9.40\ 10^{-7}$ |

1 Care should be taken below 0.1 MeV, see Section 4.
2 Generic wet soil density of 1.5 g $cm^{-3}$ and sewage sludge density 1.0 g $cm^{-3}$ assumed. Compositions of materials as given in Table 4.

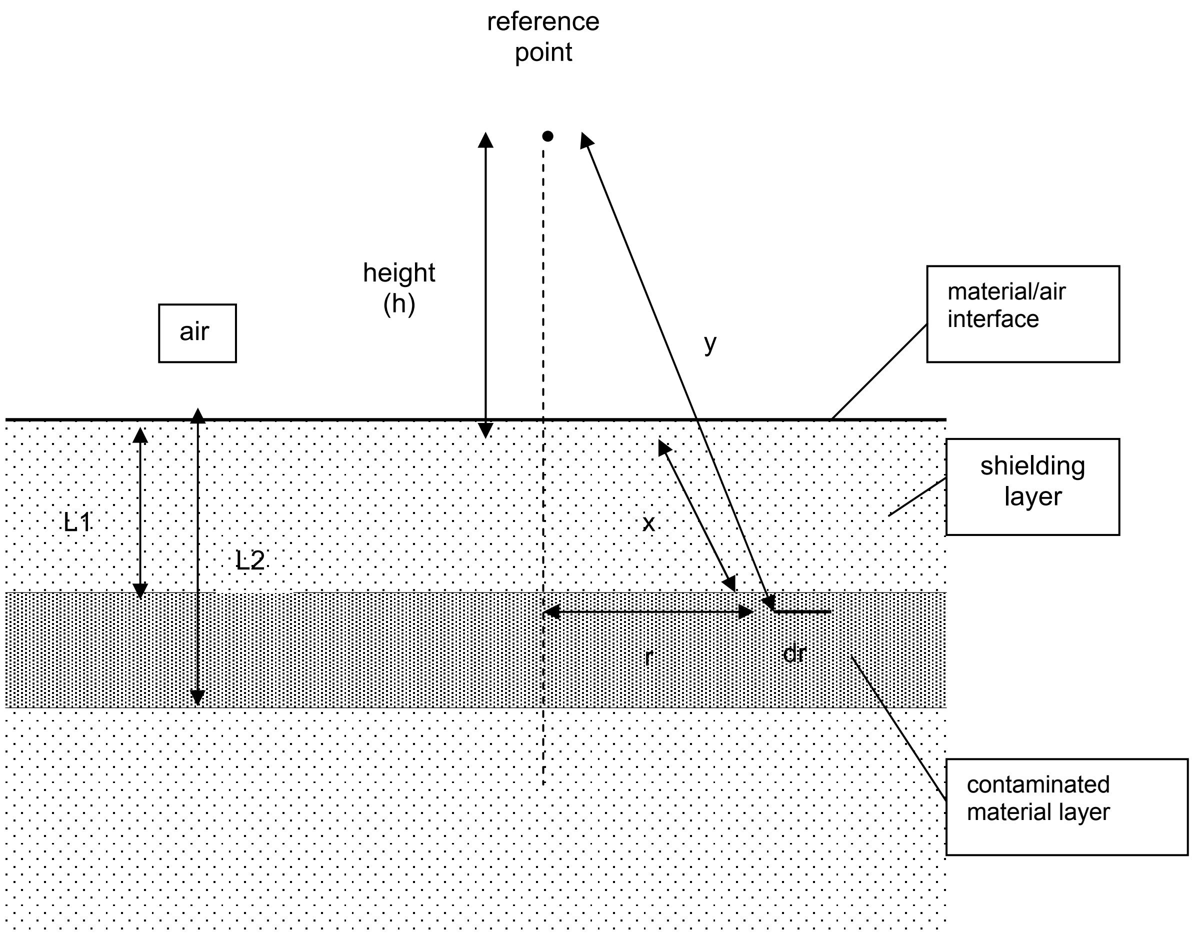


**FIGURE 1 Schematic diagram for calculation of external irradiation by photons from radionuclides distributed in soil or material of infinite lateral extent**

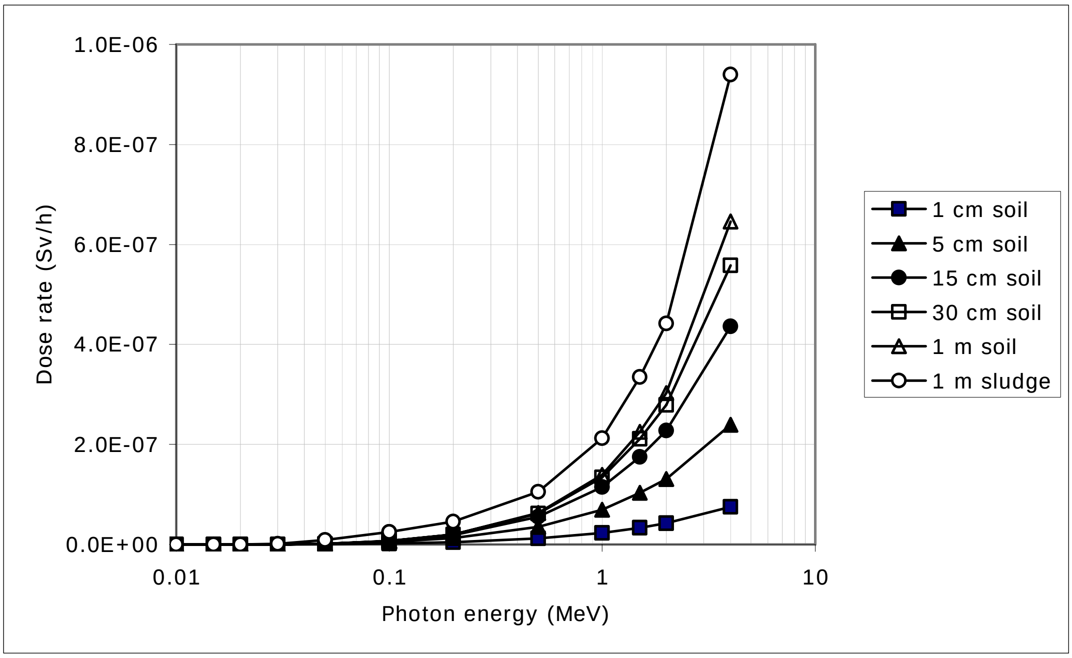


**FIGURE 2 Instantaneous effective dose rate at 1 m above depths of soil and sewage sludge contaminated with mono-energetic photons at 1 Bq cm$^{-3}$**

# APPENDIX A INTERCOMPARISON OF GRANIS V3 WITH OTHER MODELS

## A1 Comparison with analytical solutions

### A1.1 Dose at surface of semi infinite medium

For the case of an absorbing source of infinite volume and uniform activity distribution, the energy absorbed per unit volume equals the energy emitted per unit volume, i.e. a spatial equilibrium condition exists. The absorbed dose per unit volumetric activity can be simply calculated using the following equation:

$$D_{inf} = \frac{kE}{\rho}$$

where $D_{inf}$ = absorbed dose rate within an infinite medium (Gy $h^{-1}$ per Bq $m^{-3}$)

E = photon energy (MeV)

ρ = density of medium (g $cm^{-3}$)

k = units conversion factor

= $5.76\ 10^{-13}$ (Gy $h^{-1}$ g $cm^{-3}$ $MeV^{-1}$ per Bq $m^{-3}$)

The dose rate in a position where the activity concentration is uniform over half of the area around (e.g., on the surface of ground contaminated to a great depth, or on the ground when the air is contaminated) is one half of the value given above.

Figures A1 and A2 and Table A1 show the comparison of the theoretical (absorbed) dose at the surface of a semi infinite medium and the equivalent GRANIS v3 result.

Figure A1 shows that between the energy range, 0.05 to 4 MeV, GRANIS v3 agrees with the theoretical result within 5%. Below 0.05 MeV at worst, GRANIS v3 produces smaller results than theory by up to 30%. Figure A2 shows the two dose rate versus energy curves.

### A1.2 Dose from infinite slabs of finite thickness

Jaeger et al (1968) describe methods for the integration of point kernels from sources and shields of a variety of geometries, to calculate the flux from photon sources. The case appropriate for comparison with GRANIS v3 is the point kernel integration of an infinite uniform slab source with a parallel shield.

Figures A3 and A4 and Table A2 show the comparison of the results of GRANIS v3 with that of analytical calculations of dose at a height of 1 metre above slabs of finite thickness and infinite lateral extent over an energy range of 0.01 to 4 MeV. As shown, this particular analytical model gives smaller results than GRANIS v3 by up to a factor of two.

Although both of the calculations undertaken in this comparison have considered the same library data, i.e. attenuation coefficients, build-up factors and fluence to dose conversion coefficients, the discrepancy between these two models comes from the different use of build-up factors within the calculation of flux. The build-up library used in both these analyses is one directly applicable to the calculation of build-up from effectively a point source (or kernel). The GRANIS v3 calculational methodology considers the application of the build-up factor for a point kernel within a plane of activity prior to the integration of the fluence over an infinite plane, and a layer in which the plane is situated. The analytical model in Jaeger et al (1968) however, integrates the fluence then considers a single build-up factor for such a slab, i.e. it assumes that for a single slab the build-up from the kernels of which it is made are the same. This naturally results in inaccuracies, as the penetration path of the primary radiation through the source and shield are always longer for extended sources than the penetration path of the normal incident radiation from a single point source. The longer the penetration path length, the larger the build-up factor. Based on this, it would be expected that the analytical method described in Jaeger et al (1968) would produce smaller results than those calculated using GRANIS v3; this has been observed in Figures A3 and A4.

## A2 Comparison with other codes and publications

### A2.1 Comparison with the work of Chen

A Monte Carlo method has been developed by Chen (1991) and used to calculate dose above soil slabs of finite thickness but infinite lateral extent. Effective dose rate results at a height of 1 metre are presented for soil slabs, whose thickness is defined in terms of the number of mean free paths (mfp) from the ground surface to the base of the soil slab.

Figures A5 and A6 and Table A3 show the comparison of the results of GRANIS v3 with the results of Chen. The physical size of the soil slab thicknesses T (mfp) modelled in GRANIS v3 are those appropriate to the attenuation coefficients $\mu_s$ calculated from the GRANIS v3 attenuation coefficient library, these are converted into mfp to be equivalent to the physical dimension defined by Chen. Soil thicknesses are given by

$$T = \frac{1}{\left(\mu_s / \rho_s\right)} (mfp)$$

Where

$(\mu_s/\rho_s)$= mass attenuation coefficient of soil ($m^2\ kg^{-1}$) for photons

$\rho_s$ is the density of soil ($kg\ m^{-3}$).

$\mu_s$ is the linear attenuation coefficient for the photons in soil ($m^{-1}$).

The physical model used by Chen modelled both a considerable volume of soil (up to 5 mfp) below the source slab and a considerable volume of air (500 m) above the dose point, to enable photon back-scatter to be modelled.

The comparison shows that at worst (0.1 MeV and below) GRANIS v3 calculates smaller values than the results of Chen by up to 20%. Above 0.1 MeV there is good agreement between the two methods up to an energy of 4 MeV. This comparison is further discussed in Section A2.4.

### A2.2 Comparison with the computer code EGS4

Figures A7 and A8 and Table A4 show the comparison of the Monte Carlo code EGS4 (Bielajew et al, 1994) with the results of GRANIS v3 for 3 soil slab thicknesses of infinite lateral extent. The soil slabs modelled in this comparison extend from the soil surface to depths of 1, 5 and 30 cm. Dose rate is measured at a height of 1 metre above the soil surface. The EGS4 code has not been used to model back-scatter from soil below the source or from the air above the point of interest. It is expected that without back-scatter the EGS4 results should be lower than the GRANIS v3 results, which include an allowance for back-scatter through the use of build-up factors.

The results of GRANIS v3 show good agreement with EGS4 for energies in the range 0.1 to 4 MeV (within 15%). At 0.1 MeV and below, the GRANIS v3 results are smaller than EGS4 results by up to about 40%. The comparison of EGS4 and GRANIS v3 is discussed further in Section A2.4.

### A2.3 Comparison with the computer code MCNP-4

The Monte Carlo code MCNP-4 (Whalen et al, 1993) has been used to examine soil slab sources extending as the EGS4 comparison in Section A2.2, from the soil/air interface to depths of 1, 5 and 30 cm. Similarly to the EGS4 comparison, the Monte Carlo code was not used to model back-scatter.

Figures A7 and A8 and Table A5 show the results of a comparison made between the results of GRANIS v3, and those calculated using MCNP-4. At photon energies of 0.01 to 4 MeV, GRANIS v3 produces larger results than MCNP-4 by up to 30%. Below 0.05 MeV, GRANIS produces smaller results than MCNP-4, the discrepancy between the two methods in this energy region is up to about 25%.

In the energy region between 0.1 and 1.0 MeV, the discrepancy between GRANIS v3 and MCNP-4 is up to 30%. For energies in the range 1 to 4 MeV the agreement between GRANIS v3 and MCNP-4 is within 20%. Below 0.1 MeV, the discrepancies are up to 30%. Further discussion on the comparison of MCNP-4 and GRANIS v3 is provided in Section A2.4.

### A2.4 Summary of comparison of Monte Carlo soil slab results with GRANIS v3

Three Monte Carlo codes have been studied and compared with GRANIS v3: a code written by Chen (1991), and two more widely used codes EGS4 (Bielajew et al, 1994) and MCNP-4 (Whalen et al, 1993). This section describes the intercomparison of all these codes, using soil depths in terms of mean free paths (mfp) as previously discussed in Section A2.1.

Figures A9 and A10 and Table A6 show the comparison of GRANIS v3 with Chen, EGS4 and MCNP-4 for a soil depth equivalent to 5 mfp. The physical dimensions of 5 mfp modelled by each code have been based on the data library accompanying each code. The approximate size of soil depths corresponding to 5 mfp is also shown in Figure A9; the approximation is indicative of the differences in the physical size of the soil slabs modelled in each code.

Figures A9 and A10 show the ratio of Monte Carlo codes to GRANIS v3 for a range of calculated results for the dose rate above infinite soil slabs. It can be seen in Figure A9 that comparisons based on the use of mfp soil depths follow the same trends as those previously discussed in terms of soil slabs modelled with the same physical dimensions.

MCNP-4, for energies in the range 0.05 to 4 MeV, calculates results less than all other codes tested. Chen, EGS4 and MCNP-4, at energies less than 0.05 MeV, calculate doses greater than GRANIS v3. This therefore indicates a consistent order in the size of calculated dose produced by these Monte Carlo codes and GRANIS v3, as shown in Table A7.

### A2.5 Comparison with MICROSHIELD

GRANIS v3 was compared with MICROSHIELD (Negin, 1986), a widely used commercial code that analyses the shielding and estimates the exposure from gamma radiation using the point kernel method and Gaussian quadrature numerical integration. MICROSHIELD allows up to 16 different source geometries.

A rectangular slab geometry with a lateral extent of 1000 m was chosen for the purposes of this comparison. Slab (soil) thicknesses of 1, 5 and 30 cm were considered with a dose reference point 1 m above the contaminated soil surface. It is not possible to compare GRANIS v3 and MICROSHIELD directly for multi-energetic radionuclides over a range of photon energies. Therefore, eight radionuclides $^{30}$P, $^{40}$K, $^{66}$Cu, $^{81m}$Kr, $^{103m}$Rh, $^{131}$Cs, $^{155}$Sm and $^{156m1}$Tb (here the ‘m1’ denotes the most stable meta state of Tb) were considered to provide comparison at a range of mono-energetic photons of 0.02 to 1.5 MeV. A second comparison was carried out for a plane source of thickness 1 cm at dose reference heights 0.1, 1, 10 and 100 metres. These tests were carried out using the ICRP Publication 38 radionuclide library within MICROSHIELD.

The results of this comparison for soil thickness up to 30 cm are shown in Figures A11 and A12 and Table A8. The comparison shows that between 0.02 MeV and 1.5 MeV, the results between the two models compare well except for the 30 cm thickness values between 0.1 MeV and 0.2 MeV.

Figures A13 and A14 and Table A9 illustrate the comparison of dose rates for the two codes for the same set of radionuclides at heights of 0.1, 1.0, 10.0 and 100 metres above the soil-air boundary. For heights of 0.1, 1.0 and 10 metres the two models compare well between 0.02 MeV and 1.5 MeV. For the 100 metre height there is a large difference between the models at around 0.05 MeV. Beyond 0.1 MeV the ratio of the two models is within a factor of two for all heights.

## A2.6 Comparison with Eckerman and Ryman

The work of Eckerman and Ryman on exposure to external radiation above contaminated land has been published as US EPA Federal Guidance No 12 (1993), and exists as a PC database for a large number of radionuclides. The method used by Eckerman and Ryman consisted of a two-stage process, utilising two radiation transport techniques. In the case of their calculations for soil slabs, the flux at a cylindrical surface, located at the soil surface was calculated using a discrete ordinates solution of the Boltzmann transport equation. The corresponding organ and thus effective doses were assessed by Monte Carlo analysis of an anthropomorphic phantom centred within a cylindrical surface matching the boundaries of the surface used in the discrete ordinates stage. The flux from the discrete ordinates calculation was used as input (in terms of photon energy and angular distribution) to the Monte Carlo calculation. The effective dose produced by this methodology is within a few percent of the dose using ICRP Publication 60 weighting factors (ICRP, 1991) for many radionuclides.

Figures A15 and A16 and Table A10 show the comparison of Eckerman to GRANIS v3 for 5 radionuclides ($^{60}$Co, $^{137+}$Cs, $^{235}$U, $^{226}$Ra and $^{210}$Pb) which uniformly contaminate a set of 4 soil slabs of infinite lateral extent, with the following dimensions - surface to 1 cm, to 5 cm, to 15 cm and infinite depth. The dose rates are plotted at the mean energy per disintegration for each radionuclide. This comparison illustrates that GRANIS v3 again produces results for soil slabs which are similar to those provided by other calculation methods.

## A2.7 Use of GRANIS v3 for the calculation of dose at varying heights above the ground

Saito and Jacob (1995) have used a Monte Carlo code, YURI, to calculate the air kerma associated with infinite plane sources located at various depths in soil, and the variation of air kerma with height above the ground. GRANIS v3 is not capable of modelling a plane source directly, the plane sources have been considered through the use of an extremely thin source layer (0.1 mm). The initial calculations of GRANIS v3 have used the code's concrete build-up library, appropriate for representing build-up effects in soil.

Figures A17 and A18 and Table A11 show the comparisons of the results of Saito and Jacob, with those calculated using GRANIS v3. Figures A17 and A18 and Table A11 illustrate the comparison of air kerma for a plane source at a depth of 1 g cm$^{-2}$, for heights of 0.1, 1.0, 10.0 and 100 metres above the soil-air boundary. Figure A19 and Table A12 show the variation of air kerma with height as calculated by Saito and Jacob and GRANIS v3 for mono-energetic photons of 0.1 and 1.0 MeV, again for a plane source at a depth of 1 g cm$^{-2}$. For soil of 1.8 g cm$^{-3}$, a depth of 1 g cm$^{-2}$ is equivalent to a depth of approximately 6 mm.

Figures A17 and A18 show that for air kerma calculations at a height of 0.1 m, 1.0 m and 10 m, there is good agreement between the two methods in the energy range 0.2 to 2 MeV. Below 0.2 MeV the results of GRANIS v3 are smaller than those of Saito and Jacob, by margins in excess of 30%, a margin that extends considerably at larger heights above the ground surface.

GRANIS v3 has been shown to underestimate dose rate at height, compared with the results of the Monte Carlo calculations of Saito and Jacob, particularly for low energy photons. These under estimations are as a result of the GRANIS v3 treatment of build-up. An indication of the effects of the build-up problem can be investigated through the use of an alternative build-up library. GRANIS v3 does not use an air build-up library specifically, the build-up in air is considered by the application of a single material build-up library to the attenuation lengths in the shield material above the source plane and the attenuation length in air. Build-up is generally higher for low atomic number materials and in the 100 m dose point case the majority of the attenuation length from the plane to the dose point occurs within the air, where naturally most of the build-up will occur. As stated, in the initial comparisons of the results of GRANIS v3 and the work of Saito and Jacob, the concrete build-up library in GRANIS v3 has been used. The concrete build-up library gives a good approximation to the build-up effects of soil, concrete having a similar average atomic number to soil (average atomic numbers, soil = 10.9, concrete = 11.3). However, Figure A17 and Table A11 also show the comparison of the GRANIS v3 results for the 100 m dose point case using the air build-up library in place of the concrete data and the comparison with the Saito and Jacob results is much better.

This comparison suggests that GRANIS v3 is an acceptable method for calculating dose, up to height of 10 metres, for photon energies in the range 0.2 to 2 MeV. For photon energies below 0.2 MeV, doses calculated for heights up to 10 m must be treated with some caution. GRANIS v3 has been shown to underestimate dose, but is within 60% of this particular Monte Carlo method if an appropriate build-up factor is used. For heights above the ground greater than 10 metres, it is important to choose the most appropriate build-up library, e.g. the air build-up library in GRANIS v3 should be selected when the majority of the photon attenuation occurs in air.

### A2.8 Use of GRANIS v3 for shielding calculations

GRANIS v3 is capable of assessing dose in a situation where contaminated soil is shielded by another material, for example where a factory floor or a car park has been built on a contaminated site. To examine the performance of GRANIS v3 in this situation the transmission fraction calculated using GRANIS v3 has been compared with those calculated using the Monte Carlo computer code MCNP-4 (Whalen et al, 1993).

The transmission fraction is the ratio of the dose rate due to the presence of a specific thickness of shielding, to the dose rate from the un-shielded situation. The results of this comparison for concrete thickness up to 30 cm are shown in Figure A20 and Table A13, for $^{60}$Co. These results show good agreement between GRANIS v3 and MCNP-4 for $^{60}$Co contamination shielded by concrete.

## A3 Comparison with predictions of other HPA-RPD codes

### A3.1 GRANIS v3 vs BOXDOSE

Calculations of dose from contaminated soil slabs of infinite lateral extent have been calculated previously within the Environmental Assessments Department, using the computer code BOXDOSE (Charles et al, 1982). GRANIS v3 has been developed as an update and improvement to BOXDOSE. The GRANIS v3 methodology is based largely on that of BOXDOSE, its theoretical methodology was accepted as providing a method of calculating dose from contaminated material layers. The developments made in GRANIS v3 have occurred in the revision of library data and improvements within the integration routines, areas that were the cause of discrepancies between BOXDOSE and similar codes. GRANIS v3 also allows multiple media above the contaminated layer in soil, can calculate dose at different heights above the soil, and allows clean soil above the contaminated layers.

Figures A21 and A22 and Table A14 show the comparison of the results of GRANIS v3 to those of BOXDOSE for different thicknesses and depths of contaminated soil. The comparison illustrates that there is very little difference between the two codes for energies in the range 0.5 to 4 MeV. Between 0.03 and 0.5 MeV, GRANIS v3 gives results up to 2.5 times smaller than BOXDOSE, due to changes in library data (particularly build-up data). Below 0.03 MeV, GRANIS v3 generally gives results much greater than BOXDOSE, due to the manner in which the fluence contribution from each calculational material layer was calculated.

To illustrate the comparison of GRANIS v3 with BOXDOSE further, BOXDOSE has been tested using the data libraries created for GRANIS. Figures A23 and A24 and Table A15 show the results of this comparison, it can be seen that the results provided by the two codes are effectively the same for photon energies in the range 0.1 to 4 MeV. The detachment of the results of the two codes below this energy illustrates the effects of modification to the calculational algorithm in GRANIS v3, through the use of thin material layers as described above.

## A4 Conclusions of GRANIS v3 intercomparison

GRANIS v3 has been compared with analytical methods, a number of computer codes and published results for the calculation of dose from contaminated slabs of material of infinite lateral extent of a variety of thicknesses. The GRANIS v3 results for soil slabs are within the range of results produced by the Monte Carlo and discrete ordinates methods of calculation. Best agreement with other calculational methods has been observed for energies in the range 0.1 to 4 MeV, but below this energy discrepancies are generally within 40%.

GRANIS v3 has been shown to accurately predict the effects of shielding materials above contaminated materials, and is thus appropriate for use in the calculation of dose for scenarios where contaminated land has been re-developed as a car-park or factory and tarmac or concrete provide radiation shielding.

GRANIS v3 has also been shown to be acceptable for the assessment of the variation of dose above the ground, up to a height of 10 metres, particularly at photon energies in the range of 0.2 to 2 MeV. However, for heights above 10 m, care needs to be taken in the choice of appropriate build-up factors.

## A5 References

Bielajew AF, Hirayama H, Nelson WR and Rogers DWO (1994). History, overview and recent improvements of EGS4. National Research Council of Canada, Report NRC-PIRS-0436.

Charles D, Crick MJ, Fell TP and Greenhalgh JR (1982). *DOSE-MARC: The dosimetric module in the methodology for assessing the radiological consequences of accidental releases*. Chilton NRPB-M74.

Chen SY (1991). Calculation of effective dose equivalent responses for external exposure from residual photon emitters in soil. *Health Phys*, **60**(3), 411-426.

Eckerman KF and Ryman JC (1993). External exposure to radionuclides in air, water and soil. Federal Guidance Report No 12, US Environmental Protection Agency, EPA 402-R-93-081.

ICRP (1991). 1990 recommendations of the International Commission on Radiological Protection. ICRP Publication 60. *Ann ICRP*, **21**(1/3).

Jaeger RG et al (Eds) (1968). Engineering compendium on radiation shielding, Volume 1, Shielding fundamentals and methods. Springer-Verlag.

Negin CA (1986). MICROSHIELD - A Microcomputer Program for Analysing Dose Rate and Gamma Shielding. CONF-861102, ISSN 0003-018X CODEN TANSA. *Trans Am Nucl Soc*, **53**, 421-422.

Saito K and Jacob P (1995). Gamma ray fields in air due to sources in the ground. *Rad Prot Dosim*, **58**(1), 29-45.

Whalen DJ, Cardon DA, Uhle JL and Hendricks JS (1993). MCNP: neutron benchmark problems. LA-12212.

## A6 Tables and figures

**Table A1 Dose rate for theoretical semi infinite source and GRANIS v3**

| MeV | Theoretical semi infinite source (Gy $h^{-1}$ per Bq $m^{-3}$) | GRANIS v3 semi infinite[1] (Gy $h^{-1}$ per Bq $m^{-3}$) | Ratio semi inf/GRANIS v3 |
|---|---|---|---|
| 0.01 | $2.23\ 10^{-12}$ | $1.72\ 10^{-12}$ | 1.30 |
| 0.015 | $3.34\ 10^{-12}$ | $2.85\ 10^{-12}$ | 1.17 |
| 0.02 | $4.45\ 10^{-12}$ | $3.79\ 10^{-12}$ | 1.17 |
| 0.03 | $6.68\ 10^{-12}$ | $5.77\ 10^{-12}$ | 1.11 |
| 0.05 | $1.11\ 10^{-11}$ | $1.18\ 10^{-11}$ | 0.94 |
| 0.1 | $2.23\ 10^{-11}$ | $2.29\ 10^{-11}$ | 0.98 |
| 0.2 | $4.45\ 10^{-11}$ | $4.68\ 10^{-11}$ | 0.95 |
| 0.5 | $1.11\ 10^{-10}$ | $1.13\ 10^{-10}$ | 0.98 |
| 1 | $2.23\ 10^{-10}$ | $2.24\ 10^{-10}$ | 1.00 |
| 1.5 | $3.34\ 10^{-10}$ | $3.44\ 10^{-10}$ | 0.97 |
| 2 | $4.45\ 10^{-10}$ | $4.42\ 10^{-10}$ | 1.01 |
| 4 | $8.91\ 10^{-10}$ | $9.02\ 10^{-10}$ | 0.99 |

1 Semi infinite GRANIS v3 model consists of 5000 m of air (density of air = $1.29\ 10^{-3}$ g $cm^{-3}$), dose point at 0.1 m in air above semi infinite source.

**Table A2 Variation of dose rate at a height of 1 metre from Jaeger et al and GRANIS v3 with soil slab thickness**

| MeV | Jaeger (Sv $h^{-1}$ per Bq $m^{-3}$) | | | GRANIS v3 (Sv $h^{-1}$ per Bq $m^{-3}$) | | | Ratio Jaeger/GRANIS v3 | | |
|---|---|---|---|---|---|---|---|---|---|
| | 0.01 m | 0.05 m | 0.3 m | 0.01 m | 0.05 m | 0.3 m | 0.01 m | 0.05 m | 0.3 m |
| 0.01 | $4.52\ 10^{-19}$ | $4.52\ 10^{-19}$ | $4.52\ 10^{-19}$ | $4.50\ 10^{-19}$ | $4.50\ 10^{-19}$ | $4.50\ 10^{-19}$ | 1.00 | 1.00 | 1.00 |
| 0.015 | $7.74\ 10^{-18}$ | $7.74\ 10^{-18}$ | $7.74\ 10^{-18}$ | $7.92\ 10^{-18}$ | $7.92\ 10^{-18}$ | $7.92\ 10^{-18}$ | 0.98 | 0.98 | 0.98 |
| 0.02 | $3.46\ 10^{-17}$ | $3.47\ 10^{-17}$ | $3.47\ 10^{-17}$ | $3.58\ 10^{-17}$ | $3.59\ 10^{-17}$ | $3.59\ 10^{-17}$ | 0.97 | 0.97 | 0.97 |
| 0.03 | $1.6\ 10^{-16}$ | $1.8\ 10^{-16}$ | $1.8\ 10^{-16}$ | $1.73\ 10^{-16}$ | $1.92\ 10^{-16}$ | $1.92\ 10^{-16}$ | 0.93 | 0.94 | 0.94 |
| 0.05 | $4.39\ 10^{-16}$ | $7.4\ 10^{-16}$ | $7.66\ 10^{-16}$ | $6.77\ 10^{-16}$ | $1.11\ 10^{-15}$ | $1.14\ 10^{-15}$ | 0.65 | 0.67 | 0.67 |
| 0.1 | $9.9\ 10^{-16}$ | $2.24\ 10^{-15}$ | $2.83\ 10^{-15}$ | $1.96\ 10^{-15}$ | $4.73\ 10^{-15}$ | $5.75\ 10^{-15}$ | 0.51 | 0.47 | 0.49 |
| 0.2 | $2.32\ 10^{-15}$ | $5.47\ 10^{-15}$ | $7.74\ 10^{-15}$ | $4.4\ 10^{-15}$ | $1.2\ 10^{-14}$ | $1.7\ 10^{-14}$ | 0.53 | 0.46 | 0.46 |
| 0.5 | $7.38\ 10^{-15}$ | $1.82\ 10^{-14}$ | $2.82\ 10^{-14}$ | $1.16\ 10^{-14}$ | $3.31\ 10^{-14}$ | $5.46\ 10^{-14}$ | 0.64 | 0.55 | 0.52 |
| 1 | $1.59\ 10^{-14}$ | $4.1\ 10^{-14}$ | $6.8\ 10^{-14}$ | $2.24\ 10^{-14}$ | $6.53\ 10^{-14}$ | $1.20\ 10^{-13}$ | 0.71 | 0.63 | 0.57 |
| 1.5 | $2.43\ 10^{-14}$ | $6.57\ 10^{-14}$ | $1.18\ 10^{-13}$ | $3.22\ 10^{-14}$ | $9.61\ 10^{-14}$ | $1.92\ 10^{-13}$ | 0.76 | 0.68 | 0.61 |
| 2 | $3.22\ 10^{-14}$ | $8.91\ 10^{-14}$ | $1.67\ 10^{-13}$ | $4.08\ 10^{-14}$ | $1.23\ 10^{-13}$ | $2.59\ 10^{-13}$ | 0.79 | 0.72 | 0.65 |
| 4 | $5.98\ 10^{-14}$ | $1.73\ 10^{-13}$ | $3.5\ 10^{-13}$ | $7.20\ 10^{-14}$ | $2.24\ 10^{-13}$ | $4.92\ 10^{-13}$ | 0.83 | 0.77 | 0.71 |

**Table A3 Variation of dose rate at a height of 1 metre for Chen and GRANIS v3 with mean free path**

| MeV | Chen results (Sv $h^{-1}$ per Bq $m^{-3}$) | | | GRANIS v3 (Sv $h^{-1}$ per Bq $m^{-3}$) | | | Ratio Chen/GRANIS v3 | | |
|---|---|---|---|---|---|---|---|---|---|
| | 0.1 mfp | 1.0 mfp | 5.0 mfp | 0.1 mfp | 1.0 mfp | 5.0 mfp | 0.1 mfp | 1.0 mfp | 5.0 mfp |
| 0.01 | $7.30\ 10^{-20}$ | $3.95\ 10^{-19}$ | $4.87\ 10^{-19}$ | $6.94\ 10^{-20}$ | $3.59\ 10^{-19}$ | $4.67\ 10^{-19}$ | 1.05 | 1.10 | 1.04 |
| 0.015 | $1.56\ 10^{-18}$ | $6.93\ 10^{-18}$ | $8.52\ 10^{-18}$ | $1.45\ 10^{-18}$ | $6.40\ 10^{-18}$ | $7.95\ 10^{-18}$ | 1.08 | 1.08 | 1.07 |
| 0.02 | $8.65\ 10^{-18}$ | $3.18\ 10^{-17}$ | $3.93\ 10^{-17}$ | $7.29\ 10^{-18}$ | $2.94\ 10^{-17}$ | $3.59\ 10^{-17}$ | 1.19 | 1.08 | 1.09 |
| 0.03 | $4.86\ 10^{-17}$ | $1.87\ 10^{-16}$ | $2.30\ 10^{-16}$ | $4.37\ 10^{-17}$ | $1.65\ 10^{-16}$ | $2.02\ 10^{-16}$ | 1.11 | 1.13 | 1.14 |
| 0.05 | $2.94\ 10^{-16}$ | $1.11\ 10^{-15}$ | $1.45\ 10^{-15}$ | $2.71\ 10^{-16}$ | $1.13\ 10^{-15}$ | $1.45\ 10^{-15}$ | 1.09 | 0.98 | 1.00 |
| 0.1 | $1.64\ 10^{-15}$ | $7.26\ 10^{-15}$ | $1.07\ 10^{-14}$ | $1.39\ 10^{-15}$ | $6.67\ 10^{-15}$ | $9.54\ 10^{-15}$ | 1.18 | 1.09 | 1.12 |
| 0.2 | $4.53\ 10^{-15}$ | $2.21\ 10^{-14}$ | $3.32\ 10^{-14}$ | $4.15\ 10^{-15}$ | $2.03\ 10^{-14}$ | $3.05\ 10^{-14}$ | 1.09 | 1.09 | 1.09 |
| 0.5 | $1.59\ 10^{-14}$ | $6.90\ 10^{-14}$ | $1.02\ 10^{-13}$ | $1.48\ 10^{-14}$ | $6.78\ 10^{-14}$ | $9.93\ 10^{-14}$ | 1.07 | 1.02 | 1.03 |
| 1 | $3.61\ 10^{-14}$ | $1.61\ 10^{-13}$ | $2.19\ 10^{-13}$ | $3.66\ 10^{-14}$ | $1.57\ 10^{-13}$ | $2.20\ 10^{-13}$ | 0.99 | 1.03 | 1.00 |
| 1.5 | $6.22\ 10^{-14}$ | $2.44\ 10^{-13}$ | $2.30\ 10^{-13}$ | $6.17\ 10^{-14}$ | $2.56\ 10^{-13}$ | $3.52\ 10^{-13}$ | 1.01 | 0.95 | 0.65[1] |
| 2 | $8.51\ 10^{-14}$ | $3.35\ 10^{-13}$ | $4.88\ 10^{-13}$ | $8.75\ 10^{-14}$ | $3.51\ 10^{-13}$ | $4.71\ 10^{-13}$ | 0.97 | 0.95 | 1.04 |
| 4 | $1.93\ 10^{-13}$ | $7.34\ 10^{-13}$ | $9.07\ 10^{-13}$ | $1.99\ 10^{-13}$ | $7.60\ 10^{-13}$ | $9.74\ 10^{-13}$ | 0.97 | 0.97 | 0.93 |

1 The Chen result for this energy level looks low compared to the relative change in values between energy levels 1 MeV and 1.5 MeV for both 0.1 mfp and 1 mfp.

**Table A4 Variation of dose rate at a height of 1 metre for EGS4 and GRANIS v3 with soil slab thickness**

| Mev | EGS4 results (Sv $h^{-1}$ per Bq $m^{-3}$) | | | GRANIS v3 (Sv $h^{-1}$ per Bq $m^{-3}$) | | | Ratio EGS4/GRANIS v3 | | |
|---|---|---|---|---|---|---|---|---|---|
| | 0.01 m | 0.05 m | 0.3 m | 0.01 m | 0.05 m | 0.3 m | 0.01 m | 0.05 m | 0.3 m |
| 0.01 | | | | $5.3\ 10^{-19}$ | $5.3\ 10^{-19}$ | $5.3\ 10^{-19}$ | | | |
| 0.015 | $9.5\ 10^{-18}$ | $9.5\ 10^{-18}$ | $9.5\ 10^{-18}$ | $9.0\ 10^{-18}$ | $9.0\ 10^{-18}$ | $9.0\ 10^{-18}$ | 1.05 | 1.05 | 1.05 |
| 0.02 | $4.5\ 10^{-17}$ | $4.5\ 10^{-17}$ | $4.5\ 10^{-17}$ | $4.0\ 10^{-17}$ | $4.0\ 10^{-17}$ | $4.0\ 10^{-17}$ | 1.12 | 1.11 | 1.11 |
| 0.03 | $2.7\ 10^{-16}$ | $3.0\ 10^{-16}$ | $3.0\ 10^{-16}$ | $1.9\ 10^{-16}$ | $2.1\ 10^{-16}$ | $2.1\ 10^{-16}$ | 1.43 | 1.40 | 1.40 |
| 0.05 | $9.2\ 10^{-16}$ | $1.6\ 10^{-15}$ | $1.7\ 10^{-15}$ | $7.1\ 10^{-16}$ | $1.2\ 10^{-15}$ | $1.3\ 10^{-15}$ | 1.29 | 1.31 | 1.34 |
| 0.1 | $2.4\ 10^{-15}$ | $6.3\ 10^{-15}$ | $8.1\ 10^{-15}$ | $2.0\ 10^{-15}$ | $5.1\ 10^{-15}$ | $6.4\ 10^{-15}$ | 1.18 | 1.24 | 1.27 |
| 0.2 | $4.9\ 10^{-15}$ | $1.4\ 10^{-14}$ | $2.1\ 10^{-14}$ | $4.5\ 10^{-15}$ | $1.3\ 10^{-14}$ | $1.9\ 10^{-14}$ | 1.08 | 1.13 | 1.11 |
| 0.5 | $1.2\ 10^{-14}$ | $3.5\ 10^{-14}$ | $5.9\ 10^{-14}$ | $1.2\ 10^{-14}$ | $3.5\ 10^{-14}$ | $6.0\ 10^{-14}$ | 1.00 | 1.01 | 0.99 |
| 1 | $2.3\ 10^{-14}$ | $6.6\ 10^{-14}$ | $1.2\ 10^{-13}$ | $2.3\ 10^{-14}$ | $6.9\ 10^{-14}$ | $1.3\ 10^{-14}$ | 1.00 | 0.96 | 0.90 |
| 1.5 | $3.2\ 10^{-14}$ | $9.5\ 10^{-14}$ | $1.8\ 10^{-13}$ | $3.3\ 10^{-14}$ | $1.0\ 10^{-13}$ | $2.0\ 10^{-13}$ | 0.97 | 0.95 | 0.89 |
| 2 | $4.1\ 10^{-14}$ | $1.2\ 10^{-13}$ | $2.5\ 10^{-13}$ | $4.2\ 10^{-14}$ | $1.3\ 10^{-13}$ | $2.7\ 10^{-13}$ | 0.98 | 0.93 | 0.94 |
| 4 | $7.2\ 10^{-14}$ | $2.2\ 10^{-13}$ | $4.9\ 10^{-13}$ | $7.4\ 10^{-14}$ | $2.3\ 10^{-13}$ | $5.3\ 10^{-13}$ | 0.98 | 0.94 | 0.92 |

**Table A5 Variation of dose rate at a height of 1 metre for MCNP-4 and GRANIS v3 with soil slab thickness**

| MeV | MCNP-4 results (Sv $h^{-1}$ per Bq $m^{-3}$) | | | GRANIS v3 (Sv $h^{-1}$ per Bq $m^{-3}$) | | | Ratio MNCP-4/GRANIS v3 | | |
|---|---|---|---|---|---|---|---|---|---|
| | 0.01 m | 0.05 m | 0.3 m | 0.01 m | 0.05 m | 0.3 m | 0.01 m | 0.05 m | 0.3 m |
| 0.01 | $4.03\ 10^{-19}$ | $4.03\ 10^{-19}$ | $4.03\ 10^{-19}$ | $3.8\ 10^{-19}$ | $3.8\ 10^{-19}$ | $3.8\ 10^{-19}$ | 1.07 | 1.07 | 1.07 |
| 0.015 | $6.06\ 10^{-18}$ | $5.95\ 10^{-18}$ | $5.95\ 10^{-18}$ | $5.32\ 10^{-18}$ | $5.32\ 10^{-18}$ | $5.32\ 10^{-18}$ | 1.14 | 1.12 | 1.12 |
| 0.02 | $2.97\ 10^{-17}$ | $3.02\ 10^{-17}$ | $2.97\ 10^{-17}$ | $2.52\ 10^{-17}$ | $2.53\ 10^{-17}$ | $2.53\ 10^{-17}$ | 1.18 | 1.19 | 1.17 |
| 0.03 | $1.76\ 10^{-16}$ | $2.03\ 10^{-16}$ | $2.02\ 10^{-16}$ | $1.44\ 10^{-16}$ | $1.6\ 10^{-16}$ | $1.6\ 10^{-16}$ | 1.23 | 1.27 | 1.26 |
| 0.05 | $6.19\ 10^{-16}$ | $1.14\ 10^{-15}$ | $1.20\ 10^{-15}$ | $6.53\ 10^{-16}$ | $1.07\ 10^{-15}$ | $1.1\ 10^{-15}$ | 0.95 | 1.07 | 1.09 |
| 0.1 | $1.43\ 10^{-15}$ | $3.97\ 10^{-15}$ | $5.25\ 10^{-15}$ | $1.96\ 10^{-15}$ | $4.72\ 10^{-15}$ | $5.74\ 10^{-15}$ | 0.73 | 0.84 | 0.92 |
| 0.2 | $3.09\ 10^{-15}$ | $9.24\ 10^{-15}$ | $1.43\ 10^{-14}$ | $4.4\ 10^{-15}$ | $1.2\ 10^{-14}$ | $1.7\ 10^{-14}$ | 0.70 | 0.77 | 0.84 |
| 0.5 | $8.71\ 10^{-15}$ | $2.59\ 10^{-14}$ | $4.38\ 10^{-14}$ | $1.14\ 10^{-14}$ | $3.26\ 10^{-14}$ | $5.37\ 10^{-14}$ | 0.76 | 0.79 | 0.82 |
| 1 | $1.79\ 10^{-14}$ | $5.41\ 10^{-14}$ | $9.9\ 10^{-14}$ | $2.21\ 10^{-14}$ | $6.46\ 10^{-14}$ | $1.16\ 10^{-13}$ | 0.81 | 0.84 | 0.85 |
| 1.5 | $2.62\ 10^{-14}$ | $8.08\ 10^{-14}$ | $1.57\ 10^{-13}$ | $3.22\ 10^{-14}$ | $9.59\ 10^{-14}$ | $1.84\ 10^{-13}$ | 0.82 | 0.84 | 0.85 |
| 2 | $3.44\ 10^{-14}$ | $1.08\ 10^{-13}$ | $2.16\ 10^{-13}$ | $4.09\ 10^{-14}$ | $1.23\ 10^{-14}$ | $2.44\ 10^{-13}$ | 0.84 | 0.88 | 0.88 |
| 4 | $6.14\ 10^{-14}$ | $2.03\ 10^{-13}$ | $4.44\ 10^{-13}$ | $7.20\ 10^{-14}$ | $2.24\ 10^{-13}$ | $4.92\ 10^{-13}$ | 0.85 | 0.91 | 0.90 |

**Table A6 Comparison of dose rates[1] for Chen, EGS4, MCNP-4 models with GRANIS v3**

| Mev | Chen (Sv $h^{-1}$ per Bq $m^{-3}$) | EGS4 (Sv $h^{-1}$ per Bq $m^{-3}$) | MCNP-4 (Sv $h^{-1}$ per Bq $m^{-3}$) | GRANIS v3 Sv $h^{-1}$ per Bq $m^{-3}$) | Chen /GRANIS v3 | EGS4 /GRANIS v3 | MCNP-4 /GRANIS v3 |
|---|---|---|---|---|---|---|---|
| 0.01 | $4.87\ 10^{-19}$ | | $5.11\ 10^{-19}$ | $4.67\ 10^{-19}$ | 1.04 | | 1.1 |
| 0.015 | $8.52\ 10^{-18}$ | $9.38\ 10^{-18}$ | $8.84\ 10^{-18}$ | $7.95\ 10^{-18}$ | 1.07 | 1.18 | 1.11 |
| 0.02 | $3.93\ 10^{-17}$ | $4.28\ 10^{-17}$ | $4.08\ 10^{-17}$ | $3.59\ 10^{-17}$ | 1.09 | 1.19 | 1.14 |
| 0.03 | $2.3010^{-16}$ | $2.84\ 10^{-16}$ | $2.34\ 10^{-16}$ | $2.02\ 10^{-16}$ | 1.14 | 1.41 | 1.16 |
| 0.05 | $1.45\ 10^{-15}$ | $1.79\ 10^{-15}$ | $1.31\ 10^{-15}$ | $1.45\ 10^{-15}$ | 1.00 | 1.23 | 0.9 |
| 0.1 | $1.07\ 10^{-14}$ | $1.09\ 10^{-14}$ | $7.35\ 10^{-15}$ | $9.54\ 10^{-15}$ | 1.12 | 1.14 | 0.77 |
| 0.2 | $3.32\ 10^{-14}$ | $3.46\ 10^{-14}$ | $2.35\ 10^{-14}$ | $3.05\ 10^{-14}$ | 1.09 | 1.13 | 0.77 |
| 0.5 | $1.02\ 10^{-13}$ | $1.04\ 10^{-13}$ | $7.90\ 10^{-14}$ | $9.93\ 10^{-14}$ | 1.03 | 1.05 | 0.80 |
| 1 | $2.19\ 10^{-13}$ | $2.21\ 10^{-13}$ | $1.83\ 10^{-13}$ | $2.20\ 10^{-13}$ | 1.00 | 1.01 | 0.83 |
| 1.5 | $2.3\ 10^{-13}$ | $3.49\ 10^{-13}$ | $2.94\ 10^{-13}$ | $3.52\ 10^{-13}$ | 0.65[2] | 0.99 | 0.84 |
| 2 | $4.88\ 10^{-13}$ | $4.66\ 10^{-13}$ | $4.10\ 10^{-13}$ | $4.71\ 10^{-13}$ | 1.04 | 0.99 | 0.87 |
| 4 | $9.07\ 10^{-13}$ | $9.69\ 10^{-13}$ | $8.73\ 10^{-13}$ | $9.74\ 10^{-13}$ | 0.93 | 1.00 | 0.9 |

1 for slab of 5 mfp thickness

2 The Chen result for this energy level looks low compared to the relative change in values between energy levels 1 MeV and 1.5 MeV for both 0.1 mfp and 1 mfp.

**Table A7 Size of calculated doses from different codes**

| Largest calculated dose |
|---|
| EGS4 |
| Chen |
| MCNP-4 (E < 0.05 MeV) |
| GRANIS v3 |
| MCNP-4 (E > 0.05 MeV) |
| Smallest calculated dose |

**Table A8 Variation of dose rate at 1 metre above a contaminated soil surface for MICROSHIELD and GRANIS v3 with soil slab thickness**

| Radionuclide | MeV | MICROSHIELD (Sv $h^{-1}$) | | | GRANIS v3 (Sv $h^{-1}$) | | | Ratio MICROSHIELD/GRANIS v3 | | |
|---|---|---|---|---|---|---|---|---|---|---|
| | | 0.01 m | 0.05 m | 0.3 m | 0.01 m | 0.05 m | 0.3 m | 0.01 m | 0.05 m | 0.3 m |
| $^{103m}Rh$ | 0.02 | $3.80\ 10^{-18}$ | $3.97\ 10^{-18}$ | $3.69\ 10^{-18}$ | $3.15\ 10^{-18}$ | $3.45\ 10^{-18}$ | $3.47\ 10^{-18}$ | 1.21 | 1.15 | 1.06 |
| $^{131}Cs$ | 0.03 | $1.64\ 10^{-16}$ | $1.87\ 10^{-16}$ | $1.85\ 10^{-16}$ | $1.28\ 10^{-16}$ | $1.56\ 10^{-16}$ | $1.57\ 10^{-16}$ | 1.28 | 1.20 | 1.17 |
| $^{156m1}Tb$ | 0.05 | $4.24\ 10^{-16}$ | $7.62\ 10^{-16}$ | $7.92\ 10^{-16}$ | $3.40\ 10^{-16}$ | $5.85\ 10^{-16}$ | $6.09\ 10^{-16}$ | 1.25 | 1.30 | 1.30 |
| $^{155}Sm$ | 0.1 | $2.21\ 10^{-15}$ | $5.96\ 10^{-15}$ | $8.28\ 10^{-15}$ | $2.07\ 10^{-15}$ | $5.30\ 10^{-15}$ | $7.14\ 10^{-15}$ | 1.07 | 1.12 | 1.16 |
| $^{81m}Kr$ | 0.2 | $3.08\ 10^{-15}$ | $8.94\ 10^{-15}$ | $1.40\ 10^{-14}$ | $2.91\ 10^{-15}$ | $8.14\ 10^{-15}$ | $1.21\ 10^{-14}$ | 1.06 | 1.10 | 1.15 |
| $^{30}P$ | 0.5 | $2.51\ 10^{-14}$ | $7.36\ 10^{-14}$ | $1.30\ 10^{-13}$ | $2.41\ 10^{-14}$ | $7.06\ 10^{-14}$ | $1.23\ 10^{-13}$ | 1.04 | 1.04 | 1.06 |
| $^{66}Cu$ | 1 | $2.00\ 10^{-15}$ | $5.92\ 10^{-15}$ | $1.14\ 10^{-14}$ | $1.92\ 10^{-15}$ | $5.76\ 10^{-15}$ | $1.10\ 10^{-14}$ | 1.04 | 1.03 | 1.04 |
| $^{40}K$ | 1.5 | $3.55\ 10^{-15}$ | $1.06\ 10^{-14}$ | $2.13\ 10^{-14}$ | $3.45\ 10^{-15}$ | $1.05\ 10^{-14}$ | $2.12\ 10^{-14}$ | 1.03 | 1.00 | 1.00 |

**Table A9 Variation of dose rate with height above ground MICROSHIELD and GRANIS v3**

| Radionuclide | MeV | MICROSHIELD (Sv $h^{-1}$) | | | | GRANIS v3 (Sv $h^{-1}$) | | | | Ratio MICROSHIELD/GRANIS v3 | | | |
|---|---|---|---|---|---|---|---|---|---|---|---|---|---|
| | | 0.1 m | 1 m | 10 m | 100 m | 0.1 m | 1 m | 10 m | 100 m | 0.1 m | 1 m | 10 m | 100 m |
| $^{103m}Rh$ | 0.02 | $4.69\ 10^{-18}$ | $3.80\ 10^{-18}$ | $1.16\ 10^{-18}$ | $7.70\ 10^{-20}$ | $3.92\ 10^{-18}$ | $3.15\ 10^{-18}$ | $9.60\ 10^{-19}$ | $8.11\ 10^{-21}$ | 1.20 | 1.21 | 1.21 | 0.95 |
| $^{131}Cs$ | 0.03 | $1.85\ 10^{-16}$ | $1.64\ 10^{-16}$ | $8.13\ 10^{-17}$ | $1.01\ 10^{-18}$ | $1.47\ 10^{-16}$ | $1.28\ 10^{-16}$ | $5.76\ 10^{-17}$ | $7.44\ 10^{-19}$ | 1.26 | 1.28 | 1.41 | 1.36 |
| $^{156m1}Tb$ | 0.05 | $4.59\ 10^{-16}$ | $4.24\ 10^{-16}$ | $2.73\ 10^{-16}$ | $1.75\ 10^{-17}$ | $3.73\ 10^{-16}$ | $3.40\ 10^{-16}$ | $1.98\ 10^{-16}$ | $8.44\ 10^{-18}$ | 1.23 | 1.25 | 1.38 | 2.07 |
| $^{155}Sm$ | 0.1 | $2.34\ 10^{-15}$ | $2.21\ 10^{-15}$ | $1.59\ 10^{-15}$ | $2.89\ 10^{-16}$ | $2.23\ 10^{-15}$ | $2.07\ 10^{-15}$ | $1.42\ 10^{-15}$ | $2.07\ 10^{-16}$ | 1.05 | 1.07 | 1.12 | 1.40 |
| $^{81m}Kr$ | 0.2 | $3.24\ 10^{-15}$ | $3.08\ 10^{-15}$ | $2.22\ 10^{-15}$ | $5.31\ 10^{-16}$ | $3.11\ 10^{-15}$ | $2.91\ 10^{-15}$ | $2.06\ 10^{-15}$ | $4.06\ 10^{-16}$ | 1.04 | 1.06 | 1.08 | 1.31 |
| $^{30}P$ | 0.5 | $2.65\ 10^{-14}$ | $2.51\ 10^{-14}$ | $1.78\ 10^{-14}$ | $5.18\ 10^{-15}$ | $2.57\ 10^{-14}$ | $2.41\ 10^{-14}$ | $1.73\ 10^{-14}$ | $4.57\ 10^{-15}$ | 1.03 | 1.04 | 1.03 | 1.13 |
| $^{66}Cu$ | 1 | $2.11\ 10^{-15}$ | $2.00\ 10^{-15}$ | $1.42\ 10^{-15}$ | $4.54\ 10^{-16}$ | $2.04\ 10^{-15}$ | $1.92\ 10^{-15}$ | $1.39\ 10^{-15}$ | $4.18\ 10^{-16}$ | 1.03 | 1.04 | 1.02 | 1.09 |
| $^{40}K$ | 1.5 | $3.73\ 10^{-15}$ | $3.55\ 10^{-15}$ | $2.54\ 10^{-15}$ | $8.49\ 10^{-16}$ | $3.66\ 10^{-15}$ | $3.45\ 10^{-15}$ | $2.53\ 10^{-15}$ | $8.15\ 10^{-16}$ | 1.02 | 1.03 | 1.00 | 1.04 |

**Table A10 Variation of dose rate at a height of 1 metre for Eckerman and GRANIS v3 with soil slab thickness**

| Radionuclide | MeV | Eckerman (Sv $h^{-1}$ per Bq $m^{-3}$) | | | | GRANIS v3 (Sv $h^{-1}$ per Bq $m^{-3}$) | | | | Ratio Eckerman/GRANIS v3 | | | |
|---|---|---|---|---|---|---|---|---|---|---|---|---|---|
| | | 0.01 m | 0.05 m | 0.15 m | infinity | 0.01 m | 0.05 m | 0.15 m | infinity | 0.01 m | 0.05 m | 0.15 m | infinity |
| $^{210}$Pb | $4.81\ 10^{-3}$ | $2.44\ 10^{-17}$ | $3.78\ 10^{-17}$ | $3.82\ 10^{-17}$ | $3.82\ 10^{-17}$ | $2.64\ 10^{-17}$ | $4.38\ 10^{-17}$ | $4.55\ 10^{-17}$ | $4.55\ 10^{-17}$ | 0.93 | 0.86 | 0.84 | 0.84 |
| $^{226}$Ra | $6.74\ 10^{-3}$ | $1.40\ 10^{-16}$ | $3.85\ 10^{-16}$ | $5.40\ 10^{-16}$ | $5.62\ 10^{-16}$ | $1.48\ 10^{-16}$ | $4.09\ 10^{-16}$ | $5.75\ 10^{-16}$ | $6.04\ 10^{-16}$ | 0.94 | 0.94 | 0.95 | 0.93 |
| $^{235}$U | $1.54\ 10^{-1}$ | $3.19\ 10^{-15}$ | $8.82\ 10^{-15}$ | $1.24\ 10^{-14}$ | $1.2710^{-14}$ | $3.38\ 10^{-15}$ | $9.32\ 10^{-15}$ | $1.30\ 10^{-14}$ | $1.37\ 10^{-14}$ | 0.95 | 0.95 | 0.95 | 0.93 |
| $^{137+}$Cs | $5.63\ 10^{-1}$ | $1.30\ 10^{-14}$ | $3.71\ 10^{-14}$ | $5.80\ 10^{-14}$ | $6.52\ 10^{-14}$ | $1.40\ 10^{-14}$ | $4.13\ 10^{-14}$ | $6.60\ 10^{-14}$ | $7.67\ 10^{-14}$ | 0.93 | 0.90 | 0.88 | 0.85 |
| $^{60}$Co | $2.50\ 10^{0}$ | $5.29\ 10^{-14}$ | $1.54\ 10^{-13}$ | $2.49\ 10^{-13}$ | $2.97\ 10^{-13}$ | $5.62\ 10^{-14}$ | $1.70\ 10^{-13}$ | $2.84\ 10^{-13}$ | $3.52\ 10^{-13}$ | 0.94 | 0.90 | 0.88 | 0.84 |

**Table A11 Variation of dose rate at a height of 1 metre from a plane source with height above ground for Saito and Jacob model and GRANIS v3**

| MeV | Saito and Jacob (Gy $h^{-1}$ per Bq $m^{-2}$) | | | | GRANIS v3 (Gy $h^{-1}$ per Bq $m^{-2}$) | | | | | Ratio Saito and Jacob/GRANIS v3 | | | | |
|---|---|---|---|---|---|---|---|---|---|---|---|---|---|---|
| | Height 0.1 m | Height 1 m | Height 10 m | Height 100 m | Height 0.1 m | Height 1 m | Height 10 m | Height 100 m | 100 m air Buildup factor | Height 0.1 m | Height 1 m | Height 10 m | Height 100 m | 100 m air Buildup factor |
| 0.01 | 0.0 | 0.0 | 0.0 | 0.0 | 0.0 | 0.0 | 0.0 | 0.0 | 0.0 | - | - | - | - | - |
| 0.015 | $5.08\ 10^{-17}$ | $4.28\ 10^{-17}$ | 0.0 | 0.0 | $3.91\ 10^{-17}$ | $3.18\ 10^{-17}$ | $4.18\ 10^{-18}$ | 0.0 | 0.0 | 1.30 | 1.35 | - | - | - |
| 0.02 | $3.64\ 10^{-15}$ | $3.37\ 10^{-15}$ | $1.52\ 10^{-15}$ | 0.0 | $2.81\ 10^{-15}$ | $2.52\ 10^{-15}$ | $8.66\ 10^{-16}$ | $4.68\ 10^{-20}$ | $1.26\ 10^{-19}$ | 1.30 | 1.34 | 1.76 | - | - |
| 0.03 | $3.85\ 10^{-14}$ | $3.78\ 10^{-14}$ | $2.68\ 10^{-14}$ | $7.85\ 10^{-16}$ | $2.66\ 10^{-14}$ | $2.50\ 10^{-14}$ | $1.39\ 10^{-14}$ | $1.04\ 10^{-16}$ | $5.05\ 10^{-16}$ | 1.45 | 1.51 | 1.93 | - | 1.62 |
| 0.05 | $1.01\ 10^{-13}$ | $9.97\ 10^{-14}$ | $8.39\ 10^{-14}$ | $1.44\ 10^{-14}$ | $7.34\ 10^{-14}$ | $7.01\ 10^{-14}$ | $4.60\ 10^{-14}$ | $2.13\ 10^{-15}$ | $1.28\ 10^{-14}$ | 1.38 | 1.42 | 1.82 | - | 1.06 |
| 0.1 | $2.28\ 10^{-13}$ | $2.23\ 10^{-13}$ | $1.87\ 10^{-13}$ | $5.90\ 10^{-14}$ | $1.88\ 10^{-13}$ | $1.81\ 10^{-13}$ | $1.32\ 10^{-13}$ | $1.71\ 10^{-14}$ | $6.51\ 10^{-14}$ | 1.21 | 1.23 | 1.42 | - | 1.06 |
| 0.2 | $5.22\ 10^{-13}$ | $5.11\ 10^{-13}$ | $4.10\ 10^{-13}$ | $1.34\ 10^{-13}$ | $4.89\ 10^{-13}$ | $4.72\ 10^{-13}$ | $3.57\ 10^{-13}$ | $7.36\ 10^{-14}$ | $1.41\ 10^{-13}$ | 1.07 | 1.08 | 1.15 | 1.82 | 1.03 |
| 0.5 | $1.36\ 10^{-12}$ | $1.32\ 10^{-12}$ | $1.04\ 10^{-12}$ | $3.40\ 10^{-13}$ | $1.34\ 10^{-12}$ | $1.30\ 10^{-12}$ | $9.92\ 10^{-13}$ | $2.68\ 10^{-13}$ | $3.32\ 10^{-13}$ | 1.01 | 1.02 | 1.05 | 1.27 | 0.97 |
| 1 | $2.55\ 10^{-12}$ | $2.47\ 10^{-12}$ | $1.95\ 10^{-12}$ | $6.70\ 10^{-13}$ | $2.54\ 10^{-12}$ | $2.46\ 10^{-12}$ | $1.90\ 10^{-12}$ | $5.82\ 10^{-13}$ | $6.51\ 10^{-13}$ | 1.00 | 1.01 | 1.03 | 1.15 | 0.98 |
| 1.5 | - | - | - | - | $3.60\ 10^{-12}$ | $3.48\ 10^{-12}$ | $2.72\ 10^{-12}$ | $9.07\ 10^{-13}$ | $9.71\ 10^{-13}$ | - | - | - | - | - |
| 2 | $4.46\ 10^{-12}$ | $4.32\ 10^{-12}$ | $2.46\ 10^{-12}$ | $1.29\ 10^{-12}$ | $4.48\ 10^{-12}$ | $4.33\ 10^{-12}$ | $3.40\ 10^{-12}$ | $1.18\ 10^{-12}$ | $1.23\ 10^{-12}$ | 1.03 | 1.00 | 1.02 | 1.09 | 1.02 |

**Table A12 Variation of air kerma with height above ground for Saito and Jacob model and GRANIS v3**

| Height above ground (m) | Saito and Jacob ($Gy\ h^{-1}$ per $Bq\ m^{-2}$) | | GRANIS v3 ($Gy\ h^{-1}$ per $Bq\ m^{-2}$) | | Ratio Saito and Jacob /GRANIS v3 | |
|---|---|---|---|---|---|---|
| | 0.1 MeV | 1 MeV | 0.1 MeV | 1 MeV | 0.1 MeV | 1 MeV |
| 0.1 | $2.28\ 10^{-13}$ | $2.55\ 10^{-12}$ | $1.88\ 10^{-13}$ | $2.54\ 10^{-12}$ | 1.21 | 1.00 |
| 1 | $2.23\ 10^{-13}$ | $2.47\ 10^{-12}$ | $1.81\ 10^{-13}$ | $2.46\ 10^{-12}$ | 1.23 | 1.01 |
| 10 | $1.87\ 10^{-13}$ | $1.95\ 10^{-12}$ | $1.32\ 10^{-13}$ | $1.90\ 10^{-12}$ | 1.42 | 1.03 |
| 100 | $5.90\ 10^{-14}$ | $6.70\ 10^{-13}$ | $1.71\ 10^{-14}$ | $5.82\ 10^{-13}$ | 3.46 | 1.15 |

**Table A13 Comparison of MCNP-4 and GRANIS v3 transmission factors calculation for soil shielded with 30 cm of concrete, for $^{60}Co$ gamma rays**

| Concrete thickness (cm) | Transmission factor for concrete | | |
|---|---|---|---|
| | MCNP-4 | GRANISv3 | Ratio MCNP-4/GRANIS v3 |
| 0 | 1.00 | 1.00 | 1.00 |
| 1 | 0.77 | 0.78 | 0.98 |
| 5 | 0.39 | 0.40 | 0.96 |
| 10 | 0.19 | 0.20 | 0.95 |
| 30 | 0.0129 | 0.0147 | 0.87 |

**Table A14 Comparison of dose rate at a height of 1 metre for BOXDOSE and GRANIS v3 for different thicknesses and depths of contaminated soil**

| MeV | BOXDOSE (Sv $h^{-1}$ per Bq $m^{-3}$) | | | GRANIS v3 (Sv $h^{-1}$ per Bq $m^{-3}$) | | | Ratio BOXDOSE/GRANIS v3 | | |
|---|---|---|---|---|---|---|---|---|---|
| | 0 to 0.01 m | 0.01 to 0.05 m | 0 to 0.3 m | 0 to 0.01 m | 0.01 to 0.05 m | 0 to 0.3 m | 0 to 0.01 m | 0.01 to 0.05 m | 0 to 0.3 m |
| 0.01 | $3.67\ 10^{-20}$ | 0.0 | $3.67\ 10^{-20}$ | $4.50\ 10^{-19}$ | 0.0 | $4.50\ 10^{-19}$ | 0.08 | - | 0.08 |
| 0.015 | $5.72\ 10^{-18}$ | $1.60\ 10^{-23}$ | $5.72\ 10^{-18}$ | $7.92\ 10^{-18}$ | $8.06\ 10^{-23}$ | $7.92\ 10^{-18}$ | 0.72 | 0.20 | 0.72 |
| 0.02 | $3.33\ 10^{-17}$ | $7.78\ 10^{-20}$ | $3.34\ 10^{-17}$ | $3.58\ 10^{-17}$ | $1.27\ 10^{-19}$ | $3.59\ 10^{-17}$ | 0.93 | 0.62 | 0.93 |
| 0.03 | $1.94\ 10^{-16}$ | $2.64\ 10^{-17}$ | $2.20\ 10^{-16}$ | $1.73\ 10^{-16}$ | $1.92\ 10^{-17}$ | $1.92\ 10^{-16}$ | 1.12 | 1.38 | 1.15 |
| 0.05 | $7.02\ 10^{-16}$ | $5.33\ 10^{-16}$ | $1.29\ 10^{-15}$ | $6.77\ 10^{-16}$ | $4.31\ 10^{-16}$ | $1.14\ 10^{-15}$ | 1.04 | 1.24 | 1.13 |
| 0.1 | $3.39\ 10^{-15}$ | $6.59\ 10^{-15}$ | $1.43\ 10^{-14}$ | $1.96\ 10^{-15}$ | $2.7710^{-15}$ | $5.76\ 10^{-15}$ | 1.73 | 2.38 | 2.48 |
| 0.2 | $6.16\ 10^{-15}$ | $1.26\ 10^{-14}$ | $3.05\ 10^{-14}$ | $4.40\ 10^{-15}$ | $7.59\ 10^{-15}$ | $1.70\ 10^{-14}$ | 1.40 | 1.66 | 1.79 |
| 0.5 | $1.24\ 10^{-14}$ | $2.35\ 10^{-14}$ | $5.93\ 10^{-14}$ | $1.16\ 10^{-14}$ | $2.15\ 10^{-14}$ | $5.40\ 10^{-14}$ | 1.07 | 1.09 | 1.10 |
| 1 | $2.28\ 10^{-14}$ | $4.39\ 10^{-14}$ | $1.20\ 10^{-13}$ | $2.24\ 10^{-14}$ | $4.29\ 10^{-14}$ | $1.17\ 10^{-13}$ | 1.02 | 1.02 | 1.02 |
| 1.5 | $3.21\ 10^{-14}$ | $6.34\ 10^{-14}$ | $1.82\ 10^{-13}$ | $3.22\ 10^{-14}$ | $6.39\ 10^{-14}$ | $1.84\ 10^{-13}$ | 1.00 | 0.99 | 0.99 |
| 2 | $4.00\ 10^{-14}$ | $7.88\ 10^{-14}$ | $2.32\ 10^{-13}$ | $4.08\ 10^{-14}$ | $8.21\ 10^{-14}$ | $2.44\ 10^{-13}$ | 0.98 | 0.96 | 0.95 |
| 4 | $6.80\ 10^{-14}$ | $1.38\ 10^{-13}$ | $4.30\ 10^{-13}$ | $7.20\ 10^{-14}$ | $1.52\ 10^{-13}$ | $4.91\ 10^{-13}$ | 0.94 | 0.97 | 0.87 |

**Table A15 Variation of effective dose rates at a height of 1 metre for BOXDOSE and GRANIS v3 with contamination depth and thickness using GRANIS libraries**

| MeV | BOXDOSE (Sv h$^{-1}$ per Bq m$^{-3}$) | | | | GRANIS v3 (Sv h$^{-1}$ per Bq m$^{-3}$) | | | | Ratio BOXDOSE/GRANIS v3 | | | |
|---|---|---|---|---|---|---|---|---|---|---|---|---|
| | 0 to 0.01 m | 0.01 to 0.05 m | 0.05 to 0.15 m | 0.15 to 0.3 m | 0 to 0.01 m | 0.01 to 0.05 m | 0.05 to 0.15 m | 0.15 to 0.3 m | 0 to 0.01 m | 0.01 to 0.05 m | 0.05 to 0.15 m | 0.15 to 0.3 m |
| 0.01 | 2.98 10$^{-20}$ | 0.0 | 0.0 | 0.0 | 4.50 10$^{-19}$ | 0.0 | 0.0 | 0.0 | 0.07 | - | - | - |
| 0.015 | 5.25 10$^{-18}$ | 9.23 10$^{-24}$ | 0.0 | 0.0 | 7.92 10$^{-18}$ | 8.06 10$^{-23}$ | 0.0 | 0.0 | 0.66 | 0.11 | - | - |
| 0.02 | 3.15 10$^{-17}$ | 5.80 10$^{-20}$ | 0.0 | 0.0 | 3.58 10$^{-17}$ | 1.27 10$^{-19}$ | 0.0 | 0.0 | 0.88 | 0.46 | - | - |
| 0.03 | 1.68 10$^{-16}$ | 1.79 10$^{-17}$ | 1.64 10$^{-20}$ | 0.0 | 1.73 10$^{-16}$ | 1.92 10$^{-17}$ | 2.51 10$^{-20}$ | 0.0 | 0.97 | 0.93 | 0.65 | - |
| 0.05 | 6.73 10$^{-16}$ | 4.30 10$^{-16}$ | 3.11 10$^{-17}$ | 7.89 10$^{-20}$ | 6.77 10$^{-16}$ | 4.31 10$^{-16}$ | 3.26 10$^{-17}$ | 9.12 10$^{-20}$ | 0.99 | 1.00 | 0.95 | 0.87 |
| 0.1 | 1.96 10$^{-15}$ | 2.77 10$^{-15}$ | 9.72 10$^{-16}$ | 4.83 10$^{-17}$ | 1.96 10$^{-15}$ | 2.7710$^{-15}$ | 9.74 10$^{-16}$ | 5.02 10$^{-17}$ | 1.00 | 1.00 | 1.00 | 0.96 |
| 0.2 | 4.39 10$^{-15}$ | 7.58 10$^{-15}$ | 4.45 10$^{-15}$ | 5.88 10$^{-16}$ | 4.40 10$^{-15}$ | 7.59 10$^{-15}$ | 4.44 10$^{-15}$ | 5.93 10$^{-16}$ | 1.00 | 1.00 | 1.00 | 0.99 |
| 0.5 | 1.16 10$^{-14}$ | 2.15 10$^{-14}$ | 1.67 10$^{-14}$ | 4.21 10$^{-15}$ | 1.16 10$^{-14}$ | 2.15 10$^{-14}$ | 1.67 10$^{-14}$ | 4.21 10$^{-15}$ | 1.00 | 1.00 | 1.00 | 1.00 |
| 1 | 2.23 10$^{-14}$ | 4.29 10$^{-14}$ | 3.84 10$^{-14}$ | 1.34 10$^{-14}$ | 2.24 10$^{-14}$ | 4.29 10$^{-14}$ | 3.84 10$^{-14}$ | 1.34 10$^{-14}$ | 1.00 | 1.00 | 1.00 | 1.00 |
| 1.5 | 3.22 10$^{-14}$ | 6.38 10$^{-14}$ | 6.21 10$^{-14}$ | 2.60 10$^{-14}$ | 3.22 10$^{-14}$ | 6.39 10$^{-14}$ | 6.22 10$^{-14}$ | 2.60 10$^{-14}$ | 1.00 | 1.00 | 1.00 | 1.00 |
| 2 | 4.08 10$^{-14}$ | 8.21 10$^{-14}$ | 8.31 10$^{-14}$ | 3.81 10$^{-14}$ | 4.08 10$^{-14}$ | 8.21 10$^{-14}$ | 8.31 10$^{-14}$ | 3.81 10$^{-14}$ | 1.00 | 1.00 | 1.00 | 1.00 |
| 4 | 7.20 10$^{-14}$ | 1.52 10$^{-13}$ | 1.71 10$^{-13}$ | 9.62 10$^{-14}$ | 7.20 10$^{-14}$ | 1.52 10$^{-13}$ | 1.71 10$^{-13}$ | 9.62 10$^{-14}$ | 1.00 | 1.00 | 1.00 | 1.00 |

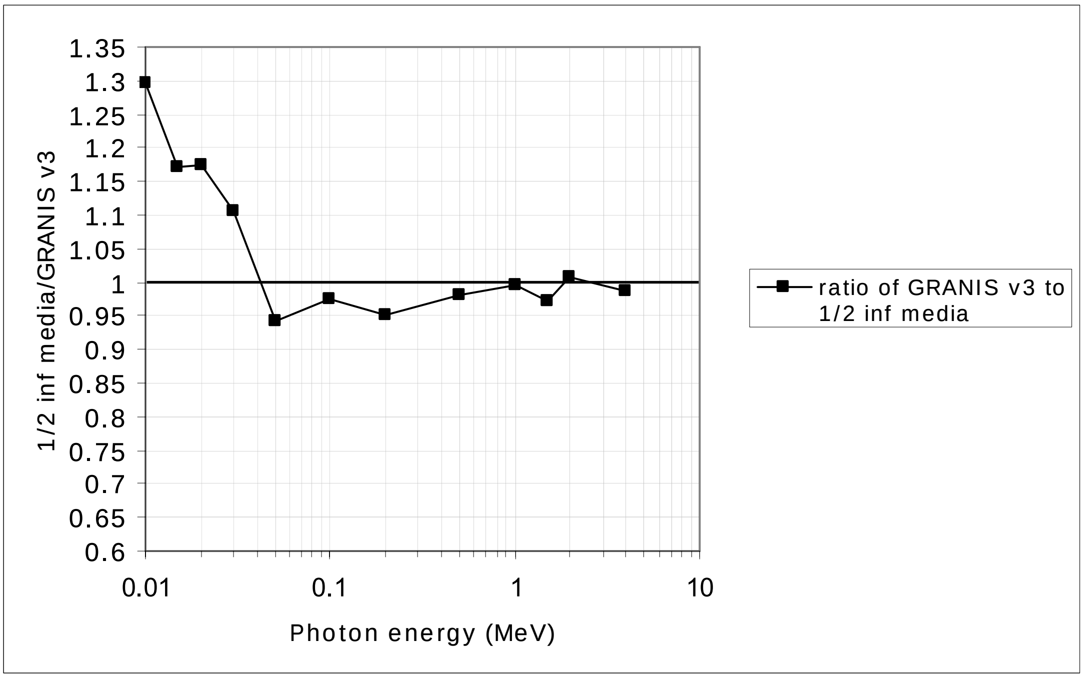


**FIGURE A1 Ratio of dose rates from GRANIS v3 and theoretical semi infinite medium**

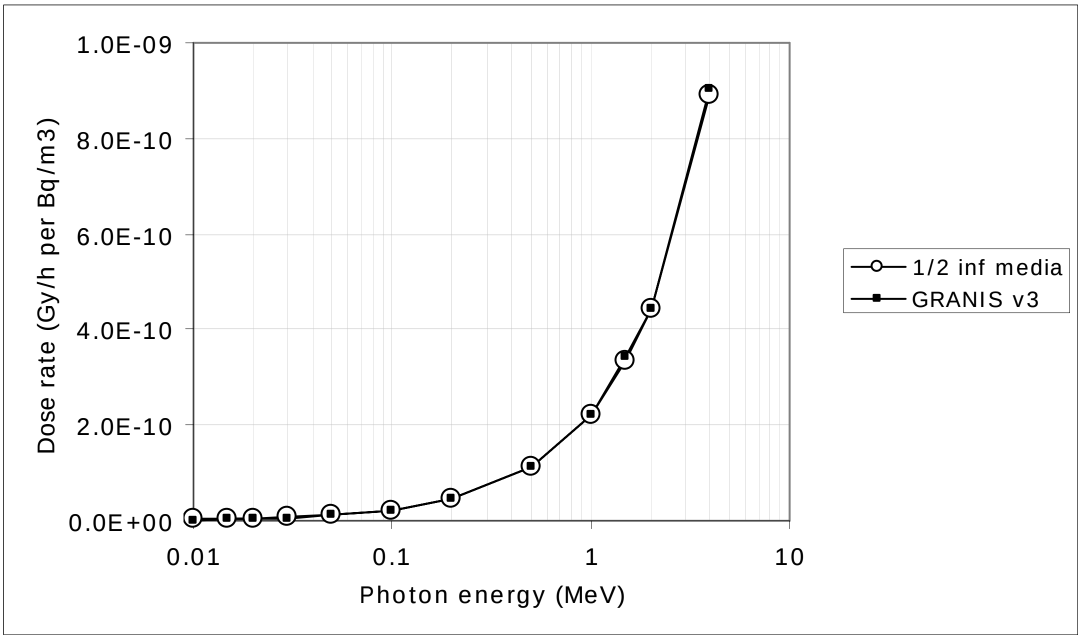


**FIGURE A2 Comparison of dose rate from GRANIS v3 and theoretical semi infinite medium**

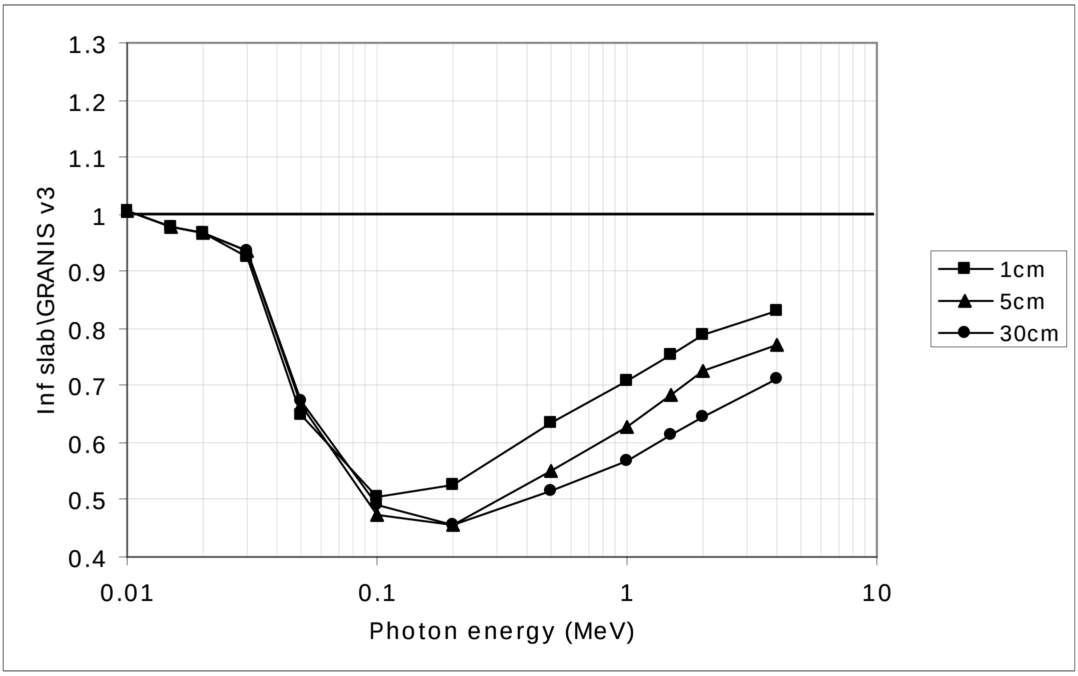


**FIGURE A3 Ratio of dose rates at a height of 1 metre of GRANIS v3 and Jaeger et al for different slab thicknesses**

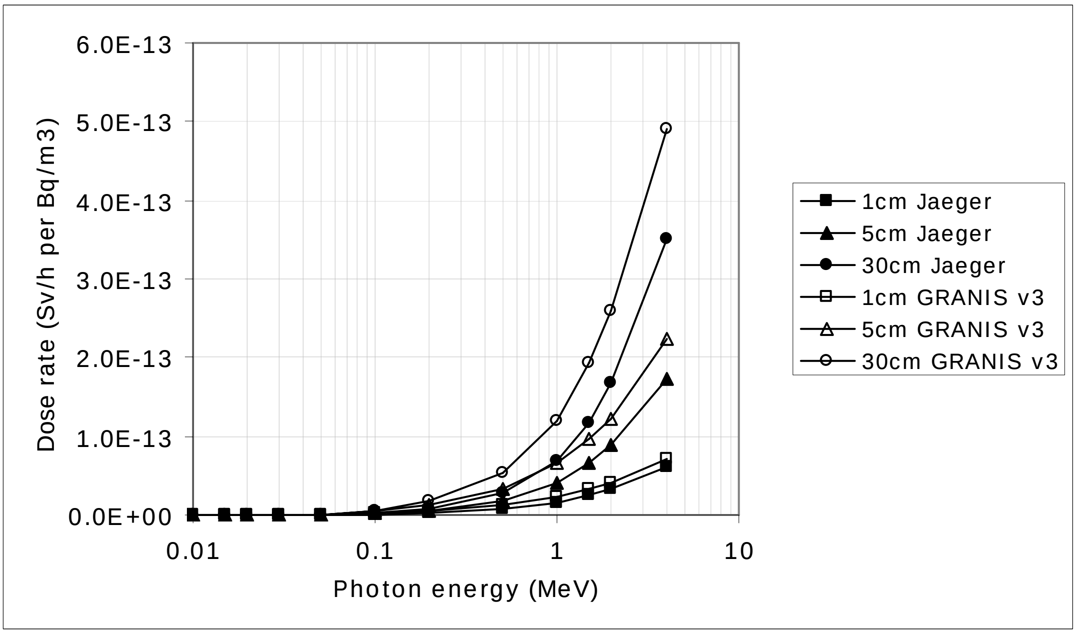


**FIGURE A4 Comparison of dose rate at a height of 1 metre for GRANIS v3 and Jaeger et al for different slab thicknesses**

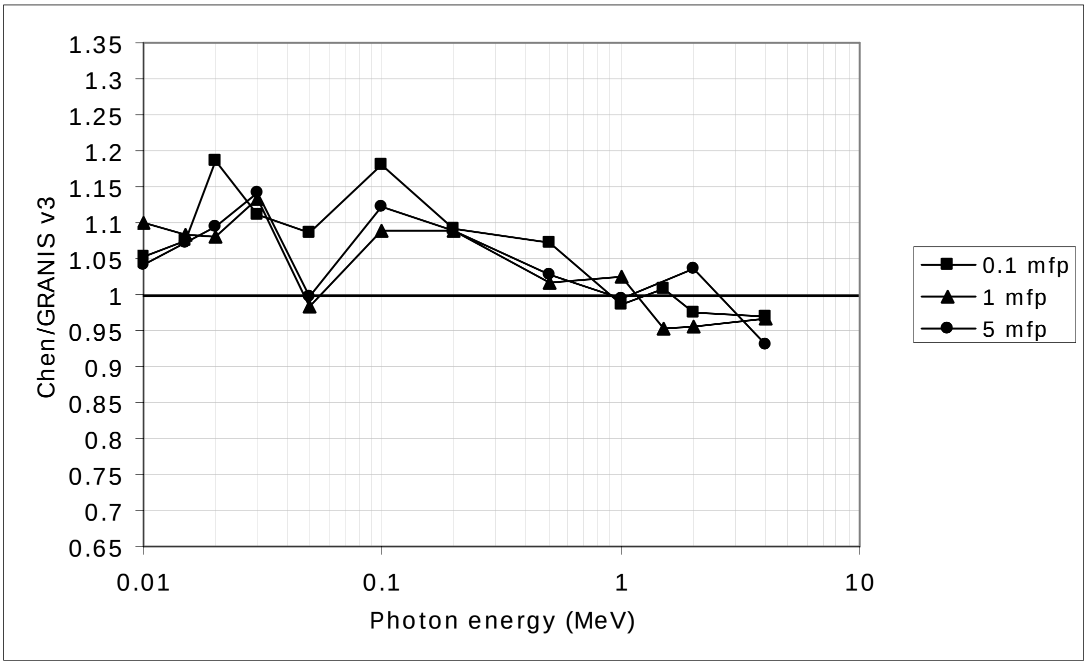


**FIGURE A5 Ratio of dose rates at a height of 1 metre of GRANIS v3 and Chen (soil slabs)**

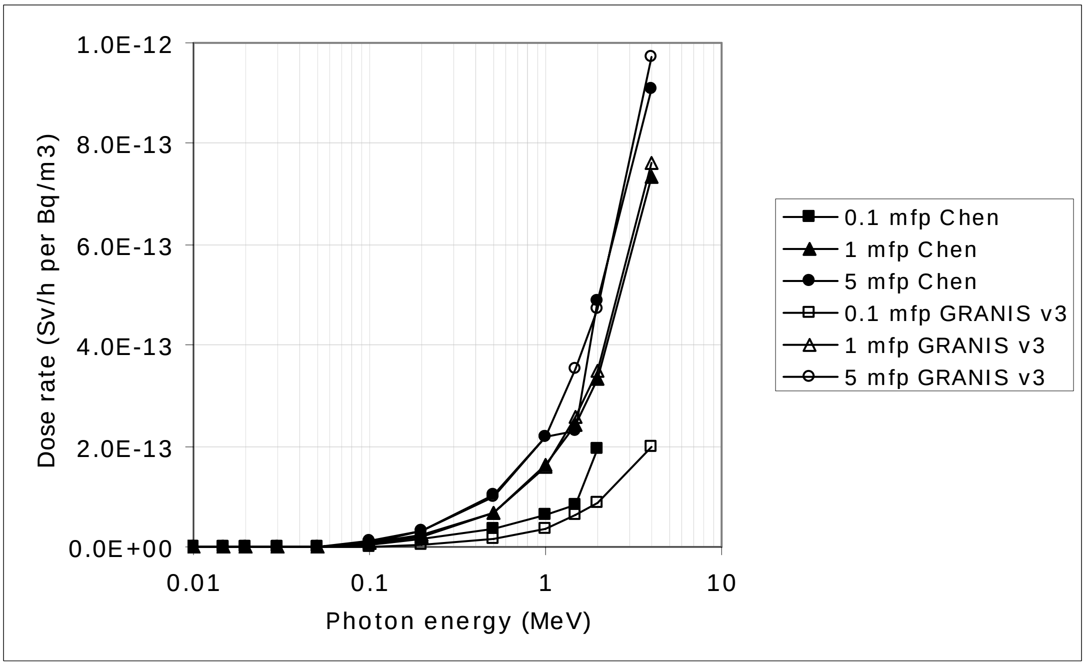


**FIGURE A6 Comparison of dose rate at a height of 1 metre for GRANIS v3 and Chen (soil slabs)**

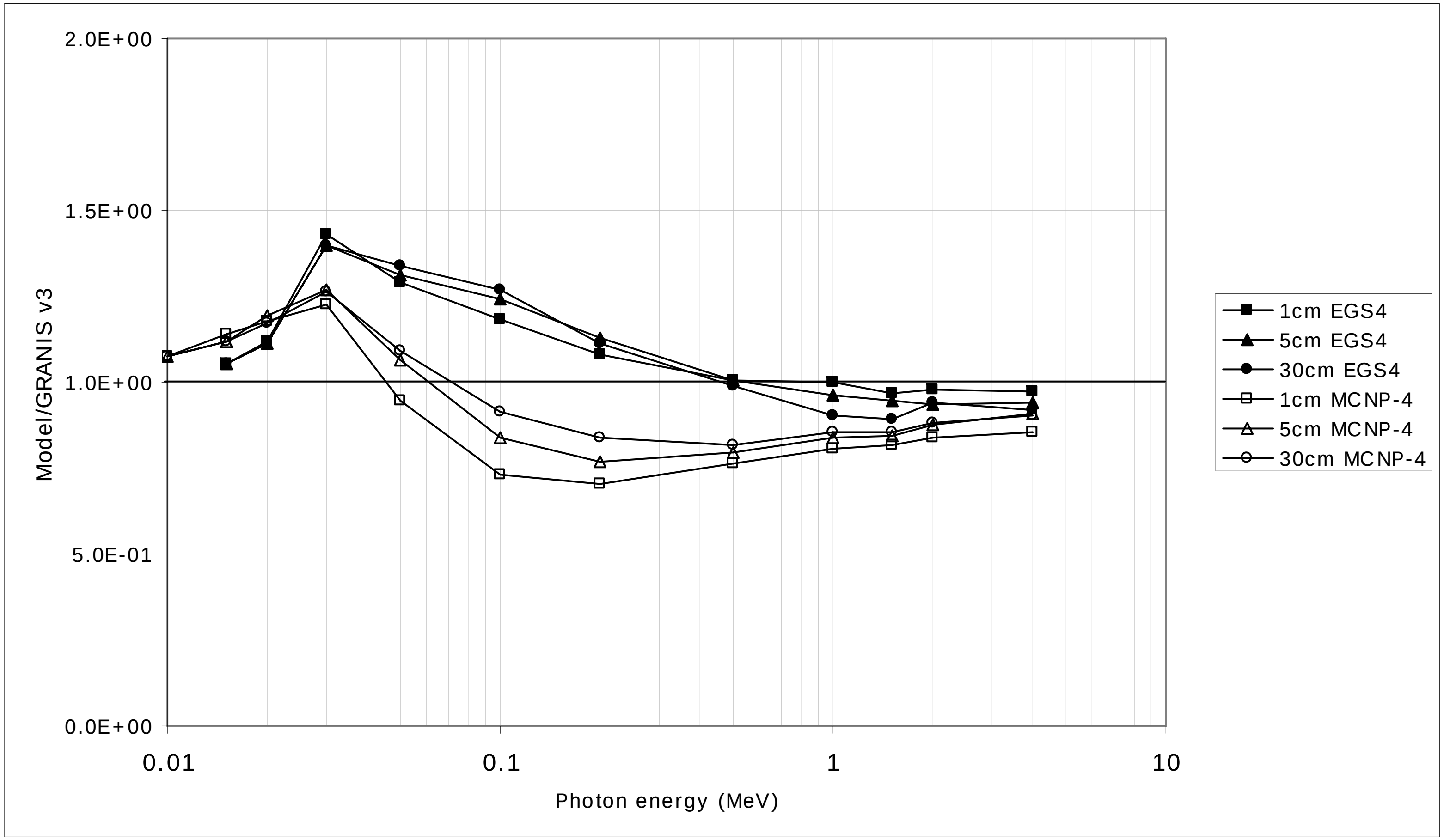


**FIGURE A7 Ratio of dose rates at a height of 1 metre of GRANIS v3 with EGS4 and MCNP-4 for different soil thickness**

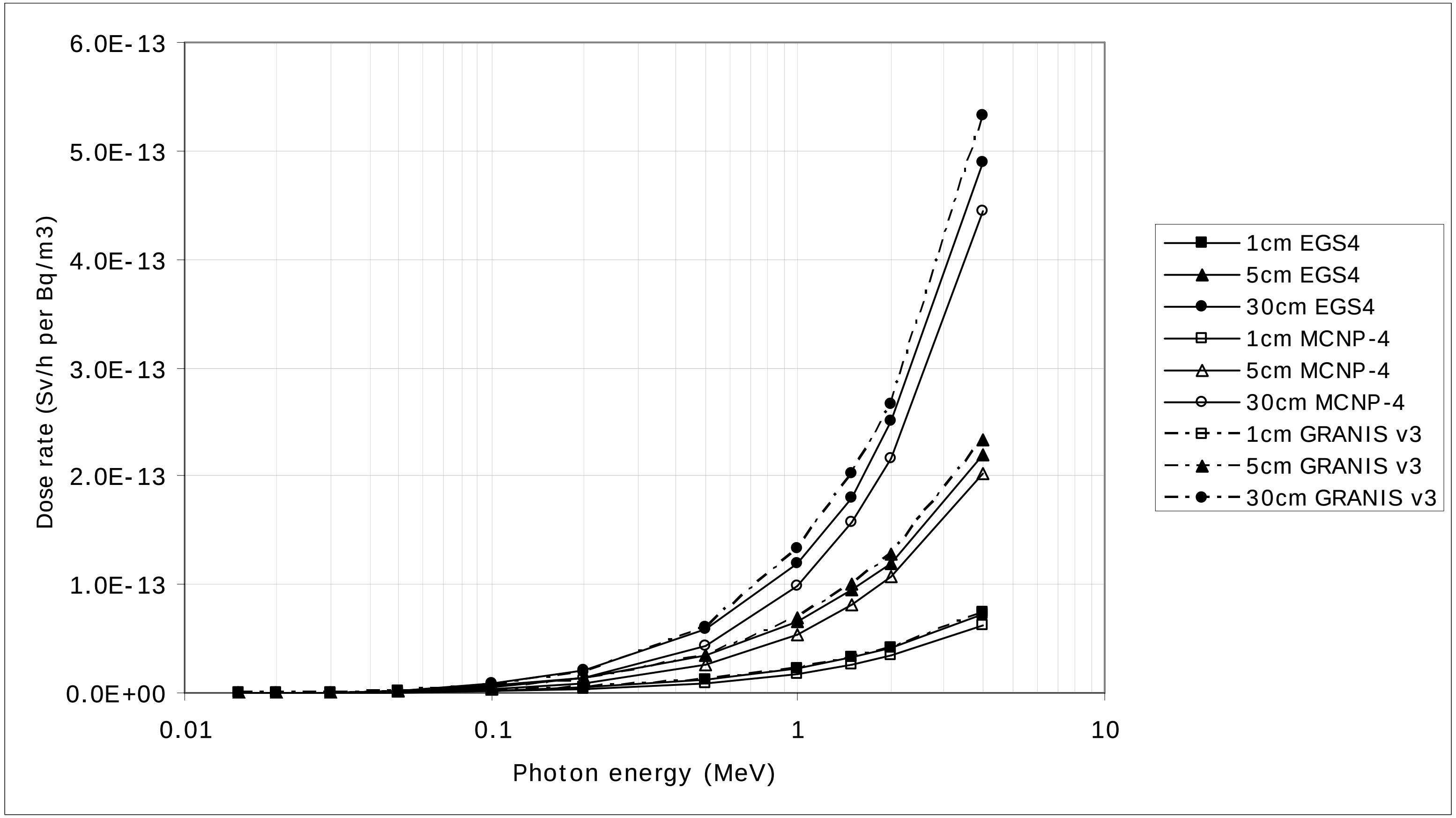


**FIGURE A8  Comparison of dose rates at a height of 1 metre of GRANIS v3 with EGS4 and MCNP-4 for different soil thickness**

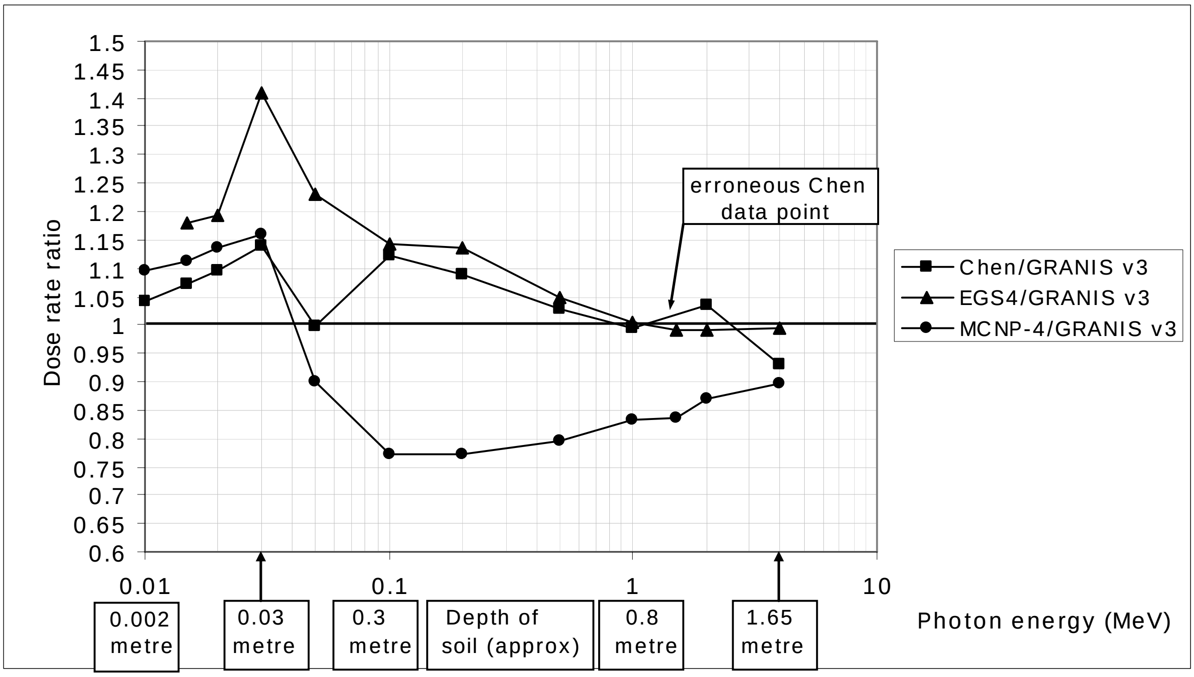


**Figure A9 Ratio of dose rates at a height of 1 metre of GRANIS v3 with Monte Carlo calculations (soil slabs of 5 mfp depth)**

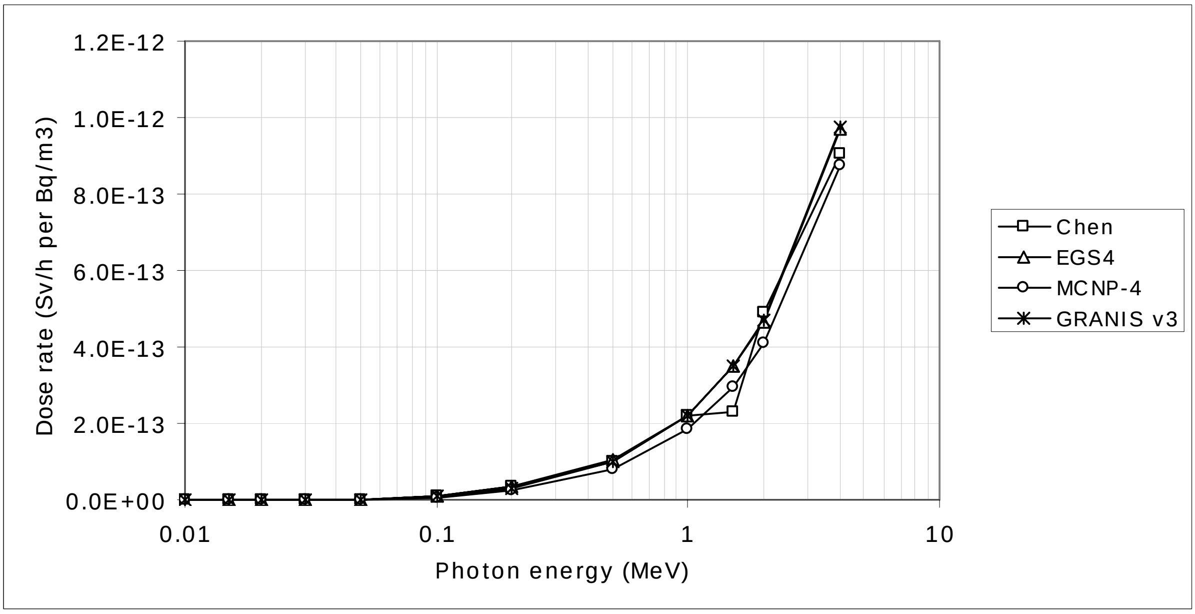


**Figure A10 Comparison of dose rates at a height of 1 metre of GRANIS v3 with Monte Carlo calculations (soil slabs of 5 mfp depth)**

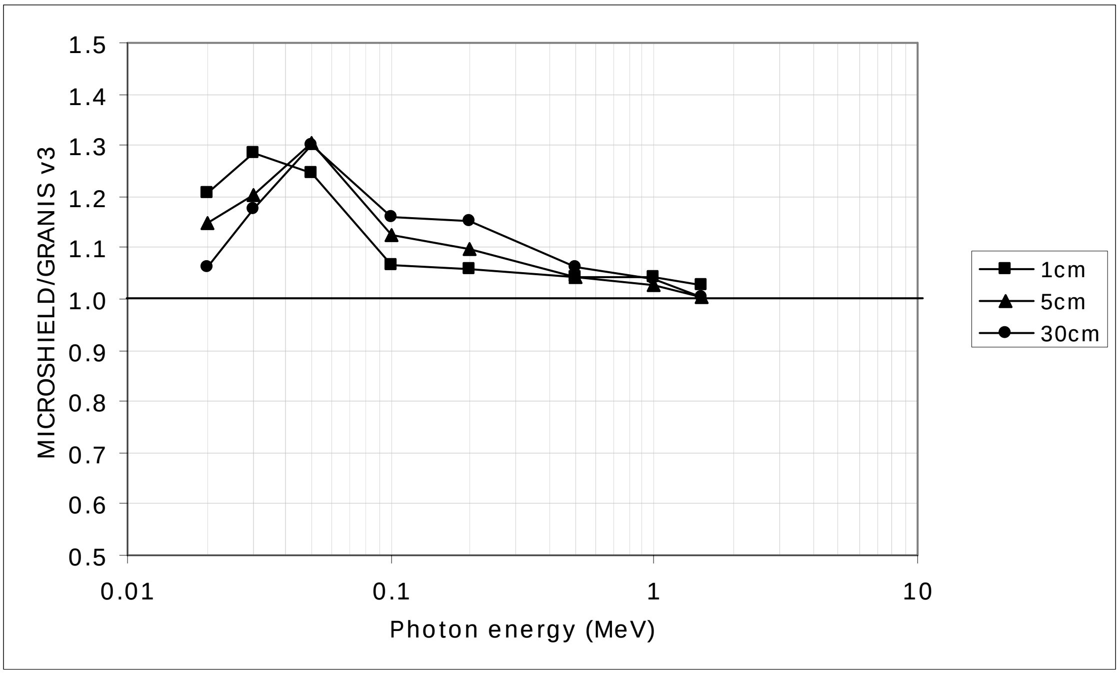


**FIGURE A11 Ratio of dose rates at 1 metre above a contaminated soil surface of GRANIS v3 with MICROSHIELD for different soil thickness**

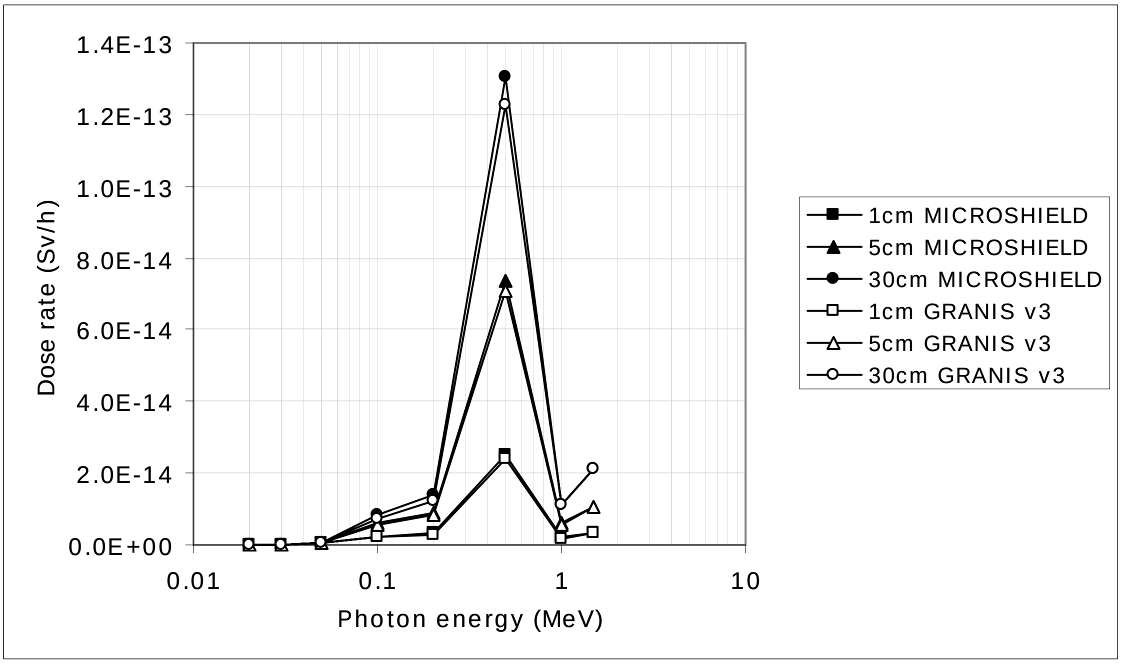


**FIGURE A12 Comparison of dose rates at 1 metre above a contaminated soil surface of GRANIS v3 with MICROSHIELD for different soil thickness**

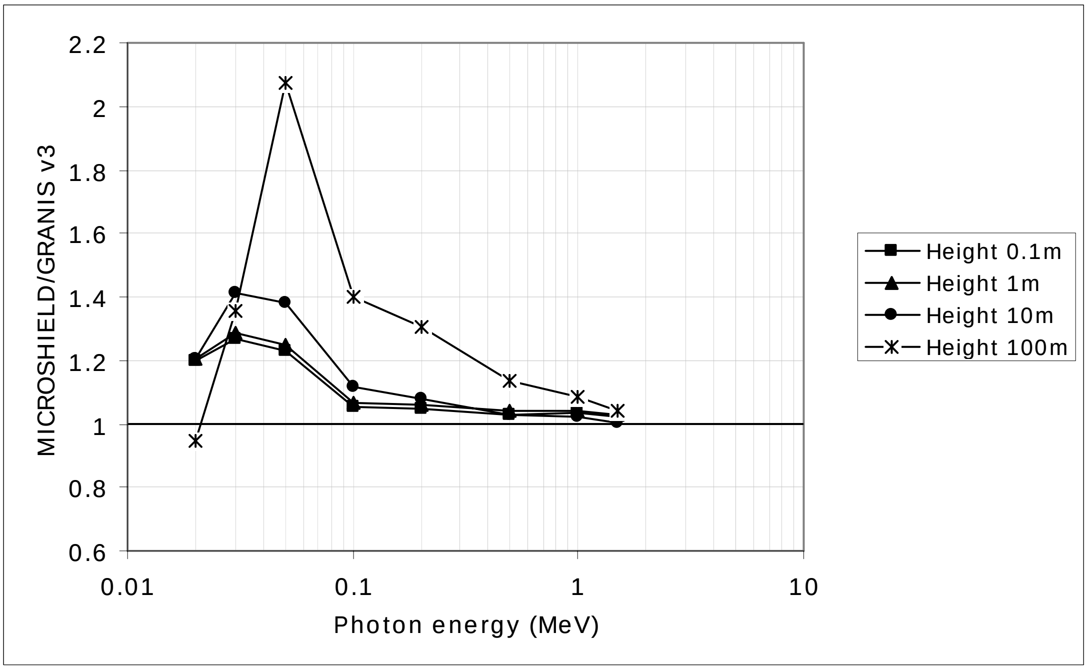


**FIGURE A13 Ratio of dose rates of GRANIS v3 and MICROSHIELD - variation of dose rate with height above the ground**

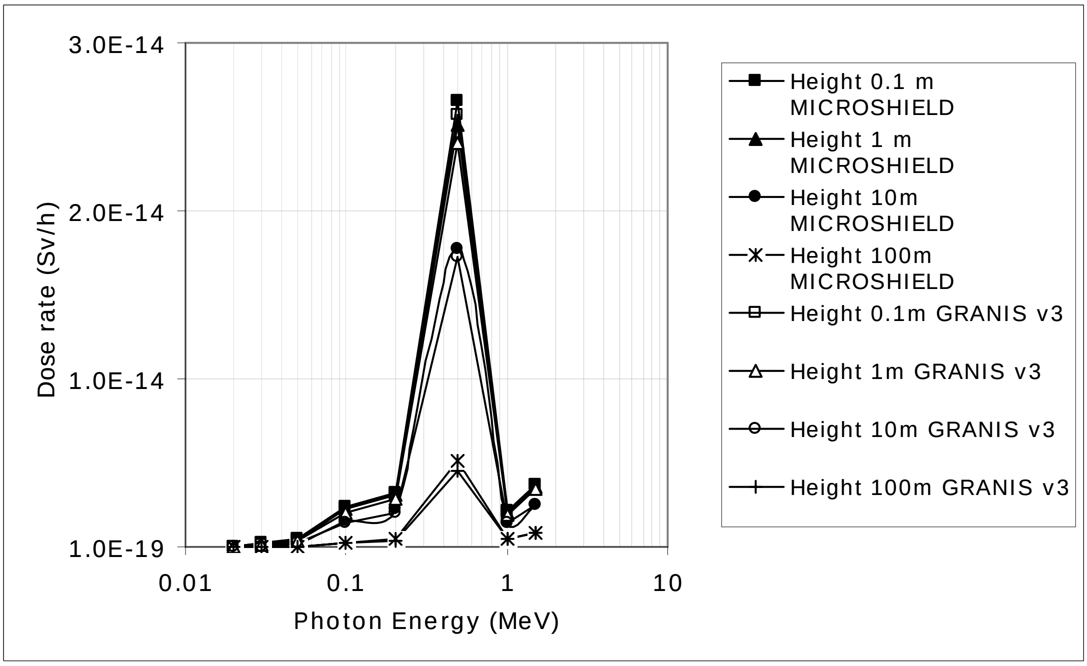


**FIGURE A14 Comparison of dose rates of GRANIS v3 and MICROSHIELD - variation of dose rate with height above the ground**

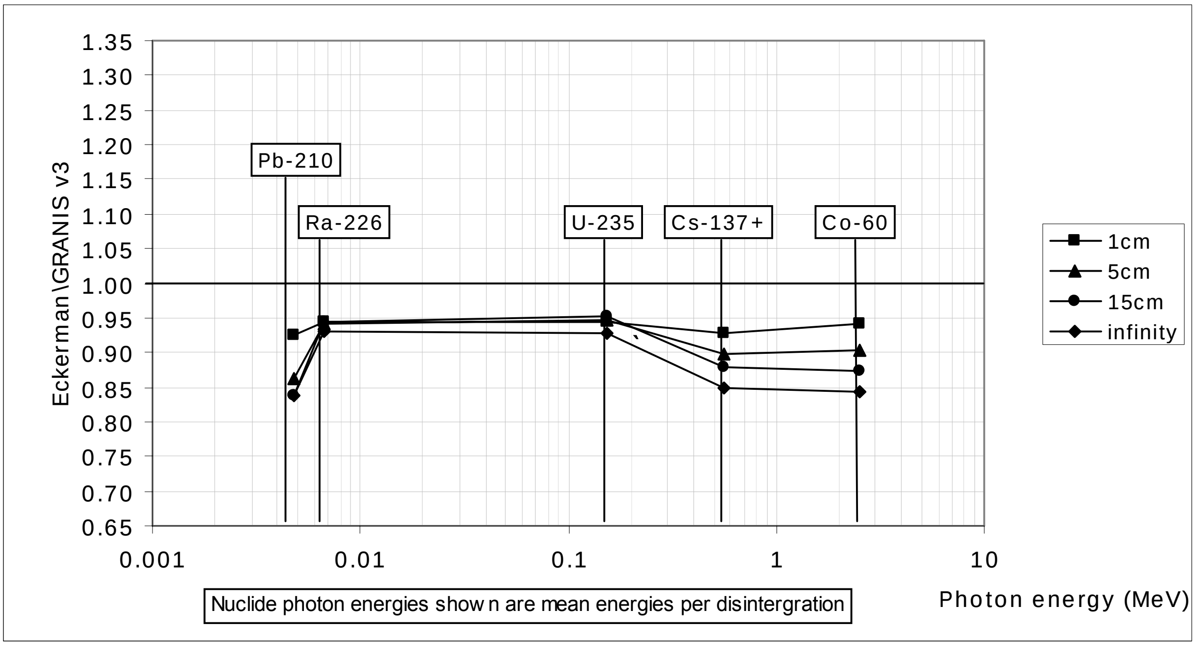


**FIGURE A15 Ratio of dose rates at a height of 1 metre of GRANIS v3 and Eckerman with soil slab thickness**

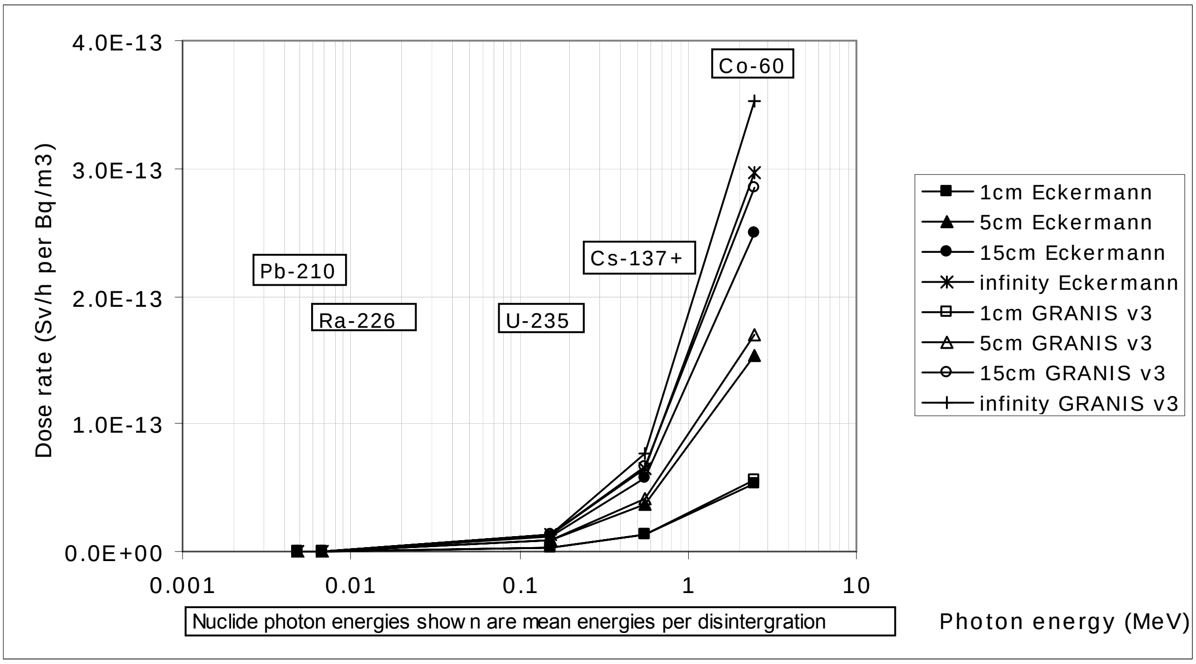


**FIGURE A16 Comparison of dose rates at a height of 1 metre of GRANIS v3 and Eckerman with soil slab thickness**

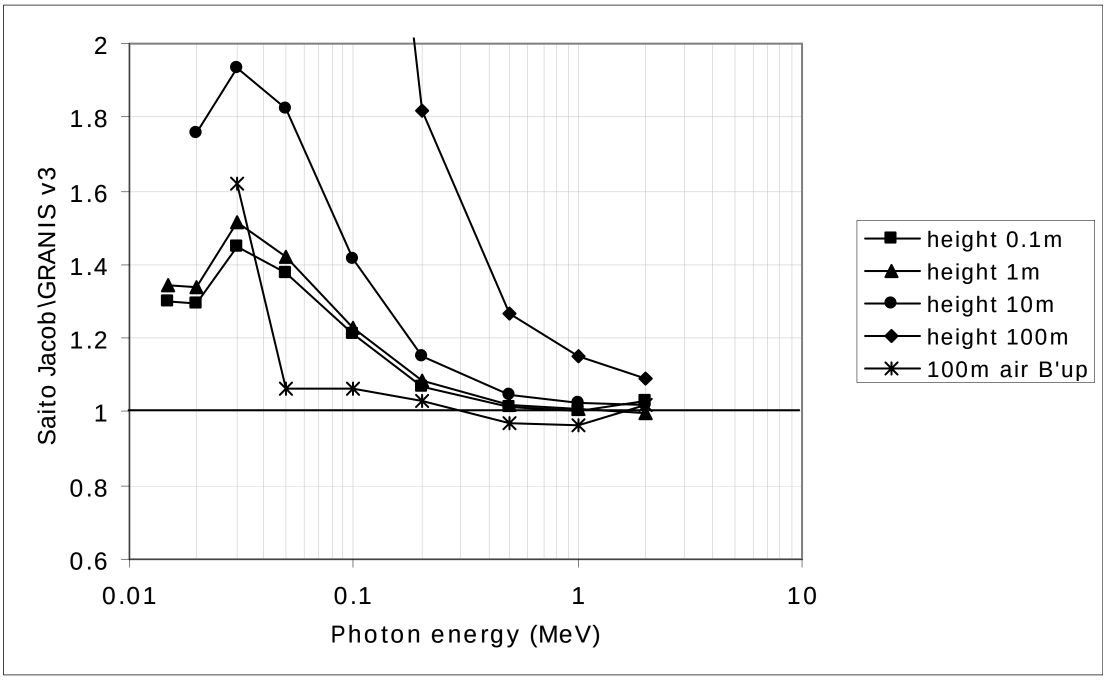


**FIGURE A17 Ratio of dose rates above plane source of GRANIS v3 and Saito/Jacob with soil build up (reference point height)**

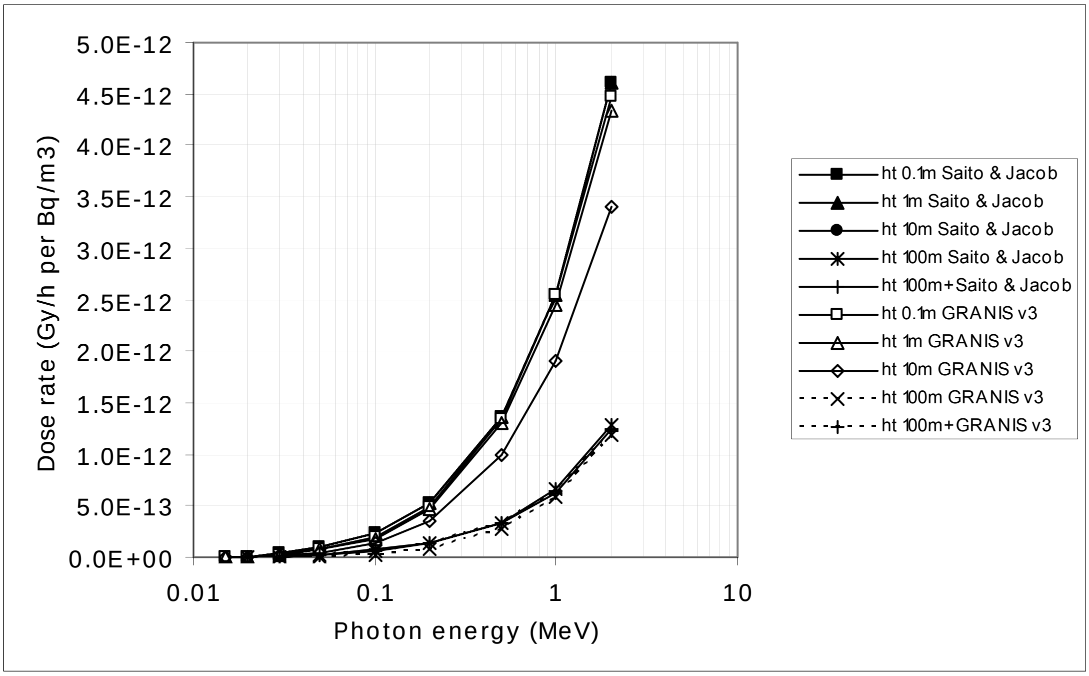


**FIGURE A18 Comparison of dose rates above plane source of GRANIS v3 and Saito/Jacob with soil build up (reference point height)**

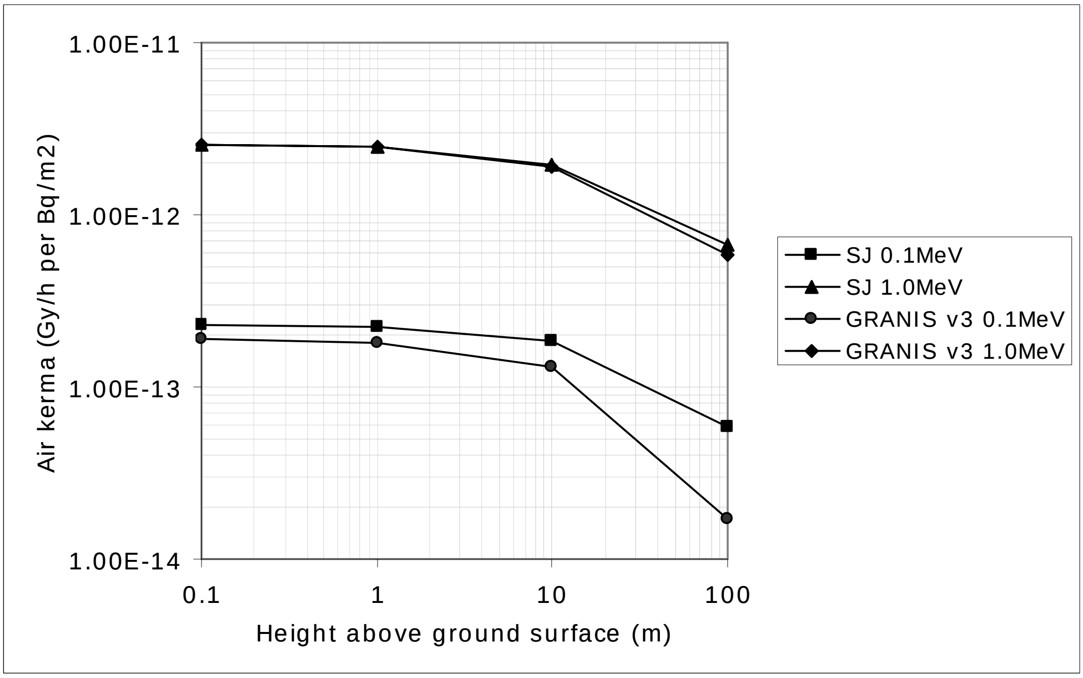


**FIGURE A19 Comparison of GRANIS v3 and Saito/Jacob - variation of dose from plane with height above the ground**

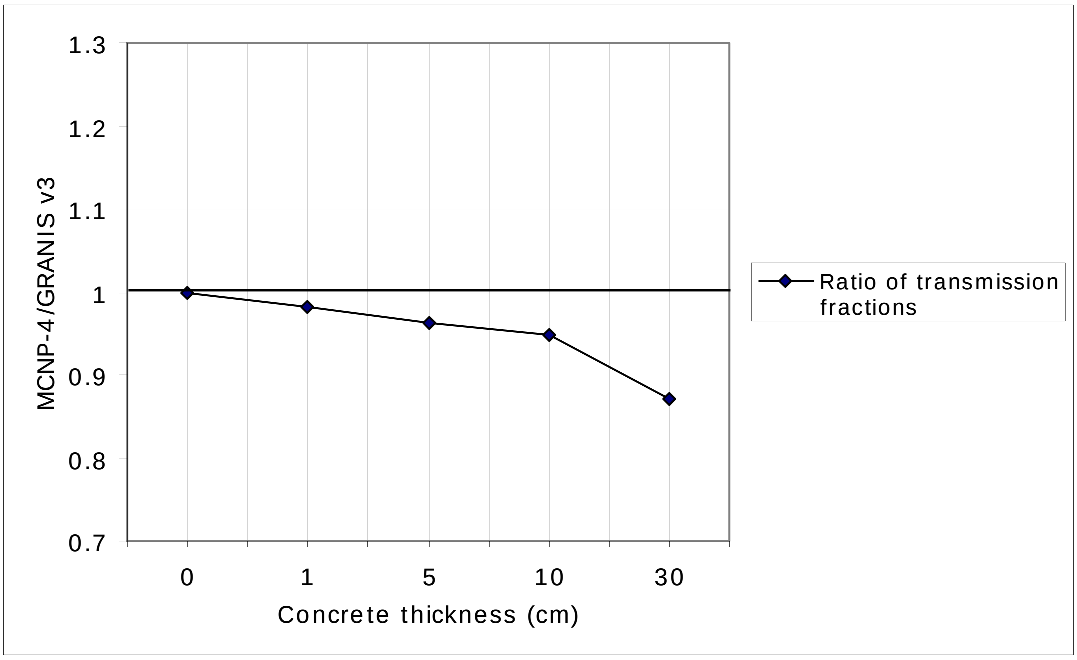


**FIGURE A20 Comparison of GRANIS v3 and MCNP-4 transmission factors for $^{60}$Co contamination shielded by concrete**

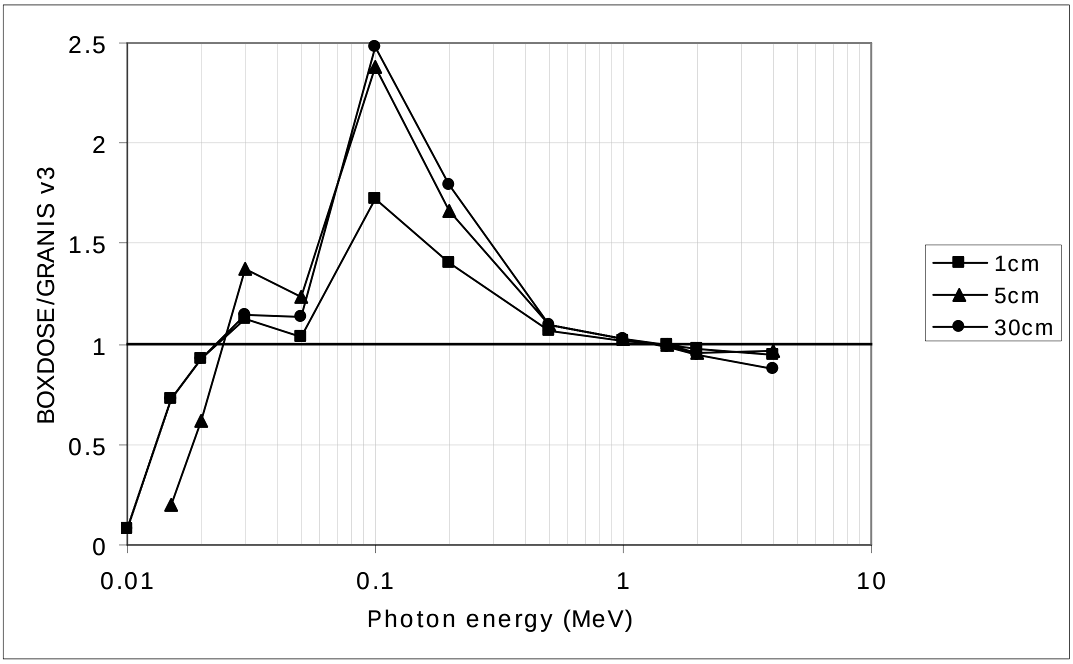


**FIGURE A21 Ratio of dose rates of GRANIS v3 and BOXDOSE (reference point height) for different soil contamination profiles**

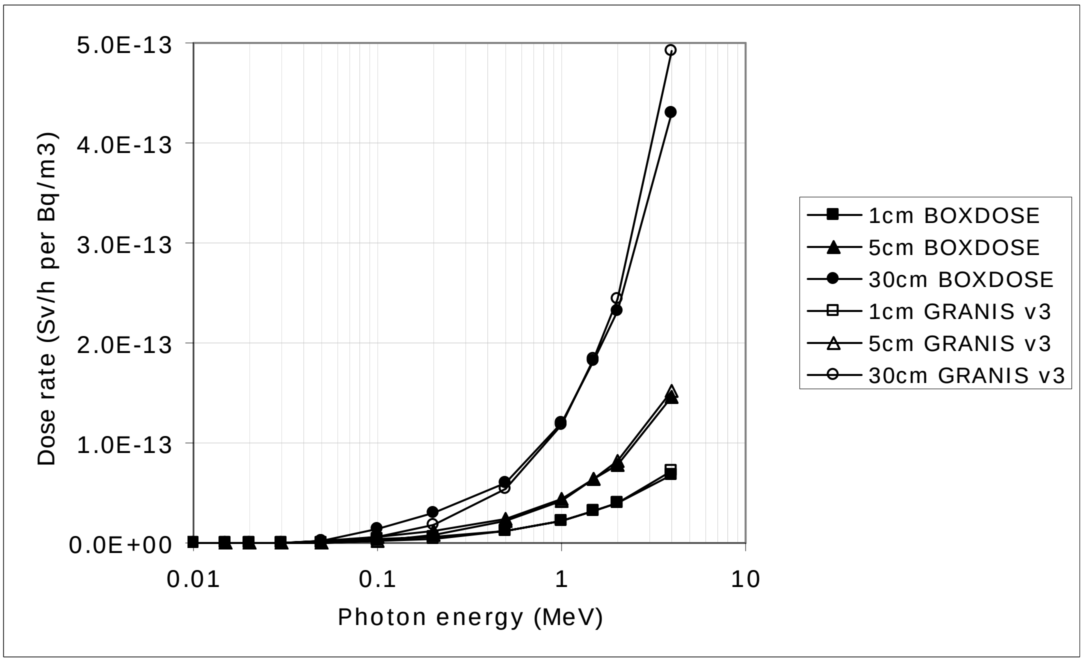


**FIGURE A22 Comparison of dose rates of GRANIS v3 and BOXDOSE (reference point height) for different soil contamination profiles**

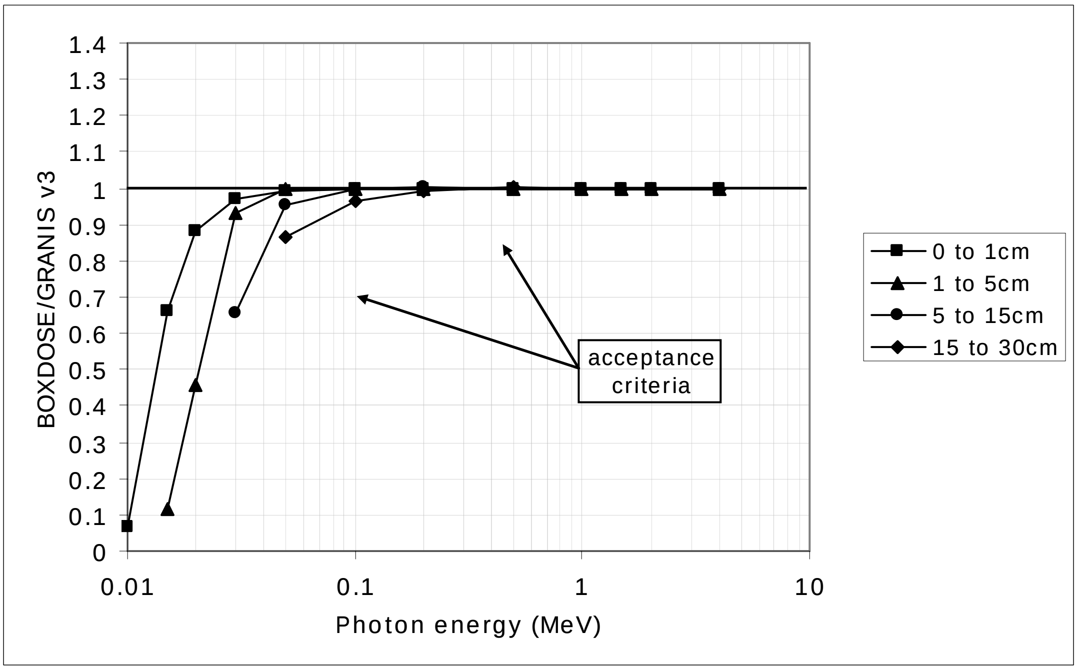


**FIGURE A23 Ratio of dose rates of GRANIS v3 and BOXDOSE (using GRANIS libraries) for different soil contamination profiles**

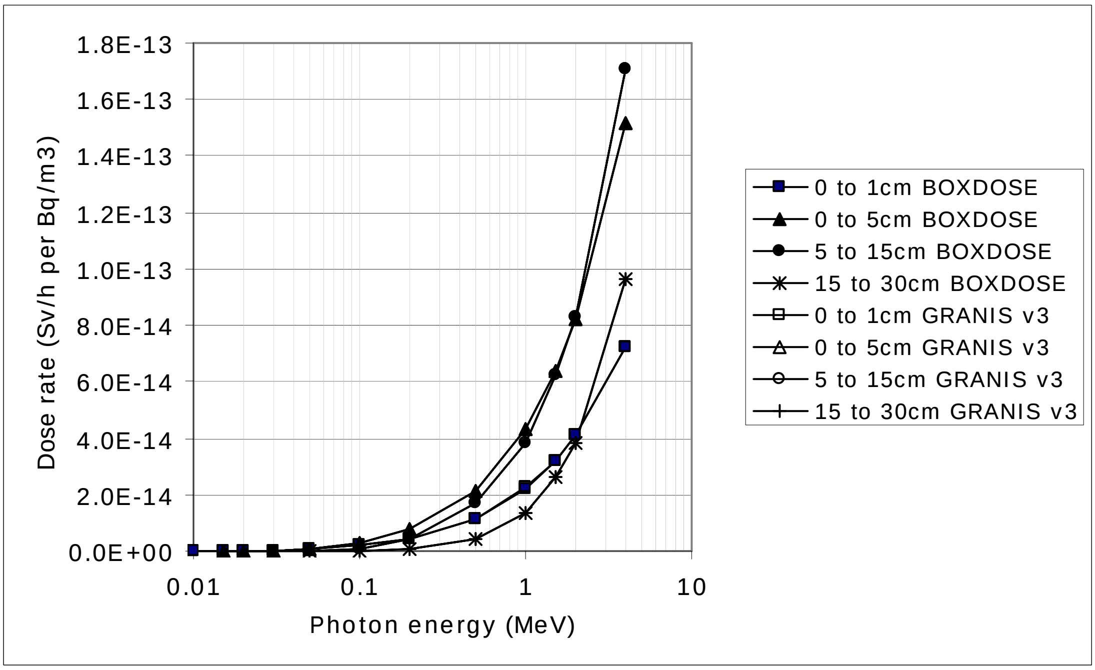


**FIGURE A24 Comparison of dose rates of GRANIS v3 and BOXDOSE (using GRANIS libraries) for different soil contamination profiles**

# APPENDIX B GRANIS V3 LIBRARY FILES

**Table B1 Mass attenuation coefficients for elements (Hubbel, 1982), data file x_sections.lib (version 1)**

| Element | Mass Attenuation Coefficients ($cm^2$ $g^{-1}$) Energy (MeV) | | | | | | | | | | | |
|---|---|---|---|---|---|---|---|---|---|---|---|---|
| | 0.01 | 0.015 | 0.02 | 0.03 | 0.05 | 0.1 | 0.2 | 0.5 | 1 | 1.5 | 2 | 4 |
| Hydrogen | 3.85 $10^{-1}$ | 3.77 $10^{-1}$ | 3.70 $10^{-1}$ | 3.57 $10^{-1}$ | 3.36 $10^{-1}$ | 2.94 $10^{-1}$ | 2.43 $10^{-1}$ | 1.73 $10^{-1}$ | 1.26 $10^{-1}$ | 1.03 $10^{-1}$ | 8.77 $10^{-2}$ | 5.81 $10^{-2}$ |
| Carbon | 2.30 $10^{0}$ | 7.87 $10^{-1}$ | 4.34 $10^{-1}$ | 2.54 $10^{-1}$ | 1.87 $10^{-1}$ | 1.51 $10^{-1}$ | 1.23 $10^{-1}$ | 8.71 $10^{-2}$ | 6.36 $10^{-2}$ | 5.18 $10^{-2}$ | 4.44 $10^{-2}$ | 3.05 $10^{-2}$ |
| Nitrogen | 3.78 $10^{0}$ | 1.21 $10^{0}$ | 6.06 $10^{-1}$ | 3.04 $10^{-1}$ | 1.97 $10^{-1}$ | 1.53 $10^{-1}$ | 1.23 $10^{-1}$ | 8.72 $10^{-2}$ | 6.37 $10^{-2}$ | 5.18 $10^{-2}$ | 4.45 $10^{-2}$ | 3.07 $10^{-2}$ |
| Oxygen | 5.83 $10^{0}$ | 1.80 $10^{0}$ | 8.50 $10^{-1}$ | 3.74 $10^{-1}$ | 2.12 $10^{-1}$ | 1.55 $10^{-1}$ | 1.24 $10^{-1}$ | 8.73 $10^{2}$ | 6.37 $10^{-2}$ | 5.19 $10^{-2}$ | 4.46 $10^{-2}$ | 3.10 $10^{-2}$ |
| Fluorine | 8.03 $10^{0}$ | 2.44 $10^{0}$ | 1.11 $10^{0}$ | 4.43 $10^{-1}$ | 2.20 $10^{-1}$ | 1.50 $10^{-1}$ | 1.18 $10^{-1}$ | 8.28 $10^{-2}$ | 6.04 $10^{-2}$ | 4.92 $10^{-2}$ | 4.23 $10^{-2}$ | 2.96 $10^{-2}$ |
| Sodium | 1.53 $10^{1}$ | 4.62 $10^{0}$ | 2.03 $10^{0}$ | 7.11 $10^{-1}$ | 2.79 $10^{-1}$ | 1.58 $10^{-1}$ | 1.20 $10^{-1}$ | 8.37 $10^{-2}$ | 6.10 $10^{-2}$ | 4.97 $10^{-2}$ | 4.28 $10^{-2}$ | 3.04 $10^{-2}$ |
| Magnesium | 2.07 $10^{1}$ | 6.26 $10^{0}$ | 2.72 $10^{0}$ | 9.19 $10^{-1}$ | 3.27 $10^{-1}$ | 1.68 $10^{-1}$ | 1.25 $10^{-1}$ | 8.65 $10^{-2}$ | 6.30 $10^{-2}$ | 5.13 $10^{-2}$ | 4.43 $10^{-2}$ | 3.16 $10^{-2}$ |
| Aluminium | 2.58 $10^{1}$ | 7.84 $10^{0}$ | 3.39 $10^{0}$ | 1.12 $10^{0}$ | 3.66 $10^{-1}$ | 1.70 $10^{-1}$ | 1.22 $10^{-1}$ | 8.45 $10^{-2}$ | 6.15 $10^{-2}$ | 5.00 $10^{-2}$ | 4.32 $10^{-2}$ | 3.11 $10^{-2}$ |
| Silicon | 3.34 $10^{1}$ | 1.02 $10^{1}$ | 4.40 $10^{0}$ | 1.42 $10^{0}$ | 4.35 $10^{-1}$ | 1.83 $10^{-1}$ | 1.28 $10^{-1}$ | 8.75 $10^{-2}$ | 6.36 $10^{-2}$ | 5.18 $10^{-2}$ | 4.48 $10^{-2}$ | 3.24 $10^{-2}$ |
| Phosphorus | 3.98 $10^{1}$ | 1.22 $10^{1}$ | 5.28 $10^{0}$ | 1.68 $10^{0}$ | 4.88 $10^{-1}$ | 1.86 $10^{-1}$ | 1.25 $10^{-1}$ | 8.51 $10^{-2}$ | 6.18 $10^{-2}$ | 5.04 $10^{-2}$ | 4.36 $10^{-2}$ | 3.17 $10^{-2}$ |
| Sulphur | 4.95 $10^{1}$ | 1.53 $10^{1}$ | 6.63 $10^{0}$ | 2.09 $10^{0}$ | 5.80 $10^{-1}$ | 2.02 $10^{-1}$ | 1.30 $10^{-1}$ | 8.78 $10^{-2}$ | 6.37 $10^{-2}$ | 5.20 $10^{-2}$ | 4.50 $10^{-2}$ | 3.29 $10^{-2}$ |
| Argon | 6.32 $10^{1}$ | 1.97 $10^{1}$ | 8.53 $10^{0}$ | 2.67 $10^{0}$ | 6.96 $10^{-1}$ | 2.04 $10^{-1}$ | 1.20 $10^{-1}$ | 7.96 $10^{-2}$ | 5.76 $10^{-2}$ | 4.70 $10^{-2}$ | 4.07 $10^{-2}$ | 3.02 $10^{-2}$ |
| Potassium | 7.82 $10^{1}$ | 2.48 $10^{1}$ | 1.08 $10^{1}$ | 3.38 $10^{0}$ | 8.61 $10^{-1}$ | 2.34 $10^{-1}$ | 1.32 $10^{-1}$ | 8.60 $10^{-2}$ | 6.22 $10^{-2}$ | 5.07 $10^{-2}$ | 4.40 $10^{-2}$ | 3.28 $10^{-2}$ |
| Calcium | 9.23 $10^{1}$ | 2.95 $10^{1}$ | 1.29 $10^{1}$ | 4.04 $10^{0}$ | 1.01 $10^{0}$ | 2.56 $10^{-1}$ | 1.37 $10^{-1}$ | 8.85 $10^{2}$ | 6.39 $10^{-2}$ | 5.21 $10^{-2}$ | 4.52 $10^{-2}$ | 3.40 $10^{-2}$ |
| Titanium | 1.10 $10^{2}$ | 3.55 $10^{1}$ | 1.57 $10^{1}$ | 4.93 $10^{0}$ | 1.20 $10^{0}$ | 2.71 $10^{-1}$ | 1.31 $10^{-1}$ | 8.19 $10^{-2}$ | 5.89 $10^{-2}$ | 4.80 $10^{-2}$ | 4.18 $10^{-2}$ | 3.17 $10^{-2}$ |
| Manganese | 1.50 $10^{2}$ | 4.98 $10^{1}$ | 2.23 $10^{1}$ | 7.08 $10^{0}$ | 1.70 $10^{0}$ | 3.35 $10^{-1}$ | 1.39 $10^{-1}$ | 8.19 $10^{-2}$ | 5.85 $10^{-2}$ | 4.77 $10^{-2}$ | 4.16 $10^{-2}$ | 3.23 $10^{-2}$ |
| Iron | 1.69 $10^{2}$ | 5.66 $10^{1}$ | 2.55 $10^{1}$ | 8.11 $10^{0}$ | 1.94 $10^{0}$ | 3.70 $10^{-1}$ | 1.46 $10^{-1}$ | 8.41 $10^{-2}$ | 5.99 $10^{-2}$ | 4.88 $10^{-2}$ | 4.27 $10^{-2}$ | 3.31 $10^{-2}$ |
| Barium | 1.86 $10^{2}$ | 6.35 $10^{1}$ | 2.94 $10^{1}$ | 9.90 $10^{0}$ | 1.38 $10^{1}$ | 2.20 $10^{0}$ | 4.05 $10^{-1}$ | 9.92 $10^{-2}$ | 5.80 $10^{-2}$ | 4.59 $10^{-2}$ | 4.08 $10^{-2}$ | 3.60 $10^{-2}$ |
| Cerium | 2.08 $10^{2}$ | 7.14 $10^{1}$ | 3.31 $10^{1}$ | 1.12 $10^{1}$ | 1.52 $10^{1}$ | 2.45 $10^{0}$ | 4.45 $10^{-1}$ | 1.04 $10^{-1}$ | 5.96 $10^{-2}$ | 4.70 $10^{-2}$ | 4.18 $10^{-2}$ | 3.70 $10^{-2}$ |
| Lead | 1.31 $10^{2}$ | 1.12 $10^{2}$ | 8.64 $10^{1}$ | 3.03 $10^{1}$ | 8.04 $10^{0}$ | 5.55 $10^{0}$ | 9.99 $10^{-1}$ | 1.61 $10^{-1}$ | 7.10 $10^{-2}$ | 5.22 $10^{-2}$ | 4.61 $10^{-2}$ | 4.20 $10^{-2}$ |

**Table B2 Build-up factor for concrete (Jaeger et al, 1968), data file buildup.lib (version 1)**

| Mean free path | Build-up factor | | | | | | | | | | | |
|---|---|---|---|---|---|---|---|---|---|---|---|---|
| | Energy (MeV) | | | | | | | | | | | |
| | 0.01 | 0.015 | 0.02 | 0.03 | 0.05 | 0.1 | 0.2 | 0.5 | 1 | 1.5 | 2 | 4 |
| 0 | 1.00 | 1.00 | 1.00 | 1.00 | 1.00 | 1.00 | 1.00 | 1.00 | 1.00 | 1.00 | 1.00 | 1.00 |
| 0.5 | 1.00 | 1.00 | 1.01 | 1.05 | 1.49 | 1.89 | 1.78 | 1.57 | 1.45 | 1.41 | 1.37 | 1.30 |
| 1 | 1.00 | 1.01 | 1.03 | 1.10 | 1.81 | 2.78 | 2.72 | 2.27 | 1.98 | 1.88 | 1.77 | 1.61 |
| 2 | 1.00 | 1.02 | 1.06 | 1.19 | 2.29 | 4.63 | 5.05 | 4.03 | 3.24 | 2.95 | 2.65 | 2.24 |
| 3 | 1.00 | 1.03 | 1.08 | 1.27 | 2.71 | 6.63 | 8.00 | 6.26 | 4.72 | 4.16 | 3.60 | 2.89 |
| 4 | 1.00 | 1.04 | 1.10 | 1.35 | 3.09 | 8.80 | 11.6 | 8.97 | 6.42 | 5.52 | 4.61 | 3.56 |
| 5 | 1.00 | 1.04 | 1.12 | 1.42 | 3.46 | 11.1 | 15.9 | 12.2 | 8.33 | 7.01 | 5.68 | 4.25 |
| 6 | 1.00 | 1.05 | 1.14 | 1.48 | 3.80 | 13.6 | 20.9 | 15.9 | 10.4 | 8.60 | 6.80 | 4.97 |
| 7 | 1.00 | 1.06 | 1.16 | 1.54 | 4.13 | 16.3 | 26.7 | 20.2 | 12.7 | 10.3 | 7.97 | 5.70 |
| 8 | 1.00 | 1.06 | 1.17 | 1.60 | 4.45 | 19.2 | 33.4 | 25.0 | 15.2 | 12.2 | 9.18 | 6.45 |
| 10 | 1.00 | 1.07 | 1.20 | 1.70 | 5.07 | 25.6 | 49.6 | 36.4 | 20.7 | 16.2 | 11.7 | 8.00 |
| 15 | 1.00 | 1.10 | 1.24 | 1.87 | 6.59 | 44.9 | 109 | 75.6 | 37.2 | 27.9 | 18.6 | 12.1 |
| 20 | 1.00 | 1.11 | 1.26 | 1.97 | 7.99 | 69.1 | 201 | 131 | 57.1 | 41.6 | 26.0 | 16.4 |
| 25 | 1.00 | 1.12 | 1.27 | 2.02 | 9.36 | 97.9 | 331 | 203 | 80.1 | 57.0 | 33.9 | 20.9 |
| 30 | 1.00 | 1.13 | 1.26 | 2.02 | 11.0 | 131 | 507 | 292 | 106 | 74.1 | 42.2 | 25.6 |
| 35 | 1.00 | 1.13 | 1.25 | 1.99 | 12.9 | 170 | 734 | 399 | 134 | 92.5 | 50.9 | 30.6 |
| 40 | 1.00 | 1.13 | 1.23 | 1.95 | 15.3 | 214 | 1020 | 523 | 164 | 112 | 59.8 | 36.5 |

**Table B3 Build-up factor for water (Jaeger et al, 1968), data file buildup.lib (version 1)**

| Mean free path | Build-up factor | | | | | | | | | | | |
|---|---|---|---|---|---|---|---|---|---|---|---|---|
| | Energy (MeV) | | | | | | | | | | | |
| | 0.01 | 0.015 | 0.02 | 0.03 | 0.05 | 0.1 | 0.2 | 0.5 | 1 | 1.5 | 2 | 4 |
| 0 | 1.00 | 1.00 | 1.00 | 1.00 | 1.00 | 1.00 | 1.00 | 1.00 | 1.00 | 1.00 | 1.00 | 1.00 |
| 0.5 | 1.00 | 1.04 | 1.13 | 1.50 | 3.19 | 2.36 | 1.92 | 1.61 | 1.47 | 1.43 | 1.38 | 1.32 |
| 1 | 1.00 | 1.09 | 1.25 | 2.00 | 5.38 | 4.52 | 3.42 | 2.45 | 2.08 | 1.96 | 1.83 | 1.66 |
| 2 | 1.00 | 1.17 | 1.49 | 3.00 | 9.82 | 11.7 | 8.22 | 4.87 | 3.62 | 3.22 | 2.82 | 2.34 |
| 3 | 1.00 | 1.24 | 1.71 | 3.98 | 14.3 | 23.5 | 15.7 | 8.29 | 5.50 | 4.69 | 3.87 | 3.04 |
| 4 | 1.00 | 1.31 | 1.92 | 4.94 | 18.8 | 40.6 | 26.4 | 12.7 | 7.66 | 6.33 | 4.99 | 3.74 |
| 5 | 1.00 | 1.38 | 2.11 | 5.90 | 23.4 | 64.0 | 41.3 | 18.1 | 10.1 | 8.13 | 6.16 | 4.47 |
| 6 | 1.00 | 1.44 | 2.29 | 6.85 | 28.1 | 94.8 | 61.0 | 24.6 | 12.8 | 10.1 | 7.38 | 5.22 |
| 7 | 1.00 | 1.49 | 2.45 | 7.78 | 32.8 | 134 | 86.2 | 32.2 | 15.7 | 12.2 | 8.66 | 5.98 |
| 8 | 1.00 | 1.54 | 2.61 | 8.70 | 37.5 | 183 | 118 | 40.8 | 18.9 | 14.4 | 9.97 | 6.75 |
| 10 | 1.00 | 1.63 | 2.89 | 10.5 | 47.2 | 314 | 202 | 61.8 | 26.0 | 19.4 | 12.7 | 8.33 |
| 15 | 1.00 | 1.79 | 3.41 | 14.8 | 72.2 | 917 | 582 | 137 | 47.4 | 33.8 | 20.1 | 12.4 |
| 20 | 1.00 | 1.88 | 3.74 | 18.9 | 98.7 | 2120 | 1310 | 247 | 73.5 | 50.8 | 28.0 | 16.7 |
| 25 | 1.00 | 1.91 | 3.92 | 22.7 | 127 | 4260 | 2580 | 395 | 104 | 70.2 | 36.4 | 21.1 |
| 30 | 1.00 | 1.92 | 3.99 | 26.3 | 156 | 7780 | 4640 | 582 | 138 | 91.6 | 45.2 | 25.7 |
| 35 | 1.00 | 1.89 | 3.97 | 29.7 | 187 | 13100 | 7890 | 809 | 175 | 115 | 54.3 | 30.3 |
| 40 | 1.00 | 1.85 | 3.89 | 32.8 | 220 | 20300 | 12800 | 1080 | 214 | 139 | 63.6 | 35.0 |

**Table B4 Build-up factor for iron (Jaeger et al, 1968), data file buildup.lib (version 1)**

| | Build-up factor | | | | | | | | | | | |
|---|---|---|---|---|---|---|---|---|---|---|---|---|
| Mean free path | Energy (MeV) | | | | | | | | | | | |
| | 0.01 | 0.015 | 0.02 | 0.03 | 0.05 | 0.1 | 0.2 | 0.5 | 1 | 1.5 | 2 | 4 |
| 0 | 1.00 | 1.00 | 1.00 | 1.00 | 1.00 | 1.00 | 1.00 | 1.00 | 1.00 | 1.00 | 1.00 | 1.00 |
| 0.5 | 1.00 | 1.00 | 1.01 | 1.00 | 1.08 | 1.26 | 1.47 | 1.48 | 1.41 | 1.38 | 1.35 | 1.30 |
| 1 | 1.00 | 1.00 | 1.02 | 1.01 | 1.11 | 1.40 | 1.86 | 1.99 | 1.85 | 1.78 | 1.71 | 1.58 |
| 2 | 1.00 | 1.00 | 1.04 | 1.02 | 1.15 | 1.61 | 2.59 | 3.12 | 2.85 | 2.67 | 2.49 | 2.14 |
| 3 | 1.00 | 1.00 | 1.05 | 1.03 | 1.17 | 1.78 | 3.33 | 4.44 | 4.00 | 3.67 | 3.34 | 2.75 |
| 4 | 1.00 | 1.00 | 1.07 | 1.03 | 1.20 | 1.94 | 4.08 | 5.96 | 5.30 | 4.78 | 4.25 | 3.40 |
| 5 | 1.00 | 1.00 | 1.09 | 1.04 | 1.22 | 2.07 | 4.85 | 7.68 | 6.74 | 5.98 | 5.22 | 4.09 |
| 6 | 1.00 | 1.00 | 1.10 | 1.05 | 1.23 | 2.20 | 5.64 | 9.58 | 8.31 | 7.28 | 6.25 | 4.82 |
| 7 | 1.00 | 1.00 | 1.11 | 1.05 | 1.25 | 2.31 | 6.44 | 11.7 | 10.0 | 8.67 | 7.33 | 5.60 |
| 8 | 1.00 | 1.00 | 1.12 | 1.06 | 1.26 | 2.41 | 7.25 | 14.0 | 11.8 | 10.1 | 8.45 | 6.40 |
| 10 | 1.00 | 1.00 | 1.15 | 1.07 | 1.28 | 2.61 | 8.90 | 19.1 | 15.8 | 13.3 | 10.8 | 8.10 |
| 15 | 1.00 | 1.00 | 1.19 | 1.09 | 1.33 | 3.01 | 13.2 | 35.1 | 27.5 | 22.5 | 17.4 | 12.9 |
| 20 | 1.00 | 1.00 | 1.21 | 1.10 | 1.36 | 3.33 | 17.6 | 55.4 | 41.3 | 33.0 | 24.6 | 18.3 |
| 25 | 1.00 | 1.00 | 1.22 | 1.10 | 1.38 | 3.61 | 22.2 | 79.9 | 57.0 | 44.8 | 32.5 | 24.4 |
| 30 | 1.00 | 1.00 | 1.23 | 1.10 | 1.41 | 3.86 | 26.9 | 108 | 74.5 | 57.7 | 40.9 | 30.9 |
| 35 | 1.00 | 1.00 | 1.23 | 1.10 | 1.42 | 4.07 | 31.7 | 141 | 93.5 | 71.7 | 49.8 | 37.9 |
| 40 | 1.00 | 1.00 | 1.22 | 1.09 | 1.44 | 4.23 | 36.4 | 177 | 114 | 86.6 | 59.1 | 45.6 |

**Table B5 Build-up factor for lead (Jaeger et al, 1968), data file buildup.lib (version 1)**

| Mean free path | Build-up factor | | | | | | | | | | | |
|---|---|---|---|---|---|---|---|---|---|---|---|---|
| | Energy (MeV) | | | | | | | | | | | |
| | 0.01 | 0.015 | 0.02 | 0.03 | 0.05 | 0.1 | 0.2 | 0.5 | 1 | 1.5 | 2 | 4 |
| 0 | 1.00 | 1.00 | 1.00 | 1.00 | 1.00 | 1.00 | 1.00 | 1.00 | 1.00 | 1.00 | 1.00 | 1.00 |
| 0.5 | 1.00 | 1.00 | 1.00 | 1.00 | 1.02 | 2.05 | 1.81 | 1.84 | 1.93 | 1.86 | 1.78 | 1.39 |
| 1 | 1.00 | 1.00 | 1.00 | 1.00 | 1.02 | 2.78 | 1.83 | 1.72 | 1.95 | 1.96 | 1.96 | 1.54 |
| 2 | 1.00 | 1.00 | 1.00 | 1.00 | 1.03 | 4.70 | 1.85 | 1.90 | 2.28 | 2.29 | 2.29 | 1.85 |
| 3 | 1.00 | 1.00 | 1.00 | 1.00 | 1.04 | 8.24 | 1.87 | 2.11 | 2.74 | 2.77 | 2.80 | 2.19 |
| 4 | 1.00 | 1.00 | 1.00 | 1.00 | 1.04 | 14.2 | 1.89 | 2.28 | 3.14 | 3.24 | 3.34 | 2.57 |
| 5 | 1.00 | 1.00 | 1.00 | 1.00 | 1.04 | 23.6 | 1.91 | 2.42 | 3.51 | 3.70 | 3.88 | 2.98 |
| 6 | 1.00 | 1.00 | 1.00 | 1.00 | 1.05 | 38.7 | 1.92 | 2.55 | 3.86 | 4.14 | 4.42 | 3.41 |
| 7 | 1.00 | 1.00 | 1.00 | 1.00 | 1.05 | 63.4 | 1.94 | 2.67 | 4.20 | 4.58 | 4.95 | 3.88 |
| 8 | 1.00 | 1.00 | 1.00 | 1.00 | 1.06 | 104 | 1.96 | 2.78 | 4.53 | 5.02 | 5.50 | 4.39 |
| 10 | 1.00 | 1.00 | 1.00 | 1.00 | 1.06 | 292 | 1.98 | 2.97 | 5.14 | 5.89 | 6.63 | 5.53 |
| 15 | 1.00 | 1.00 | 1.00 | 1.00 | 1.06 | 4150 | 2.04 | 3.37 | 6.53 | 8.04 | 9.55 | 9.28 |
| 20 | 1.00 | 1.00 | 1.00 | 1.00 | 1.07 | $5.95\ 10^{4}$ | 2.08 | 3.69 | 7.78 | 10.2 | 12.6 | 14.8 |
| 25 | 1.00 | 1.00 | 1.00 | 1.00 | 1.08 | $8.70\ 10^{5}$ | 2.11 | 3.96 | 8.93 | 12.4 | 15.8 | 22.9 |
| 30 | 1.00 | 1.00 | 1.00 | 1.00 | 1.08 | $1.30\ 10^{7}$ | 2.13 | 4.20 | 10.0 | 14.6 | 19.2 | 34.7 |
| 35 | 1.00 | 1.00 | 1.00 | 1.00 | 1.08 | $2.22\ 10^{8}$ | 2.16 | 4.40 | 11.1 | 16.8 | 22.5 | 51.6 |
| 40 | 1.00 | 1.00 | 1.00 | 1.00 | 1.08 | $3.80\ 10^{9}$ | 2.17 | 4.54 | 12.1 | 18.9 | 25.6 | 75.2 |

**Table B6 Build-up factor for air (Jaeger et al, 1968), data file buildup.lib (version 1)**

| | Build-up factor | | | | | | | | | | | |
|---|---|---|---|---|---|---|---|---|---|---|---|---|
| Mean free path | Energy (MeV) | | | | | | | | | | | |
| | 0.01 | 0.015 | 0.02 | 0.03 | 0.05 | 0.1 | 0.2 | 0.5 | 1 | 1.5 | 2 | 4 |
| 0 | 1.00 | 1.00 | 1.00 | 1.00 | 1.00 | 1.00 | 1.00 | 1.00 | 1.00 | 1.00 | 1.00 | 1.00 |
| 0.5 | 1.01 | 1.05 | 1.13 | 1.52 | 2.81 | 3.19 | 2.46 | 1.92 | 1.65 | 1.53 | 1.45 | 1.30 |
| 1 | 1.02 | 1.09 | 1.25 | 2.03 | 4.76 | 5.75 | 4.17 | 2.93 | 2.34 | 2.08 | 1.91 | 1.60 |
| 2 | 1.05 | 1.17 | 1.48 | 3.03 | 9.09 | 12.2 | 8.50 | 5.28 | 3.84 | 3.23 | 2.86 | 2.19 |
| 3 | 1.07 | 1.25 | 1.69 | 3.99 | 14.1 | 20.8 | 14.3 | 8.10 | 5.50 | 4.45 | 3.85 | 2.79 |
| 4 | 1.08 | 1.31 | 1.88 | 4.91 | 19.7 | 32.2 | 22.0 | 11.5 | 7.35 | 5.76 | 4.88 | 3.39 |
| 5 | 1.10 | 1.38 | 2.05 | 5.79 | 26.2 | 47.0 | 32.0 | 15.5 | 9.39 | 7.16 | 5.96 | 3.99 |
| 6 | 1.11 | 1.43 | 2.20 | 6.64 | 33.5 | 66.1 | 45.1 | 20.2 | 11.6 | 8.64 | 7.08 | 4.59 |
| 7 | 1.13 | 1.48 | 2.34 | 7.46 | 41.8 | 90.6 | 61.8 | 25.8 | 14.1 | 10.2 | 8.25 | 5.19 |
| 8 | 1.14 | 1.52 | 2.46 | 8.24 | 51.1 | 122 | 83.2 | 32.4 | 16.9 | 11.9 | 9.47 | 5.80 |
| 10 | 1.16 | 1.60 | 2.67 | 9.71 | 73.5 | 211 | 145 | 49.0 | 23.2 | 15.6 | 12.0 | 7.01 |
| 15 | 1.19 | 1.71 | 2.98 | 12.9 | 158 | 719 | 501 | 120 | 45.1 | 26.9 | 19.5 | 10.1 |
| 20 | 1.20 | 1.75 | 3.10 | 15.4 | 3027 | 2190 | 1540 | 265 | 78.7 | 41.9 | 28.4 | 13.2 |
| 25 | 1.20 | 1.74 | 3.08 | 17.3 | 542 | 6240 | 4470 | 547 | 130 | 61.5 | 39.1 | 16.3 |
| 30 | 1.19 | 1.71 | 2.98 | 18.8 | 936 | $1.71\ 10^{4}$ | $1.24\ 10^{4}$ | 1090 | 205 | 87.0 | 51.9 | 19.4 |
| 35 | 1.17 | 1.65 | 2.83 | 19.9 | 1570 | $4.55\ 10^{4}$ | $3.36\ 10^{4}$ | 2100 | 316 | 1200 | 67.2 | 22.6 |
| 40 | 1.16 | 1.59 | 2.66 | 20.6 | 2580 | $1.19\ 10^{5}$ | $8.89\ 10^{4}$ | 3980 | 477 | 162 | 85.2 | 25.8 |

**Table B7 Dose conversion factors for rotational geometry (ICRP, 1987), data file dose_factors.lib (version 1)**

| MeV | Air | Effective | Gonads | Breast | Thyroid | Skin |
|---|---|---|---|---|---|---|
| 0.01 | 7.43 $10^{-12}$ | 2.90 $10^{-14}$ | 9.00 $10^{-15}$ | 1.79 $10^{-13}$ | 1.00 $10^{-20}$ | 3.00 $10^{-12}$ |
| 0.015 | 3.12 $10^{-12}$ | 7.10 $10^{-14}$ | 1.40 $10^{-13}$ | 2.87 $10^{-13}$ | 7.20 $10^{-14}$ | 1.43 $10^{-12}$ |
| 0.02 | 1.68 $10^{-12}$ | 1.10 $10^{-13}$ | 1.79 $10^{-13}$ | 2.98 $10^{-13}$ | 1.62 $10^{-13}$ | 8.07 $10^{-13}$ |
| 0.03 | 7.21 $10^{-13}$ | 1.66 $10^{-13}$ | 2.16 $10^{-13}$ | 2.96 $10^{-13}$ | 2.57$10^{-13}$ | 4.03 $10^{-13}$ |
| 0.05 | 3.23 $10^{-13}$ | 2.22 $10^{-13}$ | 2.07 $10^{-13}$ | 2.43 $10^{-13}$ | 2.81 $10^{-13}$ | 2.59 $10^{-13}$ |
| 0.1 | 3.71 $10^{-13}$ | 3.57 $10^{-13}$ | 3.41 $10^{-13}$ | 3.44 $10^{-13}$ | 4.43 $10^{-13}$ | 3.65 $10^{-13}$ |
| 0.2 | 8.56 $10^{-13}$ | 7.31 $10^{-13}$ | 6.94 $10^{-13}$ | 7.25 $10^{-13}$ | 8.67 $10^{-13}$ | 8.02 $10^{-13}$ |
| 0.5 | 2.38 $10^{-12}$ | 1.96 $10^{-12}$ | 1.91 $10^{-12}$ | 1.94 $10^{-12}$ | 2.25 $10^{-12}$ | 2.15 $10^{-12}$ |
| 1 | 4.47 $10^{-12}$ | 3.75 $10^{-12}$ | 3.73 $10^{-12}$ | 3.72 $10^{-12}$ | 4.28 $10^{-12}$ | 4.17 $10^{-12}$ |
| 1.5 | 6.12 $10^{-12}$ | 5.24 $10^{-12}$ | 4.99 $10^{-12}$ | 5.30 $10^{-12}$ | 6.08 $10^{-12}$ | 5.73 $10^{-12}$ |
| 2 | 7.50 $10^{-12}$ | 6.56 $10^{-12}$ | 6.25 $10^{-12}$ | 6.68 $10^{-12}$ | 7.62 $10^{-12}$ | 7.04 $10^{-12}$ |
| 4 | 1.20 $10^{-11}$ | 1.10 $10^{-11}$ | 1.07 $10^{-11}$ | 1.09 $10^{-11}$ | 1.26 $10^{-11}$ | 1.14 $10^{-11}$ |

**Table B8 Modified dose conversion factors for rotational geometry (ICRP, 1996), data file dose_factors.lib (version 1)**

| MeV | Air | Effective | Gonads | Breast | Thyroid | Skin |
|---|---|---|---|---|---|---|
| 0.01 | 7.43 $10^{-12}$ | 2.42 $10^{-14}$ | 2.76 $10^{-14}$ | 6.46 $10^{-14}$ | 2.15 $10^{-15}$ | 1.49 $10^{-12}$ |
| 0.015 | 3.12 $10^{-12}$ | 4.77 $10^{-14}$ | 8.89 $10^{-14}$ | 2.33 $10^{-13}$ | 7.08 $10^{-14}$ | 1.03 $10^{-12}$ |
| 0.02 | 1.68 $10^{-12}$ | 7.76 $10^{-14}$ | 1.28 $10^{-13}$ | 3.33 $10^{-13}$ | 2.03 $10^{-13}$ | 7.27 $10^{-13}$ |
| 0.03 | 7.21 $10^{-13}$ | 1.38 $10^{-13}$ | 1.61 $10^{-13}$ | 3.24 $10^{-13}$ | 2.95$10^{-13}$ | 4.19 $10^{-13}$ |
| 0.05 | 3.23 $10^{-13}$ | 2.14 $10^{-13}$ | 2.09 $10^{-13}$ | 2.62 $10^{-13}$ | 3.13 $10^{-13}$ | 2.68 $10^{-13}$ |
| 0.1 | 3.71 $10^{-13}$ | 3.56 $10^{-13}$ | 3.44 $10^{-13}$ | 3.55 $10^{-13}$ | 4.56 $10^{-13}$ | 3.62 $10^{-13}$ |
| 0.2 | 8.56 $10^{-13}$ | 7.31 $10^{-13}$ | 7.13 $10^{-13}$ | 7.49 $10^{-13}$ | 9.49 $10^{-13}$ | 7.93 $10^{-13}$ |
| 0.5 | 2.38 $10^{-12}$ | 1.93 $10^{-12}$ | 1.87 $10^{-12}$ | 2.03 $10^{-12}$ | 2.43 $10^{-12}$ | 2.14 $10^{-12}$ |
| 1 | 4.47 $10^{-12}$ | 3.71 $10^{-12}$ | 3.55 $10^{-12}$ | 3.90 $10^{-12}$ | 4.61 $10^{-12}$ | 4.09 $10^{-12}$ |
| 1.5 | 6.14 $10^{-12}$ | 5.23 $10^{-12}$ | 5.03 $10^{-12}$ | 5.45 $10^{-12}$ | 6.40 $10^{-12}$ | 5.69 $10^{-12}$ |
| 2 | 7.54 $10^{-12}$ | 6.57 $10^{-12}$ | 6.36 $10^{-12}$ | 6.80 $10^{-12}$ | 7.95 $10^{-12}$ | 7.08 $10^{-12}$ |
| 4 | 1.21 $10^{-11}$ | 1.10 $10^{-11}$ | 1.09 $10^{-11}$ | 1.12 $10^{-11}$ | 1.29 $10^{-11}$ | 1.15 $10^{-11}$ |

**Table B9 Gamma ray production data (Eckerman et al, 1993), data file orlnspec.dat (version 1)**

| Nuclide | Gamma production fraction | | | | | | | | | | | |
|---|---|---|---|---|---|---|---|---|---|---|---|---|
| | Energy (MeV) | | | | | | | | | | | |
| | 0.01 | 0.015 | 0.02 | 0.03 | 0.05 | 0.1 | 0.2 | 0.5 | 1 | 1.5 | 2 | 4 |
| $^{51}$Cr | 0.0144 | - | - | - | - | - | 5.89 $10^{-2}$ | 3.94 $10^{-2}$ | - | - | - | - |
| $^{54}$Mn | - | - | - | - | - | - | - | 3.31 $10^{-1}$ | 6.71 $10^{-1}$ | - | - | - |
| $^{59}$Fe | - | - | - | - | - | 8.06 $10^{-3}$ | 3.20 $10^{-2}$ | - | 6.32 $10^{-1}$ | 3.66 $10^{-1}$ | - | - |
| $^{60}$Co | - | - | - | - | - | - | - | - | 9.89 $10^{-1}$ | 1.01 $10^{0}$ | - | - |
| $^{65}$Zn | 8.06 $10^{-3}$ | - | - | - | - | - | - | 2.86 $10^{-2}$ | 3.90 $10^{-1}$ | 1.18 $10^{-1}$ | - | - |
| $^{75}$Se | 4.61 $10^{-1}$ | 6.73 $10^{-2}$ | - | - | 9.77 $10^{-3}$ | 5.65 $10^{-1}$ | 9.69 $10^{-1}$ | 2.75 $10^{-1}$ | - | - | - | - |
| $^{86}$Rb | - | - | - | - | - | - | - | - | 7.43 $10^{-2}$ | 1.35 $10^{-2}$ | - | - |
| $^{89}$Sr | - | - | - | - | - | - | - | 1.69 $10^{-5}$ | 7.61 $10^{-5}$ | - | - | - |
| $^{95}$Zr | - | - | - | - | - | - | - | 5.13 $10^{-1}$ | 4.82 $10^{-1}$ | - | - | - |
| $^{95}$Nb | - | - | - | - | - | - | - | 4.68 $10^{-1}$ | 5.32 $10^{-1}$ | - | - | - |
| $^{99}$Mo | - | 1.11 $10^{-2}$ | 2.19 $10^{-2}$ | 5.48 $10^{-3}$ | 6.16 $10^{-3}$ | 4.10 $10^{-2}$ | 7.47 $10^{-2}$ | 9.09 $10^{-2}$ | 8.46 $10^{-2}$ | - | - | - |
| $^{103}$Ru | - | - | - | - | - | - | 1.06 $10^{-2}$ | 9.08 $10^{-1}$ | 1.27 $10^{-2}$ | - | - | - |
| $^{106}$Ru | - | - | - | - | - | - | 3.32 $10^{-4}$ | 2.88 $10^{-1}$ | 5.10 $10^{-2}$ | 4.52 $10^{-3}$ | 1.27 $10^{-3}$ | 8.40 $10^{-5}$ |
| $^{110m}$Ag | - | - | - | - | - | - | 6.53 $10^{-3}$ | 1.28 $10^{0}$ | 1.55 $10^{0}$ | 3.67 $10^{-1}$ | 2.79 $10^{-3}$ | - |
| $^{125}$Sb | - | - | 1.01 $10^{-1}$ | 3.97 $10^{-1}$ | 1.66 $10^{-2}$ | 1.66 $10^{-2}$ | 1.49 $10^{-1}$ | 6.03 $10^{-1}$ | 8.26 $10^{-2}$ | - | - | - |
| $^{127m}$Te | - | - | 7.93 $10^{-2}$ | 2.91 $10^{-1}$ | 8.53 $10^{-3}$ | 1.44 $10^{-3}$ | - | 1.08 $10^{-4}$ | 4.55 $10^{-5}$ | - | - | - |
| $^{129m}$Te | - | - | 6.16 $10^{-2}$ | 2.23 $10^{-1}$ | 2.90 $10^{-3}$ | 1.40 $10^{-3}$ | 8.17 $10^{-5}$ | 2.46 $10^{-2}$ | 1.70 $10^{-2}$ | 5.47 $10^{-5}$ | - | - |
| $^{132}$Te | - | - | 8.54 $10^{-2}$ | 6.04 $10^{-1}$ | 1.58 $10^{-1}$ | 3.26 $10^{-2}$ | 8.05 $10^{-1}$ | 8.30 $10^{-2}$ | - | - | - | - |
| $^{129}$I | - | - | 1.89 $10^{-2}$ | 6.96 $10^{-1}$ | 6.08 $10^{-2}$ | - | - | - | - | - | - | - |
| $^{131}$I | - | - | 1.33 $10^{-3}$ | 3.87 $10^{-2}$ | 1.04 $10^{-2}$ | 1.65 $10^{-2}$ | 4.15 $10^{-1}$ | 5.33 $10^{-1}$ | 2.87 $10^{-2}$ | - | - | - |
| $^{132}$I | - | - | - | - | - | - | 1.28 $10^{-2}$ | 1.56 $10^{0}$ | 1.23 $10^{0}$ | 1.35 $10^{-1}$ | 2.98 $10^{-2}$ | 7.54 $10^{-4}$ |
| $^{133}$I | - | - | - | - | - | - | 4.06 $10^{-3}$ | 8.75 $10^{-1}$ | 1.34 $10^{-1}$ | 2.29 $10^{-2}$ | - | - |
| $^{134}$I | - | - | - | - | - | 2.48 $10^{-2}$ | 6.69 $10^{-2}$ | 9.87 $10^{-1}$ | 1.71 $10^{0}$ | 1.76 $10^{-1}$ | 7.07 $10^{-2}$ | 9.33 $10^{-4}$ |
| $^{135}$I | - | - | - | - | - | - | 4.99 $10^{-2}$ | 1.37 $10^{-1}$ | 5.21 $10^{-1}$ | 4.71 $10^{-1}$ | 1.28 $10^{-1}$ | 3.16 $10^{-3}$ |
| $^{134}$Cs | - | - | - | - | - | - | 1.20 $10^{-3}$ | 1.37 $10^{0}$ | 8.24 $10^{-1}$ | 2.90 $10^{-2}$ | - | - |

**Table B9 Cont'd Gamma ray production data (Eckerman et al, 1993), data file orlnspec.dat (version 1)**

| Nuclide | Gamma production fraction | | | | | | | | | | | |
|---|---|---|---|---|---|---|---|---|---|---|---|---|
| | Energy (MeV) | | | | | | | | | | | |
| | 0.01 | 0.015 | 0.02 | 0.03 | 0.05 | 0.1 | 0.2 | 0.5 | 1 | 1.5 | 2 | 4 |
| $^{136}$Cs | - | - | - | $8.57\ 10^{-2}$ | $1.11\ 10^{-1}$ | $1.72\ 10^{-1}$ | $5.21\ 10^{-1}$ | $6.25\ 10^{-1}$ | $1.47\ 10^{0}$ | $1.70\ 10^{-1}$ | - | - |
| $^{137}$Cs | - | - | - | $5.14\ 10^{-2}$ | $5.90\ 10^{-3}$ | - | - | $5.75\ 10^{-1}$ | $2.75\ 10^{-1}$ | - | - | - |
| $^{140}$Ba | $4.33\ 10^{-2}$ | - | $4.15\ 10^{-4}$ | $1.47\ 10^{-1}$ | $1.75\ 10^{-3}$ | $2.47\ 10^{-2}$ | $8.01\ 10^{-2}$ | $2.82\ 10^{-1}$ | $1.83\ 10^{-2}$ | - | - | - |
| $^{140}$La | - | - | - | - | - | - | $1.45\ 10^{-1}$ | $6.93\ 10^{-1}$ | $3.01\ 10^{-1}$ | $7.74\ 10^{-1}$ | $2.17\ 10^{-1}$ | $1.07\ 10^{-2}$ |
| $^{144}$Ce | $8.20\ 10^{-3}$ | - | - | $7.27\ 10^{-2}$ | $4.84\ 10^{-2}$ | $8.78\ 10^{-2}$ | $3.62\ 10^{-2}$ | - | - | - | - | - |
| $^{169}$Yb | $3.46\ 10^{-1}$ | - | - | $6.08\ 10^{-3}$ | $2.07\ 10^{0}$ | $5.15\ 10^{-1}$ | $6.58\ 10^{-1}$ | $3.90\ 10^{-2}$ | - | - | - | - |
| $^{192}$Ir | - | - | - | - | $6.57\ 10^{-2}$ | $2.94\ 10^{-2}$ | $9.96\ 10^{-1}$ | $1.15\ 10^{0}$ | $3.97\ 10^{-2}$ | - | - | - |
| $^{226}$Ra | $2.25\ 10^{-3}$ | $4.90\ 10^{-3}$ | $3.40\ 10^{-4}$ | - | $1.77\ 10^{-3}$ | $8.98\ 10^{-3}$ | $2.83\ 10^{-2}$ | $1.12\ 10^{-5}$ | - | - | - | - |
| $^{235}$U | $4.07\ 10^{-2}$ | $1.68\ 10^{-1}$ | $5.34\ 10^{-2}$ | - | $1.43\ 10^{-2}$ | $2.73\ 10^{-1}$ | $6.16\ 10^{-1}$ | $1.35\ 10^{-3}$ | - | - | - | - |
| $^{238}$U | $1.33\ 10^{-2}$ | $5.53\ 10^{-2}$ | $1.82\ 10^{-2}$ | $1.14\ 10^{-2}$ | $1.54\ 10^{-2}$ | $5.07\ 10^{-5}$ | $1.54\ 10^{-4}$ | $2.88\ 10^{-4}$ | $4.04\ 10^{-3}$ | $1.05\ 10^{-4}$ | $9.77\ 10^{-5}$ | $4.28\ 10^{-5}$ |
| $^{238}$Pu | $1.25\ 10^{-2}$ | $6.31\ 10^{-2}$ | $3.55\ 10^{-2}$ | $4.99\ 10^{-4}$ | $2.63\ 10^{-4}$ | $7.46\ 10^{-5}$ | $3.91\ 10^{-9}$ | $7.29\ 10^{-9}$ | $1.52\ 10^{-7}$ | $2.53\ 10^{-9}$ | $2.33\ 10^{-9}$ | $1.04\ 10^{-9}$ |
| $^{239}$Pu | $4.70\ 10^{-2}$ | $2.39\ 10^{-2}$ | $1.35\ 10^{-2}$ | $1.81\ 10^{-4}$ | $2.34\ 10^{-4}$ | $1.33\ 10^{-4}$ | $4.72\ 10^{-5}$ | $3.49\ 10^{-5}$ | - | - | - | - |
| $^{241}$Pu | $7.20\ 10^{-6}$ | $3.57\ 10^{-5}$ | $1.95\ 10^{-5}$ | $2.77\ 10^{-7}$ | $6.58\ 10^{-7}$ | $1.25\ 10^{-5}$ | $1.30\ 10^{-6}$ | - | - | - | - | - |
| $^{241}$Am | $6.01\ 10^{-2}$ | $3.54\ 10^{-1}$ | $2.30\ 10^{-1}$ | $2.35\ 10^{-2}$ | $2.90\ 10^{-1}$ | $6.84\ 10^{-2}$ | - | - | - | - | - | - |

## B1 References

Eckerman KF, Westfall RJ, Ryman JC and Cristy M (1993). Nuclear decay data files of the dosimetry research group. Health Sciences Division, Oak Ridge National Laboratory, ORNL/TM-12350.

Hubbell JH (1982). Photon mass attenuation and energy-absorption coefficients from 1 keV to 20 MeV. *Int J Appl Radiat Isot*, **33**, 1269-1290.

ICRP (1987). Data for use in protection against external radiation. ICRP Publication 51. *Ann ICRP*, **17**(2/3).

ICRP (1996). Conversion coefficients for use in radiological protection against external radiation. ICRP Publication 74. A*nn ICRP*, **26**(3/4).

Jaeger RG et al (Eds) (1968). Engineering Compendium on Radiation Shielding **1**, Shielding Fundamentals and Methods. New York, Springer and Verlag.